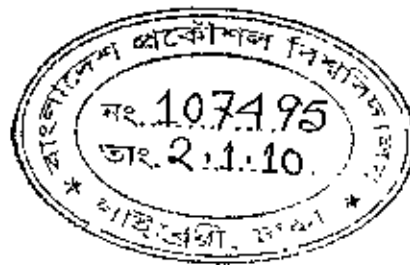# EFFECTS OF HIGH PRESSURE COOLANT ON MACHINABILITY OF STEELS

By

Md. Kamruzzaman

A Thesis
Submitted to the
Department of Industrial & Production Engineering
in Partial Fulfilment of the
Requirements for the Degree
of
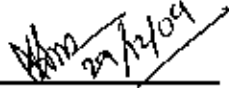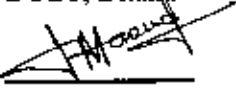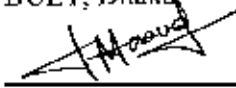DOCTOR OF PHILOSOPHY IN INDUSTRIAL & PRODUCTION
ENGINEERING

DEPARTMENT OF INDUSTRIAL & PRODUCTION ENGINEERING
BANGLADESH UNIVERSITY OF ENGINEERING & TECHNOLOGY
DHAKA, BANGLADESH

December 2009

The thesis titled **Effects of High Pressure Coolant on Machinability of Steels** submitted by **Md. Kamruzzaman**, Student No. P04050801F, Session- April 2005, has been accepted as satisfactory in partial fulfillment of the requirement for the degree of Doctor of Philosophy in Industrial & Production Engineering on December 29, 2009.
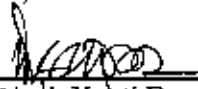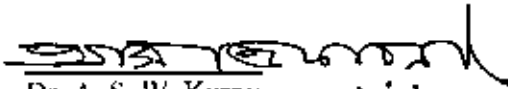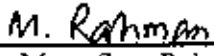
BOARD OF EXAMINERS

1.   Dr. Nikhil Ranjan Dhar   Chairman
      Professor
      Department of Industrial & Production Engineering
      BUET, Dhaka

2.   Head   Member
      Department of Industrial & Production Engineering   (Ex-officio)
      BUET, Dhaka

3.   Dr. A. K. M. Masud   Member
      Professor
      Department of Industrial & Production Engineering
      BUET. Dhaka.

4.   Dr. Abdullahil Azeem   Member
      Associate Professor
      Department of Industrial & Production Engineering
      BUET, Dhaka

5.   Dr. Dipak Kanti Das   Member
      Professor
      Department of Mechanical Engineering
      BUET, Dhaka.

6.   Dr. A. S. W. Kurny   Member
      Professor
      Department of Materials and Metallurgical Engineering
      BUET, Dhaka

7.   Dr. Mustafizur Rahman   Member
      Professor   (External)
      Department of Mechanical Engineering
      National University of Singapore
      Singapore 119260

Declaration

It is hereby declare that this thesis or any part of it has not been submitted elsewhere for the award of any degree or diploma.

Md. Kamruzzaman

Table of Contents

List of Tables

List of Figures

xiii

List of Symbols

a	:	Thermal diffusivity of the chip
BUE	:	Built up edge
B_t	:	Fraction of secondary heat source transfer into the chip
CBN	:	Cubic boron nitride
C_p	:	Specific heat of the coolant
D	:	Depth of cut
F	:	Feed rate
F_c	:	Main cutting force
F_t	:	Radial force
F_t	:	Feed force
h_{eff}	:	Effective heat convection coefficient
h_m	:	Maximum theoretical roughness
HPC	:	High-pressure coolant
KB	:	Crater width
KM	:	Distance of centre of crater from the tool edge
K_o	:	Modified Bessel function of the second kind of order zero
KT	:	Crater depth
L	:	Length of shear plane
l	:	characteristic length
L_c	:	Natural chip-tool contact length
L_t	:	Insert thickness
MQL	:	Minimum Quantity Lubrication
MRR	:	Material removal rate
Nu	:	Nusselt number
$PCBN$	:	Poly Crystalline Cubic boron nitride
PCD	:	Poly Crystalline Diamond
Pr	:	Prandtl number
q_{hl}	:	Heat intensity of the heat loss due to HPC
q_p	:	Heat intensity of the primary heat source
q_s	:	Heat intensity of the secondary heat source

R	:	Nose radius of the turning tool
R_a	:	Surface roughness
r_c	:	Chip thickness ratio$=\dfrac{t_a}{t_c}$
Re	:	Reynolds number
SEM	:	Scanning electron microscope
t_c	:	Chip thickness
t_o	:	Uncut chip thickness
V	:	Cutting speed
V_m	:	Velocity of a moving plane heat source
v	:	Characteristic velocity
VB	:	Average flank wear
V_c	:	Chip velocity
VM	:	Maximum flank wear
VN	:	Flank notch wear
VS	:	Average auxiliary flank wear
VSM	:	Maximum auxiliary flank wear
w	:	Width of cut
α	:	Rake angle
β	:	Friction angle
ε	:	Average cutting strain
θ	:	Average chip-tool interface temperature
$\Delta\theta_{c-p}$	:	Temperature rise in the chip due to the primary heat source
$\Delta\theta_{c-s}$	:	Temperature rise in the chip due to the secondary heat source
θ_o	:	Ambient temperature
θ_i	:	Temperature at the rake face
$\Delta\theta_{t-f}$	:	Temperature rise in the tool due to the secondary heat source
$\Delta\theta_{t-hl}$	:	Temperature change in the tool due to the heat loss
λ	:	Thermal conductivity of the chip material
λ_c	:	Thermal conductivity of the coolant
λ_t	:	Thermal conductivity of the tool insert
μ	:	Viscosity of the coolant
ρ	:	Density of the coolant

τ_s	:	Shear strength of the work material
ϕ	:	Principal cutting edge angle
$\emptyset$	:	Diameter of the job
φ	:	Shear plane angle
Ω	:	Constant
Λ	:	Percentage elongation of the work material
Δd	:	Reduction in depth of cut

Acknowledgement

I would like to express my heartfelt and sincere thanks to my esteemed supervisor, Dr. Nikhil Ranjan Dhar, Professor of the Department of Industrial and Production Engineering (IPE) for his priceless guidance and support during my post-graduate career at Bangladesh University of Engineering and Technology (BUET). I consider it to be a great honor to work under him. His constant encouragement to try new ideas during our research association greatly helped me to mold myself as competent engineer motivating me to accomplish laurels and novel ways of thinking. In addition to being my supervisor, he was also my guardian, taking a personal interest in my well-being, for which I will be truly grateful.

I would also like to thank Dr. A. K. M. Masud, Dr. A. Azeem, Dr. D. K. Das and Dr. A. S. W. Kurny for being on my doctoral thesis committee and providing valuable suggestions to improve the content of this thesis. I also express my gratitude to Dr. Md. Mohar Ali, Professor, Department of Materials and Metallurgical Engineering (MME), BUET for his valuable suggestions and encouragement.

I wish also to thank to all of the teachers and employees of the Department of Industrial & Production Engineering especially to the Head of the Department of IPE. I acknowledge the help rendered by the Director, DAERS, BUET who provided machine shop facilities whenever required. The help extended by the Head of the Department of MME, BUET for obtaining the scanning electron micrographs (SEM) is also sincerely acknowledged.

I am deeply obliged to all of my colleagues- Dr. S.M.A. Choudhury, M. H. Rashid and M. M. H. Chowdhury for their availability whenever I needed them and for

· Abstract

High production machining at high cutting speed and feed rate generates large heat and high cutting temperature. which shortens the tool life and deteriorates the job quality. This problem becomes more acute when the jobs are difficult to machine and are to be used under dynamic loading. The conventional cutting fluids are not that effective in such high production machining particularly in continuous cutting of materials like steels. Further the conventional cutting fluids are not environmentally friendly. The disposal of the cutting fluids often leads to local water pollution and soil contamination. Recycling and reuse of conventional cutting fluids also lead to other problems. Machining of soft, sticky and ductile materials yields long continuous chips and rapid tool wear due to inefficient action of the cutting fluids. In the present decade, with increased environmental awareness, the researchers are striving to develop environment friendly machining technology; one such technology is to use cutting oil with high-pressure. The benefits of reduction in machining temperature are significant reduction in cutting force and feed force. The benefits of high-pressure coolant are dependent on the process parameters and the tool geometry.

The role of application of high-pressure coolant jet on machinability of three different steels (C-60 steel, 17CrNiMo6 steel and 42CrMo4 steel) by two different uncoated carbide inserts (SNMG 120408 and SNMM 120408) have been extensively studied in terms of mechanics and mechanism of chip formation, cutting zone temperature, pattern and extent of tool wear and its growth with machining time along with machined surface quality in comparison to dry and wet machining.

A high-pressure coolant jet was impinged on the rake face of the cutting tool through a specially designed and developed nozzle. Application of high-pressure coolant jet showed significant effect on chip formation, cutting zone temperature and cutting forces. Expectedly, compared to dry and wet machining, tool wear under high-pressure coolant machining decreased, especially under moderate cutting speed-feed combination through control of cutting zone temperature, cutting forces, favorable chip-tool interaction and retention of cutting edge sharpness. SEM studies of the worn out inserts revealed that the notching and grooving, which are very detrimental and may cause premature and catastrophic failure of the cutting tools, are remarkably reduced by high-pressure coolant jet. The present high-pressure coolant system increased tool life by 30% to 75% when turning C-60 steel by SNMG insert and 80% to 140% when machining by SNMM insert. The surface quality of the machined surface improved possibly due to lesser damage of the cutting tool nose.

In order to implement the high-pressure coolant machining technology, an analytical model for cutting temperature has been developed. It is found that according to the selected cutting conditions in the model-based comparisons, the predicted cutting temperature under high pressure coolant conditions is reduced as high as about 18% compared with those in dry cutting.

Chapter-1

Introduction

1.1 Introduction

Traditionally, the manufacture of a product had been attempted to be done as quickly with high MRR and inexpensively without sacrificing quality of the product as possible. Now, more environmental regulations are being put in place, manufacturers are forced to re-evaluate their manufacturing processes and reduce or eliminate their harmful and environment polluting waste streams. The waste streams present in machining include cutting fluid flow, chip flow, and cutting tool usage.

The performance and service life of engineering components depend on their material, dimensional and form accuracy and surface quality. The preformed blanks are finished by machining and grinding to attain the desired accuracy and surface integrity. The growing demand for higher productivity, product quality and overall economy in manufacturing by machining and grinding, particularly to meet the challenges thrown by liberalization and global cost competitiveness, insists high material removal rate and high stability and long life of the cutting tools.

But high production machining and grinding with high cutting speed, feed and depth of cut is inherently associated with generation of large amount of heat and high cutting temperature at the cutting zone. Such high cutting temperature not only reduces dimensional accuracy and tool life but also impairs the surface integrity of the product.

The greater the energy consumption, the more severe are the thermal/frictional conditions, consequently making the metal cutting process more and more inefficient in terms of tool life, dimensional accuracy and material removal rate. Elevated tool temperatures have negative impact on a tool life. The temperature of the tool plays an important role in the thermal distortion and the machined part's dimensional accuracy, as well as in the tool life in machining. It also weakens the surface integrity of the product by inducing tensile residual stresses and surface and subsurface micro-cracks in addition to rapid oxidation and corrosion. Tools become softer and wear more rapidly by abrasion as temperatures are increased, and in many cases constituents of the tool may diffuse into the chip or react chemically with the work piece or cutting fluid. So, prime focus for machining operation is to reduce the cutting temperature as far as possible.

With the advent of carbide tools and other new methods of machining, the efficiency of the metal cutting operations has improved to a certain extent under normal cutting conditions. Currently the high temperature problems are tried to be controlled by reducing heat generation and removing heat from the cutting zone through optimum selection of machining parameters, proper cutting fluid selection and application. Some recent techniques have enabled partial control of the machining temperature by using heat resistant tools like coated carbides, PCD, CBN, PCBN etc. However, diamond and CBN tools are very expensive and the practices in the industry are still not wide spread.

In industries, the machining temperature and its detrimental effects are generally controlled or reduced to some extent by:

i. appropriate selection of

  • process parameters, i.e., cutting speed, feed and depth of cut

2

- cutting tool geometry

ii. proper selection of cutting tools

iii. proper selection and application of cutting fluids

iv application of special techniques, if feasible

1.2 Problem in Conventional Cutting Fluid Application

The most common way to reduce cutting temperature is application of water soluble cutting fluid from overhead position. Such cutting fluid not only cools the tool and job but also provides lubrication and handles the chip to clean the cutting zone and protects the nascent finished surface from contamination by the harmful gases present in the atmosphere. But the conventional types and methods of application of cutting fluid have been found to become less effective with the increase in cutting speed and feed when the cutting fluid cannot properly enter the chip-tool interface to cool and lubricate due to bulk plastic contact of the chip with the tool rake surface Besides that, often in high speed machining the cutting fluid may cause premature failure of the cutting tool by fracturing due to close curling of the chips and thermal shocks. For which application of high cooling type water base cutting fluids are generally avoided in machining steels by brittle type cutting tools like carbides and ceramics. The more serious concern by use of cutting fluid, particularly oil-based type is the pollution of the working environment. The major socio-economic problems that arise due to conventional type and method of application of cutting fluids are:

i. inconveniences due to wetting and dirtiness of the working zone

ii. possible damage of the machine tool slide ways by corrosion

iii. inhalation problem of the operator due to break down of the cutting fluid

3

into its constituents and produce obnoxious and nerve racking gases

iv.   biological hazards to the operators from bacterial growth in the cutting fluids like skin irritation, bronchitis etc

v.   water pollution and soil contamination when mixes the fluid with them and

vi.   requirement of additional systems for local storage, pumping, filtration, recycling, and re-cooling

1.3   Limitations of Conventional Cutting Fluid Application and Probable Solutions

Application of conventional cutting fluids offers several important benefits in machining processes such as:

i.   cooling the tool and job particularly at their interface

ii.   lubrication of the chip-tool and work-tool interfaces

iii. cleaning of the machining zone by flushing away the machined chips/debris

iv.   protection of the nascent machined surface from atmospheric contamination

Though it would appear that generous use of coolant and lubricants always assist in controlling the cutting zone temperature, it may not be the case always, especially under high speed machining as the tool-chip/workpiece contact will be under seizure condition and no coolant/lubricant can penetrate into the interfaces. Conventional coolants undergo film boiling at around 350°C and loose their cooling property [Paul and Chattopadhyay 1995].

The cutting zone in machining is often flooded with coolant without taking into account the requirements of the specific process. Scientific investigations and industrial applications have indeed shown that the type of coolant and its supply influence the

4

component quality and tool life in machining for which coolants and lubricants are important technological parameters in machining. But in some cases application of cutting fluids is considered undesirable, especially in machining some advanced and exotic materials.

Also, coolants and lubricants incur a significant part of the manufacturing cost. A recent survey indicated that the cost of cutting fluids and the auxiliary equipments compromise nearly 7-17% of the total machining costs [Klocke and Eisenblaetter 1997]. Compared with the cost of the cutting tools (2-4%), the cutting fluid cost is significantly high. As a result, there is a need to reduce the use of the cutting fluids. Furthermore, machining processes often produce small lubricant droplets in the form of mist, smoke and gases that are harmful to the environment and human health.

During machining operations, workers could be exposed to cutting fluids by skin contact and inhalation [Bennett and Bennett 1987]. Skin contact usually occurs in the following situations:

i.   the worker directly touches cutting fluid without any protective equipment

ii.   the worker handles work, machine, and equipment that are covered with cutting fluid

iii. the worker is exposed to cutting fluid splashes from the machine tool or workpiece

Skin exposure to cutting fluid can cause various skin diseases [NIOSH 1998]. In general, skin contact with straight cutting oils cause folliculitis, oil acne, and keratoses while skin exposure to soluble, semi-synthetic and synthetic cutting fluid would result in irritant contact dermatitis and allergic contact dermatitis.

5

Another source of exposure to cutting fluids is by inhalation of mists or aerosols. The inhalation exposure will be higher if the worker is close to the machine that is not enclosed, if the metal cutting is operated with high cutting speeds and deep cuts, or if ventilation equipment was not properly selected or maintained. Airborne inhalation diseases have been occurring with cutting fluid aerosols exposed workers for many years. These diseases include lipid pneumonia, hypersensitivity pneumonitis, asthma, acute airways irritation. chronic bronchitis, and impaired lung function [**NIOSH 1998**].

In response to these health effects through skin contact or inhalation, the National Institute for Occupational Safety and Health (NIOSH) has recommended that the permissible exposure level (PEL) is 0.5 mg/m^3 as the metalworking fluid concentration on the shop floor [**NIOSH 1998, Thornburg and Leith 2000**].

Thus from technological, economical and ecological perspectives, as well as increasing legislations, efforts are being made to reduce or eliminate the use of coolants in machining. But with the need for high production machining, the control of cutting temperature is an important aspect of modern machining and grinding operations. Dry machining technologies and minimum quantity lubrication (MQL) will only be acceptable condition that the main tasks of coolants in machining processes can be successfully replaced The tasks that will have to be addressed are heat reduction, machined surface protection, cleaning of the cutting zone [**Dhar**[a] **et al. 2006, Dhar**[b] **et al. 2006**]. Cryogenic machining with liquid nitrogen has improved machinability index but cryogenic machining is costly due to high cost of liquid nitrogen [**Dhar**[a] **et al. 2002, Dhar**[b] **et al. 2002**].

6

1.4   Machining with High-Pressure Coolant Jet

The use of conventional coolants and lubricants in high production machining and grinding is being reviewed or minimized because of the following concerns:

i.   lack of significant technological benefits

ii. increasing cost of storage and disposal of used cutting fluids

iii. potential health hazards to worker

iv. environmental pollution due to disposal of used coolants

Strict legislation in most of the countries has imposed stringent conditions on use and disposal of used metal cutting fluids. Under these circumstances, the used metal cutting fluid disposal costs have spiraled up. All these factors have focused the machining industries to look for alternative ways and methods of controlling the high cutting temperatures. The focus is on effective and efficient cooling and lubrication with eco-friendliness as well as cost competitiveness. Under these considerations, the concept of high-pressure coolant presents itself as a possible solution for high speed machining in achieving slow tool wear while maintaining cutting forces/power at reasonable levels, if the high pressure cooling parameters can be strategically tuned. Mazurkiewicz et al. [1989] reported that a coolant applied at the cutting zone through a high-pressure jet nozzle could reduce the contact length and coefficient of friction at chip-tool interface and thus could reduce cutting forces and increase tool life to some extent. High-pressure coolant injection technique not only provided reduction in cutting forces and temperature but also reduced the consumption of cutting fluid by 50% [Aronson 2004, Wrethim et al. 1992] It has been reported that the cooling and lubrication is improved in high speed machining of

7

difficult-to-machine materials by the use of high-pressurized coolant/lubricant jet [Wrethim et al. 1992].

The success of implementing this technology across the metal removal industries will therefore depend on increased research activities providing credible data for depth understanding of high-pressure coolant supplies at the chip-tool interface and integrity of machined components. In this regard, the present research work is carried out to experimentally investigate the role of high-pressure coolant on chip formation mechanism, cutting temperature, cutting force, tool wear, dimensional accuracy and surface finish in machining different steels at different cutting speed and feed combinations by uncoated carbide insert under completely dry and high-pressure coolant conditions and to find out the benefit of high-pressure coolant machining over dry cutting.

1.5   Scope of the Thesis

One of the possible and emerging technologies to overcome the aforesaid problems associated with conventional cutting fluid on the shop floor is application of high-pressure coolant (HPC) in achieving high productivity and product quality in high production machining. In a machining operation tool life achieved, metal removal rate (MRR), component of forces and power consumption, surface finish generated and surface integrity of the machined component as well as the shape of the chips can all be used to measure machinability Keeping in view, the present research work has been carried out to explore the role of high-pressure coolant on major machinability characteristics in turning steel by uncoated carbide inserts under different machining conditions.

Chapter 1 presents the general requirements in machining industries, role of cutting tools, techno-environmental and socio-economical problems associated with the

high cutting temperature and the conventional cooling practice and expected role of high-pressure coolant. Survey of previous work and objective of the present work are presented in **Chapter 2** and **Chapter 3** respectively.

Chapter 4 deals with fabrication of high-pressure coolant system for the present work to enable proper cooling of the cutting zone. Calibration of tool-work thermocouple comprising of different materials and different inserts are also presented in the chapter. This chapter also presents the procedure and conditions of the machining experiments carried out and the experimental results on the effects of high-pressure coolant (HPC), relative to dry machining, on chip morphology, cutting zone temperature, cutting forces, cutting tool wear, tool life and surface integrity in turning different steels under different cutting conditions.

Chapter 5 provides development of a mathematical model for cutting temperature at the chip-tool interface from the characterization of the physical processes taking place during machining and its validation. **Chapter 6** contains the detailed discussion on the experimental results and possible interpretations on the results obtained.

Finally, a summary of major contributions is given in **Chapter 7** and **references and publications** are provided at the end.

Chapter-2

Literature Review

Machinability of materials usually judged mainly in respect of chip morphology, chip-tool interaction, cutting temperature, cutting forces, dimensional accuracy, surface integrity and wear and life of cutting tool with using cutting fluid and without using cutting fluid. Heat generation and high cutting temperature is inherent characteristics of machining due to shearing of work material, friction between the flowing chips and rake face of the tool as well as friction of auxiliary flank with finished surface. At such elevated temperature the cutting tool if not enough hot hard may loose their form or stability quickly or wear out rapidly resulting in increased cutting forces, dimensional inaccuracy of the product and shorter tool life. The magnitude of this cutting temperature increases, though in different degree, with the increase of speed, feed and depth of cut, as a result, high production machining is constrained by rise in temperature. This problem increases further with the increase in strength and hardness of the work material.

It appears that the high temperature in cutting zone is the main problem and hence methods were tried out over the years to tackle this problem. Application of proper cutting fluids at times, reduced the above problems to some extent through cooling and lubrication of the cutting zone. The commonly used fluids are neat oil, semi synthetic and synthetic fluids with or without additives and inorganic salts. The application procedures of these fluids are generally by flood cooling, or in the form of jet or even mist. Ample research has been done in various directions and is still going on aiming improvement in overall

machining efficiency through controlling the aforesaid problems.

2.1 Causes and Effects of Cutting Temperature

The high specific energy required in machining under high cutting speed and unfavorable condition of machining results in very high temperature which reduces the dimensional accuracy and tool life by plastic deformation and rapid wear of the cutting points [Chattopadhyay and Bhattacharya 1968; Chattopadhyay and Chattopadhyay 1982; Singh et al. 1997]. On the other hand, such high temperature impairs the surface integrity of the machined component by severe plastic flow of work material, oxidation and by inducing large tensile residual stresses, surface and subsurface cracks Chattopadhyay and Chattopadhyay 1982].

The mechanisms of material deformation, friction and material removal lead to the initiation of machined components, where the temperature of the rake and flank is the most important factor to affect the chip formation, tool wear, cutting forces and surface integrity [Jaspers and Dautzenberg 2002; Aronson 2004]. At elevated temperature and pressure the cutting edge deforms plastically and wears rapidly, which lead to dimensional inaccuracy, increased cutting forces and premature tool failure [List et al. 2005].

Ng et al. [2002] proposed that there is a peak cutting temperature at an intermediate cutting speed and when cutting speed is increased from this point, there is a reduction in temperature. Since this claim most of the literature has concluded that there is no corresponding reduction in temperature at higher cutting speeds. Conversely, Vernon and Ozel [2003] stated that the limit of cutting speed is a function of the cutting tools used. Ekinovic et al. [2005] suggested that temperature is increased with cutting speed up to maximum which is equal to the melting point of the work piece. No temperature reduction

occurred at higher cutting speeds. But there is no fixed limit to the cutting speed when machining aluminum alloy because the melting point of this alloys (up to 600°C) is lower than the temperature at which cemented carbide and ceramic tool materials begin to lose their strength and wear rapidly.

Cutting chips becomes blue in color due to intensive high temperature during machining. With the increase in cutting speed, feed, depth of cut and hardness of the work material the chips turns to gradual deep blue. Kosa and Ney [1989] suggested that in machining ductile metals, the heat and temperature developed due to plastic deformation and rubbing of the chips with tool, may cause continuous built-up of welded debris which affects machining operation. Austenitic stainless steels are generally considered difficult-to-machine because of high work-hardening rate, toughness and ductility. Therefore, tools will be subjected to high frictional heat, and chips will have a tendency to stick and cause severe built-up edge formation. It was observed that, in machining ductile metals, producing long chips, the chip-tool contact length have a direct influence on the cutting temperature and thermo-chemical wear of cutting tools [Jawahir and Luttervelt 1993]. The cutting temperature becomes the maximum on the rake face of the tool at a certain distance from the cutting edge where cratering occurs. Such high rake face temperature can also raise the temperature at the flank of the tool.

Komanduri and Schroeder [1993] reported that machining Inconel with hot-pressed ceramic and cubic boron nitride cutting tool produces different types of longitudinal chips. At lower speed (<30 m/min) the chips are mechanically continuous although highly coiled. With increased speed (up to about 91.5 m/min), shear localization is initiated. The chips formed are comprised of many segments strongly joined together forming a continuous tight coil. With a further increase in speed, the extent of contact

12

between the segments decreases. At about 152.5 in/min, short chips with only a few segments joined together are produced, and from this speed onward, the chip segments are completely isolated. Pashby et al. [1993] proposed that the cutting speed at which a change in chip form occurs varied from tool material to tool material. Kitagawa et al. [1997] conducted experiments with ceramic tool under flood cooling condition and concluded that with increase in cutting speed, serrations in the chip become obvious and the chip thickness decreases.

Vleugels [1995] observed that the contact length between the tool and chip has a direct influence on the cutting temperatures and the amount of heat energy that is dissipated in the tool which enhances thermally activated chemical wear. Toropov and Ko [2003] also reported that, in machining ductile metals, the chip contact length plays significant role on the chip and tool temperature which becomes maximum almost at the centre of the chip-tool contact surface where crater wear begins and grooves intensively.

Generally, shear angle decreases with increase in cutting speed and a high shear angle improves the machinability of steel. Masatoshi Hirao et al. [1996] concluded that molybdenum and vanadium mixed nitriding steel produces long cutting chips at low cutting speed but the cutting tool is sometimes broken by long continuous chips which affects shear angle. Duan and Wang [2005] suggested that an increase of work material hardness increases the shear angle, the temperature and the yield strength but reduces the average stress ratio on the primary deformation zone. Sutter [2005] reported that continuous chip forms during machining material having good thermal property and low hardness, whereas ribbon like chip or a segmental (or shear localized) chip forms during machining material having poor thermal property and high hardness.

Strafford and Audy [1997] investigated the relationship between hardness and machining forces during turning of AISI 4340 steel with mixed alumina tools. The results suggest that an increase in hardness leads to an increase in the machining forces. Tool geometry is another important factor affecting machining forces, especially the feed (axial) and thrust (radial) force components [Thiele and Melkote 1999]. The use of large nose radius together with low depths of cut leads to low true side cutting edge angle values, thus resulting in high thrust forces [Muller and Blumke 2001]. Liu et al. [2002] observed that the cutting temperature is optimum when the work piece material hardness is HRC 50. With further increase in the work piece hardness, the cutting temperature shows a descending tendency Liu et al. [2002] also suggests that under different cutting parameters, the role of cutting force changes with work piece hardness. The main cutting force features an increasing tendency with the increase of the work piece hardness.

According to Trent [1983], the cutting tool generally undergoes both flank wear and crater wear during machining. Flank wear generally causes an increase in the cutting forces, dimensional inaccuracy and vibration. Crater wear takes place on the rake face of the tool where the chip slides over the tool surface. Reed and Clark [1983] reported that the hardness, plastic modulus and the fracture toughness of the tool decline with increase in cutting temperature, which accelerates tool wear rate. Moreover, thermal stresses in the tool increase with the temperature resulting in more cracks in the tool and premature failure of the tool. The amount of energy dissipated through the rake face of the tool raises the temperature at the flanks of the tool [Wu and Matsumoto 1990]. Wang et al. [1996] reported that the normal turning chips often have considerable strength and cause crater wear, crack development or other kinds of surface damage on the rake face of the tool. Liao and Shiue [1996] reported that built-up edge (BUE) is formed with chipping of the cutting edge during machining Inconel with carbide. They also observed Ni and Fe

14

diffusion into the cutting tool. This diffusion of the work elements into the cutting tool may be explained by the very high cutting temperature during the experiments.

Kitagawa et al. [1997] investigated tool wear and cutting tool temperature by means of turning experiment in the presence of 10% water base coolant. Temperature rose monotonically, up to about 1200° C, with increasing cutting speed. They confirmed that notch wear VN were the major types of wear observed. However taking into account the decreasing of notch wear at higher cutting speed, they estimated that the wear characteristics observed cannot be exclaimed by temperature alone and the wear is rather developed by an abrasive process than a thermally activated adhesion mechanism.

Rahman et al. [1997] investigated the machinability index of Inconel 718 subjected to various machining parameters including tool geometry, cutting speed and feed rate on flank wear of the coated carbide inserts, work piece surface roughness and cutting force components as the performance indicators for tool life. They observed that tool life increases with the increase in side cutting edge angle for the inserts and the heat generated during the cutting process is distributed over a greater length of cutting edge. This improves the heat removal from the cutting edge, distributes the cutting forces over a larger portion of the cutting edge, reduces tool notching and substantially improves tool life.

Most of the major parameters including the choice of tool and coating materials, tool geometry, machining method, cutting speed, feed rate, depth of cut, lubrication, must be controlled in order to achieve adequate tool lives and surface integrity of the machined surface [Ezugwu and Tang 1995]. A crater is usually formed at some distance from the cutting edge and it is most frequently observed when cutting steels and other high-melting-

15

point metals at relatively high cutting speeds [**Choudhury and Appa Rao 1999**]. This crater gradually becomes deeper with time and may lead to the breakage of the cutting edge, rendering the tool useless.

Luo et al. [1999] reported that when turning AISI 4340 steel using mixed alumina and PCBN tools the flank wear is reduced as work material hardness increased up to a critical value. A further increase in the work piece hardness accelerates the tool wear rate. The reduction in tool wear up to critical is attributed to the elevation of the cutting temperature, which reduces the shear strength of the work material; however, this effect is not observed when the hardness exceeded critical value. The material transfer leads to the formation of a crater on the tool rake face and consequently reduces the tool mechanical resistance and its efficiency Diffusion phenomena were first reported by Molinari and Nouari [2000] who showed that at conventional speed, tool wear is mainly due to abrasion and adhesion, but is dominated by diffusion process at higher speeds

Severe flank wear and notching at the tool nose and/or the depth of cut line are the dominant failure modes when machining nickel-based alloys with carbide tools [**Ezugwu and Wang 1996; Wang et al. 1996; Kaminski and Alvelid 2000**]. The recommended cutting speeds range is from 10 to 30 m/min when machining nickel-based alloys with cemented carbide tools [**Fang 2002**]. Cemented carbide tools cannot be used to machine nickel-based alloys at high speed since they cannot withstand the conditions of extreme high temperature and stress in the cutting zone. Rapid increase in notching occurs on carbide tools at higher cutting speed. This usually leads to the premature fracture of the entire insert edge [**Ezugwu and Bonney 2004**]. Flank wear generally causes an increase in the cutting force and the interfacial temperature, leading normally to dimensional inaccuracy in the work pieces machined and to vibration which makes the cutting

16

operation less efficient [Bouzid et al. 2004].

High production and finish machining and grinding are inherently associated with generation of intense heat and cutting temperature at the cutting zone. Such high cutting temperature not only reduces tool life but also impairs the surface integrity of the job. The problems become more acute when the materials are hard and tough and the finished products are used in dynamic loading conditions. Such problems arising out of high cutting temperatures are tried to be controlled or reduced to some extent by.

i.   application of conventional cutting fluid

ii.   using heat and wear resistance cutting tool materials

iii.   application of liquid nitrogen (cryogenic machining)

iv.   application of minimum quantity lubrication (MQL machining)

v.   application of high-pressure coolant (HPC machining)

Usually water soluble cconventional cutting fluid is applied to control such elevated cutting temperature but it is ineffective in high speed machining and also is a major source of environmental pollution in the machining industries. Research has also been initiated on control such pollution by neat and clean machining like Cryogenic cooling, MQL cooling and high-pressure coolant (HPC) machining and their technological effects particularly in temperature intensive machining and grinding. A brief review of some of the interesting and important contributions in the closely related areas is presented in this section.

2.2   Controlling of Cutting Temperature

The application of conventional cutting fluid during machining is believed to reduce this cutting temperature either by removing heat as coolant or by reducing the heat generation as a lubricant and increase tool life. But it has been experienced that lubrication is effective at low cutting velocities when it is accomplished by diffusion through the workpiece and by forming solid boundary layers from the extreme pressure additives, but at high cutting velocities no sufficient lubrication effect is evident [Cassin and Boothroyed 1965; Sokovic and Mijanovic 2001].

Generally, suitable cutting fluid is employed to reduce cutting temperature through cooling and lubrication at the cutting zone. The cutting fluids are believed to reduce cutting temperature either by removing heat as a coolant or reducing the heat generation as a lubricant. In addition, the cutting fluid has a practical function as a chip-handling medium [Beaubien and Cattaneo 1964]. But it has been reported that lubrication is effective at low speeds when it is accomplished by diffusion through the work piece and by forming solid boundary layers from the extreme pressure additives, but at high speeds no sufficient lubrication effect is evident [Cassin and Boothroyed 1965]. The primary function of cutting fluids is to reduce this cutting temperature and increase tool life [Shigeki et al. 1993]. The ineffectiveness of lubrication of the cutting fluid at high speed machining is attributed to the inability of the cutting fluid to reach the actual cutting zone and particularly at the chip-tool interface due to bulk or plastic contact at high cutting speed [Dhar[a] et al. 2002; Dhar[b] et al. 2002].

The effect of the heat generated at the primary shear zone is less significant for its lesser intensity and distance from the rake surface. However, the heat generated at the

chip-tool interface is of much greater significance, particularly under high cutting speed conditions where the heat source is a thin flow-zone seized to the tool [Trent 1983, 1984, 1991]. The coolant cannot act directly on this thin zone but only externally cools the chip, work piece and the tool, which are accessible to the coolant. Removal of heat by conduction through the chip and the work piece is likely to have relatively little effect on the temperature at the chip-tool and work-tool interface. The cooling and lubricating affects by cutting fluid influence each other and diminish with increase in cutting speed [Kitagawa et al. 1997]. Since the cutting fluid does not enter into the chip-tool interface during high speed machining, the cutting fluid action is limited to bulk heat removal only.

A cutting fluid may impart two more actions, namely the mechanical strength reducing action and the electro-chemical action. The mechanical strength reducing action seemed to be negligible when steel jobs are machined at moderate cutting speeds with carbide tools [Kurimoto and Barroe 1982]. The influence of the electric current flowing through the cutting zone on the rate of tool wear is also well known [Sadik and Lindstro̎m 1993]. However, most commercial cutting fluids are non electro-conductive, and as such the situation with respect to current flow is not vary significantly from the dry cutting case. The electrochemical action is treated as a corrosion phenomenon in respect of tool wear.

However, the application of abundant cutting fluid, increases the cutting process costs and in hardened steel cutting, does not allow the work piece soften, which is good for the process [Novaski and Do̎rr 1999]. Ekinovic et al. [2002] suggested that, the use of abundant cutting fluid (wet condition) has the advantages of providing chip transportation, reducing friction and cooling the work piece. For example if cutting fluid is not used in machining of both aluminum alloys and soft steels, the wear caused by attrition is

unacceptable.

Seah et al. [1995] also reported that at the first stage of machining (first 40 seconds or so), tool wear is faster in wet cutting than in dry cutting. Later on, the wear rate is stabilized and is somewhat the same for both dry and wet cutting. Minimum volume of oil technique may represent a compromise between the advantages and disadvantages of completely dry cutting and cutting with abundant soluble oil [Heisel et al. 1994; Heisel et al. 1998]. The application of cutting fluid may not always reduce the cutting tool wear as is commonly believed. Rather some conditions like machining steels by carbide tools, the use of coolant may increase tool wear. It has also been experienced that there was more tool wear when cutting with coolant than cutting dry in case of machining AISI 1060 and AISI 4340 steels by carbide cutting tool [Dhar[c] et al. 2002; Dhar[d] et al. 2002].

The application of cutting fluid may not always reduce the cutting tool wear as is commonly believed. Rather some conditions like machining steels by carbide tools, the use of coolant may increase tool wear. It has been experienced [Shaw et al. 1951] that there was more tool wear when cutting with coolant than cutting dry in case of machining AISI 1020 and AISI 4340 steels by M-2 high speed steel cutting tool. The high cutting temperature is controlled by profuse cooling [Kurimoto and Barroc 1982; Wrethim et al. 1992; Alaxender et al. 1998]. But such profuse cooling with conventional cutting fluids is not able to solve these problems fully even when employed in the form of jet or mist. Cutting fluids also help in machining of ductile materials by reducing or preventing formation of a built-up edge (BUE), which degrades the surface finish [Kaminski and Alvelid 2000].

During machining, the cutting tool generally undergoes [**Trent 1983**] both flank
wear and crater wear. Flank wear generally causes an increase in the cutting forces,
dimensional inaccuracy and vibration. Crater wear takes place on the rake face of the tool
where the chip slides over the tool surface. Another experimental investigation was
conducted [**Cozzens et al. 1995**] on single point boring. This was aimed to study the role
of cutting fluid, tool and workpiece material, tool geometry and cutting conditions on
machinability. The results indicated that the cutting fluid conditions had no significant
effect on surface texture, forces and built-up edge. Since boring is a high-speed operation
and lubrication is ineffective, no effect was seen on the forces. However, the cutting fluid
was found to have a significant effect on surface integrity.

Proper selection and application of cutting fluid generally improves tool life. At
low cutting speed almost four times longer tool life was obtained by such cutting fluid
[Satoshi et al. 1997]. But surface finish did not improve significantly.

Manufacturing by machining constitutes major industrial activities in global
perspective. Like other manufacturing activities, machining also leads to environmental
pollution [**Ding and Hong 1998; Hong et al. 1999**] mainly because of use of cutting
fluids. These fluids often contain sulphur, phosphorus, chlorine or other extreme-pressure
additives to improve the lubricating performance. These chemicals present health hazards.
Furthermore, the cost of treating the waste liquid is high and the treatment itself is a source
of air pollution. The major problems that arise due to use of cutting fluids are [**Aronson
1995**].

i.   environmental pollution due to breakdown of the cutting fluids into harmful
      gases at high cutting temperature,

21

ii.   biological hazards to the operators from the bacterial growth in the cutting fluids

iii. requirements of additional systems for pumping, local storage, filtration, temporary recycling, cooling and large space requirement

iv.   disposal of the spent cutting fluids which also offer high risk of water pollution and soil contamination

Since beginning of twentieth century people [Peter et al.1996; Welter 1978; Kennedy 1989 and Thony et al. 1975] were concerned with possible harmful effects of various cutting fluid application.

It has been estimated that about one million workers are exposed to cutting fluids in the United States alone [Bennett 1983]. Since cutting fluids are complex in composition, they may be more toxic than their constituents and may be irritant or allergenic. Also, both bacteria and fungi can effectively colonize the cutting fluids and serve as source of microbial toxins. Hence significant negative effects, in terms of environmental, health, and safety consequences, are associated with the use of cutting fluids. The effects of exposure to the fluids on health have been studied for over 50 years; beginning with the concern that cutting fluid (oil) is a potential etiologic factor for occupational skin cancer. The international Agency for Research on Cancer has concluded that there is sufficient evidence that mineral oils used in the workplace are carcinogenic [Peter et al. 1996]. Basically, workers are exposed to metal cutting fluids via three routes like skin exposure, aerial exposure and ingestion [Bennett and Bennett 1985].

Skin exposure is the dominant route of exposure, and it is believed that about 80 percent of all occupational diseases are caused by skin contact with fluids [Bennett and

Bennett 1985]. Cutting fluids are important causes of occupational contact dermatitis, which may involve either irritant or allergic mechanisms. Water mixed fluids generally determine irritant contact dermatitis and allergic contact dermatitis when they are in touch with workers skin. Non-water-miscible fluids usually cause skin disorders such as folliculitis, oil acne, keratoses and carcinomas.

Iowa Waste Reduction Centre [1996] reported that besides potential skin and eye contact, inhalation is also a way to occupational exposure. Mists are aerosols comprised of liquid particles (<20 μm). During machining process, a considerable amount of heat is generated for which the cutting fluid may attain a temperature sufficiently higher than the saturation temperature. The vapour is produced at the solid-liquid interface as a result of boiling. Vapour may be generated also at the liquid-air interface when the fluid vapour pressure is less than the saturation pressure, namely as evaporation phenomena. Vapour generated then may condense to form mist. The potential health effects of exposure to cutting fluid mists have been the subjects of epidemiological studies in the automotive industry The mist droplets can cause throat, pancreas, rectum, and prostate cancers, as well as breathing problems and respiratory illnesses. One acute effect observed is mild and reversible narrowing of airways during exposure to cutting fluid mist [Kennedy 1989].

Growing demand for high MRR in machining necessitated much increase in cutting speed, which eventually required the efficiency of cooling to be increased in order to cope with the increase in the cutting temperature. On the other hand, legislation in many countries is restricting much use of coolants, because of environmental issues. There are limits on the amount of coolant mist, and some coolants and coolant-coated chips have been treated as toxic materials. Outside the plant, the rising cost of chip disposal and the potential secondary effects of coolant vented to the atmosphere are new concerns

[Aronson 1995] In some applications the consumption of cutting fluids has been reduced drastically by using mist lubrication. However, mist in the industrial environment can have a serious respiratory effect on the operator [Kennedy 1989]. Consequently, high standards are being set to minimize this effect. Use of cutting fluids will become more expensive as these standards are implemented leaving no alternative but to consider environmentally friendly manufacturing.

The machining temperature can be reduced to some extent by improving the machinability characteristics of the work material metallurgically, optimizing the tool geometry and by proper selection of the process parameters [Muraka et al. 1979; Jawahir 1988]. But for higher productivity in manufacturing by machining to meet the global cost competitiveness, insists high material removal rate as well as high process parameters.

With the advent of some modern machining process and harder materials and for demand for precision machining, the control of machining temperature by more effective and efficient cooling has become extremely essential. Some recent techniques have enabled partial control of the machining temperature and eliminated pollution by using heat resistance tools like coated carbides, CBN etc under dry condition. The thermal deterioration of the cutting tools can be reduced by using CBN tools [Narutaki and Yamane 1979]. If properly manufactured, selected and used, CBN tool provides much less cutting forces, temperature and hence less tensile residual stresses [Davies et al. 1996]. However, CBN tools are very expensive. Recent studies have reported that *CBN* tools can be used for machining high temperature super alloys, especially titanium alloys, at higher cutting speeds despite the high reactivity of titanium-alloys with the tool materials in addition to their relatively high cost [Hong et al. 2001]. Owing to their high hardness and

high melting point, CBN tools can withstand the heat and pressure developed during cutting without compromising surface integrity of the machined component because of their ability to maintain a sharp cutting edge for longer periods [Ezugwu 2004].

Farook et al. [1998] modified the contact surface of turning inserts by deposition of a soft bearing material by EDM. Although the modified inserts offered reduced cutting force, their beneficial effect on surface finish was marginal. At higher cutting velocities, the brought on layers are fast depleted with cutting time and do not contribute to wear resistance of the tool, especially at the flanks. The machining of hardened steel is usually done using dry cutting, because the increase of the temperature makes chip deformation and shearing of the hardened material easier. Nevertheless high temperatures cause an inconvenience such as work piece dilation, which affects dimensional and geometric accuracy and runs the risk of surface integrity damage. On the other hand, the complete absence of lubrication harms chip transportation and causes increases of tool-chip and tool-work piece friction, which generate the increase of abrasive wear and attrition [Novaski and Dörr 1999].

Thoors and Chandrasekaran [1994] observed that CO_2 snow could function as a good coolant under certain circumstances, which are very much related to the tool-work combination and the actual mode of feeding the coolant to the cutting zone. Machining temperature can be controlled by the use of CO_2 snow as the coolant in machining [Chandrasekaran et al. 1998]. This is feasible if CO_2 in liquid form under pressure of 60 bar is fed to the cutting zone and diffused through a capillary jet. This results in a change of state and the formation of CO_2 snow (endothermic reaction resulting in a temperature of -79^0C). But under intense temperature CO_2 produces harmful CO gas.

Recently the process of cryogenic turning has been investigated [Bhattacharya et al.1972]. The forces and cutting energy reportedly decreased when machined cryogenically compared to those with dry machining. Significant improvement in surface finish and other surface properties were noticed and such beneficial affects were attributed to low temperature and controlled tool wear. It has been further reported [Uhera and Kumagai 1968; Uhera and Kumagai 1969; Fillippi and Ippolito 1970] that cryogenic machining with liquid nitrogen resulted in relatively lesser cutting forces, longer tool life and better surface conditions.

Cryogenic machining with liquid nitrogen has improved machinability of steel to a certain extent under normal cutting conditions [Paul and Chattopadhyay 1995]. Chilling the cutting tool by liquid nitrogen jets enhances tool hardness and life, dimensional accuracy and improves surface roughness. Cooling the chip makes it brittle and aids removal. Because nitrogen is an abundant atmospheric constituent and the quantities used are small, there is no unfavorable environmental or health impact nor are coolant disposal cost and the chips readily recycled. [Paul et al. 2000; Paul et al. 2001; Dhar[a] et al. 2002; Dhar[b] et al. 2002]. Their results indicate substantial benefit of cryogenic cooling on cutting force, tool life, dimensional accuracy and surface roughness due to mainly reduction of cutting zone temperature and favorable changes in the chip-tool interaction.

Dhar[a] and Kamruzzaman [2005] investigate the role of cryogenic cooling by liquid nitrogen jet on chip formation, grinding zone temperature and surface roughness in grinding alloy steels. Their experimental results indicate significant reduction in grinding temperature on application of cryogen, which enables favorable chip formation. Though cryogenic grinding provides relatively more surface roughness for less plastic deformation

and rubbing, shearing and fracturing modes of chip formation and retention of the grit's sharpness, it provides environment friendliness and improves the grindability characteristics.

It has also been reported that the machining of steel with liquid nitrogen improves the machinability index in respect of lowering cutting force as well as energy consumption due to decrease in chip reduction coefficient, increasing tool life by retaining sharpness of the cutting tool for a long time preventing formation of built up edge, increase product quality by decreasing surface roughness and thermal stress [Dhar[d] et al. 2002; Dhar[b] and Kamruzzaman 2005; Dhar et al. 2006; Dhar and Kamruzzaman 2007] but cryogenic machining is costly due to high cost of liquid nitrogen. Also accelerated notch wear on the principal flank of the carbide insert was observed at nitrogen rich atmosphere of cryogenic machining.

Minimal quantity lubrication (MQL) is a recent technique introduced in machining to obtain safe, environmental and economic benefits, reducing the use of coolant lubricant fluids in metal cutting. Machado and Wallbank [1997] conducted experiments on turning medium carbon steel using a Venturi to mix compressed air with small quantities of liquid lubricant, water or soluble oil with a mean flow rate of 3 and 5 ml/min. The mixture was directed onto the rake face of a carbide tool against the chip flow direction. The application of a mixture of air and soluble oil was able to reduce the consumption of cutting fluid, but it promoted a mist in the environment with problems of odors, bacteria and fungi growth of the overhead flooding system.

Attanasio et al. [2004] reported that when MQL is applied to the tool rake, tool life is generally no different from dry conditions, but MQL applied to the tool flank can

increase tool life. Lubricating the flank surface of a tip by the MQL technique reduces the tool wear and increases the tool life. Traces of lubricant compounds have been found on the worn surfaces only when MQL has been applied on the flank surface.

Dhar et al. [2006] investigated the influence of near dry lubrication on cutting temperature, chip formation and dimensional accuracy when turning AISI 1040 steel. The lubricant was supplied at 60 ml/hr through an external nozzle in a flow of compressed air (7 bar). Based on the machining tests, the authors found that near dry lubrication resulted in lower cutting temperatures compared with dry and flood cooling. The dimensional accuracy under near dry lubrication presented a notable benefit of controlling the increase of the workpiece diameter when the machining time elapsed where tool wear was observed. Dimensional accuracy was improved with the use of near dry lubrication due to the diminution of tool wear and damage.

Dhar et al. [2005], Dhar^e et al. [2006] and Dhar et al. [2007] also suggested that MQL reduced the cutting temperature; such reduction has been more effective for those tool-work combinations and cutting conditions, which provided higher value of chip reduction coefficient, ζ for adverse chip-tool interaction causing large friction and built-up edge formation at the chip-tool interface. Favorable change in the chip-tool interaction and retention of cutting edge sharpness due to reduction of cutting zone temperature seemed to be the main reason behind reduction of cutting forces by the MQL. Dimensional accuracy also substantially improved mainly due to significant reduction of wear and damage at the tool tip by the application of MQL. Though MQL gives some advantages during the turning operation, it presents some limits due to the difficulty of lubricant reaching the cutting surface.

Pollution free manufacturing is increasingly gaining interest due to recent development of pollution-prevention legislation, European initiatives on product take-back or recycling, which affect many export industries in the US, and a growing consumer, demand for green products and production processes. Concern for the environment, health and safety of the operators, as well as the requirements to enforce the environmental protection laws and occupational safety and health regulations are compelling the industry to consider a high-pressure coolant (HPC) machining process as one of the viable alternative instead of using conventional cutting fluids.

2.3   High-Pressure Coolant (HPC) Machining

Machining of alloys at high speed conditions can be achieved by a combination of the appropriate tool material, machining technique and the choice of a suitable cooling technology. High pressure coolant (HPC) assisted cooling is one of the preferred technologies, currently, under exploitation especially in the aerospace and power plant industries for machining exotic materials. The credibility of high-pressure coolant (HPC) assisted machining had been thoroughly investigated over the years [Mazurkiewicz et al. 1989; Ezugwu et al. 1990; Machado and Wallbank 1994; Kovacevic 1994; Ezugwu et al. 2005]. The system not only provides adequate cooling at the tool-workpiece interface but also provides an effective removal (flushing) of chips form the cutting area. The coolant jet under such high pressure is capable of creating a hydraulic wedge between the tool and workpiece, penetrating the interface deeply with a speed exceeding that necessary even for very high speed machining. This phenomenon also changes the chip flow condition [Kovacevic et al. 1995]. The penetration of the high-energy jet at the tool-chip interface reduces the temperature gradient and minimizes the seizure effect, offering an adequate lubrication at the tool-chip interface with a significant reduction in friction.

29

Excellent chip breakability has been reported when machining difficult-to-cut materials with high-pressure coolant supply [Wertehim et al. 1992; Crafoord et al. 1999; Nabhani 2001]. This is attributed to a coolant wedge, which forms between the chip and tool forcing the chip to bend upwards giving it a desirable up curl required for segmentation. There is a drastic reduction in the cutting forces required to remove material from the work piece with the application of high-pressure coolant jet.

Nagpal and Sharma [1973] proposed that tool-chip interface temperature initially decreases with an increase in jet pressure, up to critical pressure, above which it rise to a relatively constant value for pressures in excess of the critical pressure.

Mazurkiewicz et al. [1989] reported that a coolant applied at the cutting zone through a high-pressure jet nozzle can reduce the contact length and coefficient of friction at chip-tool interface and thus can reduce cutting forces and increase tool life to some extent. In machining ductile metals even with cutting fluid, the increase in cutting speed reduces the ductility of the work material and causes production of long continuous chips, which raises the cutting temperature further [Nedess and Hintze 1989].

Kovacevie et al. [1995] suggested that the application of high-pressure water jet through the tool rake face, friction is reduced at the tool-chip interface due to formation of a cushion layer, which prevents intimate contact at the tool-chip interface, consequently leading to bending and self-breakage of chips. Whereas in the case of high-pressure water jet through an external nozzle, tool-chip contact area is reduced due to the breakage of the chip by the impinging jet. The enhance effectiveness of the coolant/lubrication by applying the cutting fluid at high pressures in the form of a narrow jet, leads to a reduction in the quantity of the cutting fluid being used, reducing the amount of disposal which is a

primary concern of Environmental Protection Authorities.

Cozzens et al. [1995] conducted an experimental investigation on single point boring aiming to study the role of cutting fluid, tool and workpiece material, tool geometry and cutting conditions on machinability. The results indicated that the cutting fluid conditions have no significant effect on surface texture, forces and built-up edge. Since boring is a high-speed operation and lubrication is ineffective, no effect was seen on the forces. However, the cutting fluid was found to have a significant effect on surface integrity.

Ezugwu et al. [1990] Observed that coolant supply at high-pressure tends to lift up the chip after passing through the deformation zone resulting to a reduction in the tool-chip contact length/area. Chip segmentation is considerably enhanced, as the chip curl radius is reduced significantly, due to targeted maximum coolant pressure/force on to the chip which aids the chip shearing process and consequently lowering cutting forces. Coolant is one of the most influential factors affecting tool performance when machining nickel-based alloys [Ezugwu et al. 1990; Khamsehzadeh 1991]. The use of a high-pressure coolant supply when machining nickel-based (Inconel 901) superalloy with cemented carbide tools gives higher tool lives than when machining with the conventional coolant supply [Ezugwu et al. 1990]. The use of a high-pressure coolant supply results in a significant reduction in the tool-chip contact length, and hence in the contact area, which in turn decreases the compressive stress at the tool edge with little change in the cutting forces. This prevents the formation of notching, thus leading to a higher tool life.

Proper selection and application of cutting fluid generally improves tool life. At low cutting speed almost four times longer tool life is obtained by proper cutting fluid

[Satoshi et al. 1997] However, surface finish does not improve significantly. Wearing of cutting tools not only causes loss of the cutting edges or tips of the inserts but loss of the entire insert after wear of all the corners. It was reported that coolant injection offers better cutting performance in terms of surface finish, tool force and tool wear when compared to flood cooling [Alaxender et al. 1998]. The chip curl radius also depends on the coolant pressure and the flow rate. Therefore at a given power, smaller chip curl radius can be achieved at a lower coolant pressure with a high coolant flow rate [Crafoord et al. 1999]. From an environmental perspective, therefore, the significant waste is not the portion of the tool worn away by the tool-work contact, but the remaining portion of the tool that is disposed after its useful life [Arunachalam and Mannan 2000]. Cutting tools operate within a safety temperature zone with minimal tool wear when machining at the critical coolant pressure as thermal stresses are kept to a minimum, thereby prolonging tool life [Ezugwu and Bonney 2003].

Ezugwu and Bonney [2004] reported that machining Inconel-718 with coated carbide inserts under high-pressure coolant supplies improve tool life by up to 7 folds, especially at high speed conditions. Tool life tends to improve with increasing coolant pressure. There is also evidence that once a critical pressure has been reached any further increase, in coolant pressure may only result to a marginal increase in tool life. Lower cutting forces are recorded with increasing coolant supply pressure when machining Inconel-718 with SiC whisker reinforced alumina ceramic tool [Ezugwu et al. 2005]. The reduction in cutting forces observed is also partly due to the chip segmentation when machining with high-pressure coolant supplies.

Chip segmentation is another advantage of employing the high-pressure cooling technique. Because the tool contact time is shorter, the tool is less susceptible to

32

dissolution wear caused by chemical reaction with newly generated chips [Dhar[a] et al. 2006]. A more recent study of the effect of high-pressure coolant flow in turning of alloy steel with carbide tools reported a 2.5 times increase in tool life than when machining with conventional coolant flow [Dhar et al. 2007]. Studies have shown that it is possible to increase cutting speed by over 67 and 150% when machining alloy steel with carbides under high coolant pressure of 70 bar, compared to conventional coolant supply [Dhar and Kamruzzaman 2008].

2.4   Summary of the Review

A review of the literature on machinability of different commercial steels highlights the immense potential of the control of machining temperature and its detrimental effects. It is realized that the machining temperature has a critical influence on chip formation, cutting forces, tool wear and tool life. All these responses are very important in deciding the overall performance of the tool. The conventional cutting fluids are not that effective in high speed machining particularly in continuous cutting of materials likes steels. Further the conventional cutting fluids are not environment friendly. Cryogenic machining can improve the machinability index as well as provide environmental friendliness machining but cryogenic machining is costly due to high cost of liquid nitrogen. Application of minimum quantity lubricant (MQL) jet not only can reduce cutting fluid requirement but also substantial technological benefits has been observed in machining different steels by different inserts. Though MQL gives some advantages during the turning operation, it presents some limits due to the difficulty of lubricant reaching the cutting surface.

From all these investigations, it is evident that applying cutting fluid in the form

33

of a jet at higher pressure into the cutting zone is more beneficial than conventional cooling techniques. In general, low pressure the cutting fluids is not capable of penetrating deep enough into the tool-chip interface to dissipate heat as quickly as possible from the appropriate regions in the cutting zone. Further, all these investigations are limited to stationary single edge cutting tool operations. However there is a great need to improve machining performance by improving cooling methods in the case of turning, drilling and milling especially while machining difficult to machine materials.

High-pressure coolant (HPC) jet cooling is a promising technology in high speed machining, which economically addresses the current processes, environmental and health concerns. In this unique process cutting oil is impinged through a nozzle precisely at the narrow cutting zone. The success of implementing this technology across the metal removal industries is therefore depend on increased research activities providing credible data for in depth understanding of high-pressure coolant supplies at the chip-tool interface and integrity of machined components. The growing demands for high MRR, precision and effective machining of exotic materials is restrained mainly by the high cutting temperature. It is revealed from the aforesaid literature survey that the cutting temperature, which is the cause of several problems restraining productivity, quality and hence machining economy, can be substantially controlled by high-pressure coolant jet. Thorough investigation is essential to explore the potential benefits of high-pressure coolant jet machining in such cases.

34

Chapter-3

Objectives of the Present Work

3.1   Objectives of the Present Work

It is evident from the previous discussion and literature review that the cutting temperature, which is the cause of several problems restraining productivity, quality and hence machining economy, can be substantially controlled by high-pressure coolant. The growing demands for high material removal rate, precision and effective machining of exotic materials is restrained mainly by the high cutting temperature. Thorough investigation is essential to explore the potential benefits of high-pressure coolant machining in such cases. However, enough work has not been done systematically yet in this direction. The main objectives of the present work, keeping in view the overall improvement in productivity, quality and economy in machining different steels (C-60 steel, 17CrNiMo6 steel and 42CrMo4 steel), are:

a)   Experimental study on the effects of high pressure coolant on the machinability characteristics of different steels at different cutting speeds and feeds in terms of

i.   form and geometry of the chips

ii.   cutting forces i.e. main cutting force and feed force

iii. average chip-tool interface temperature

iv.   pattern and mechanism of deformation of the cutting tools

v.   extent of tool damage and tool life

vi.   surface integrity along with surface finish and

vii. product quality (dimensional deviation)

b)   Design and fabrication of a suitable nozzle for effective and efficient cooling by impinging high velocity cutting oil jet at high pressure along the rake face.

c)   Development of a predictive model for cutting temperature within the chip-tool interface from the characterization of the physical processes taking place during machining and its validation.

3.2   Outline of Methodology

The research work was mainly experimental and partly analytical in nature. Proper design of experiment was done for reasonably quantitative assessment of the role of the machining and the high-pressure coolant parameters on the technological responses. The methodology was as follows:

i.   A high-pressure coolant delivery system has been designed and fabricated for supplying coolant at high pressure from the coolant tank and impinged at high speed through the nozzle into the chip-tool interface. Considering the conditions required for the present research work and uninterrupted supply of coolant at pressure around 100 bar over a reasonably long cut, a coolant tank of capacity of 200 liter has been designed, fabricated and used. The coolant tank comprises of a motor-pump assembly, a flow control valve, a relief valve and a directional control valve. The nozzle of 0.50 mm

36

bore diameter has been fixed to the tool post and was connected with standard connecting end to supply high-pressure cutting oil in the form of thin jet at the chip-tool interface.

ii. A nozzle for application of the high-pressure coolant jet has been fabricated for controlling the spray pattern, covering area and coolant flow rate.

iii. Chip shape, chip color and chip thickness ratio under both dry and high-pressure coolant conditions have been studied and also the metallurgical study of the chips has been carried out to explore the nature of chip tool interaction.

iv. The average chip-tool interface temperatures have been monitored by tool-work thermocouple technique. A tool-work thermocouple calibration has been carried out to measure the interface temperatures.

v. Main cutting force (F_c) and feed force (F_f) under both dry and high-pressure coolant conditions have been recorded with the help of a tool dynamometer, charge amplifier and computer. Computer was used for monitoring the profile of the cutting forces during machining under both the environments.

vi. The growths of average principal flank wear, average auxiliary flank wear and maximum auxiliary flank wear have been observed under metallurgical microscope. The cutting insert has been withdrawn at regular intervals to examine the pattern and extent of wear on main and auxiliary flanks for all the trials. The average width of the principal flank wear and auxiliary flank has been measured using the metallurgical microscope.

vii. The pattern and extent of wear that developed at different surfaces of the tool tips after being used for machining the different steels over reasonably long period have been observed under scanning electron microscope (SEM) to see the actual effects of different environments on wear of the carbide inserts.

viii. The surface roughness and variation in finished diameter along the job-axis have been monitored by a Talysurf and precision dial gauge respectively to study the effects of high-pressure coolant on surface finish and dimensional deviation.

ix. An analytical model has been developed for the temperature rise in metal cutting based on pioneering work of Hahn [1951] on the moving oblique band heat source with an appropriate image source and boundary conditions for the shear plane heat source and frictional heat source at the chip-tool interface using the modified Jeager's [1942] moving band for the chip and stationary rectangular heat source for the tool solutions with non uniform distribution of heat intensity. The proposed model has been verified by experimental data of turning C-60 steel under high-pressure coolant condition.

Chapter-4

Experimental Investigations

4.1 Introduction

The high cutting temperature generated during machining not only reduces tool life but also impairs the product quality. The temperature becomes more intensive when cutting speed and feed rate are increased for higher MRR and the work materials are relatively difficult to machine for their high strength, hardenability and lesser thermal conductivity. Cutting fluids are widely used to reduce the cutting temperature. But the major problems associated with the use of conventional methods and type of cutting fluids, which are mostly oil based, are:

    i   ineffectiveness in desired cooling and lubrication

    ii.   health hazards due to generation of obnoxious gases and bacterial growth

    iii.   inconvenience due to uncleanliness of the working zone

    iv.   corrosion and contamination of the lubricating system of the machine tools

    v.   need of storage, additional floor space, pumping system, recycling and disposal

    vi.   environmental pollution and contamination of soil and water

In this regard, it has already been observed through previous research that proper application of high-pressure coolant may play vital role in providing not only environment friendliness but also some techno-economical benefits.

For achieving substantial technological and economical benefits in addition to environment friendliness, the high-pressure coolant system needs to be properly designed considering the following important factors:

i.   effective cooling by enabling high-pressure coolant jet reaches as close to the actual hot zones as possible

ii. avoidance of bulk cooling of the tool and the job, which may cause unfavorable metallurgical changes

iii. minimum consumption of coolant by pin-pointed impingement and only during chip formation

iv. control of pressure and flow rate of coolant according to need

4.2   Design and Fabrication of High-Pressure Coolant System

The cutting fluid needs to be drawn at high pressure from the coolant tank and impinged at high speed through the nozzle. Considering the conditions required for the present research work and uninterrupted supply of coolant at pressure around 100 bar over a reasonably long cut, a coolant tank of large capacity (200 liter) has been designed, fabricated and used. The photographic view of the coolant tank along with motor-pump assemble, flow control valve, relief valve and directional control valve is shown in Fig.4.1.

The coolant is contained in the coolant tank and a pump is used to ensure desired high driving pressure during the high withdrawal periods. This is accomplished by controlling relief valve through flow control valve that creates a high pressure. When the flow control valve is open, coolant taken from the tank at normal pressure is pressurized at a required pressure by controlling relief valve. A relief valve installed in the discharge line with a return line back to the supply tank is to provide complete protection against an

40

unexpected over pressure situation? The flow control valve is pressure and temperature compensating type valve and maintain a constant flow rate independent of change in system pressure (load) and temperature (viscosity of the fluid). The valve with an integral check valve allows a controlled flow and reverses free flow. The high-pressure coolant is impinged through a nozzle at the chip-tool interface. A direction control valve is used to control the flow direction of the jet during machining.
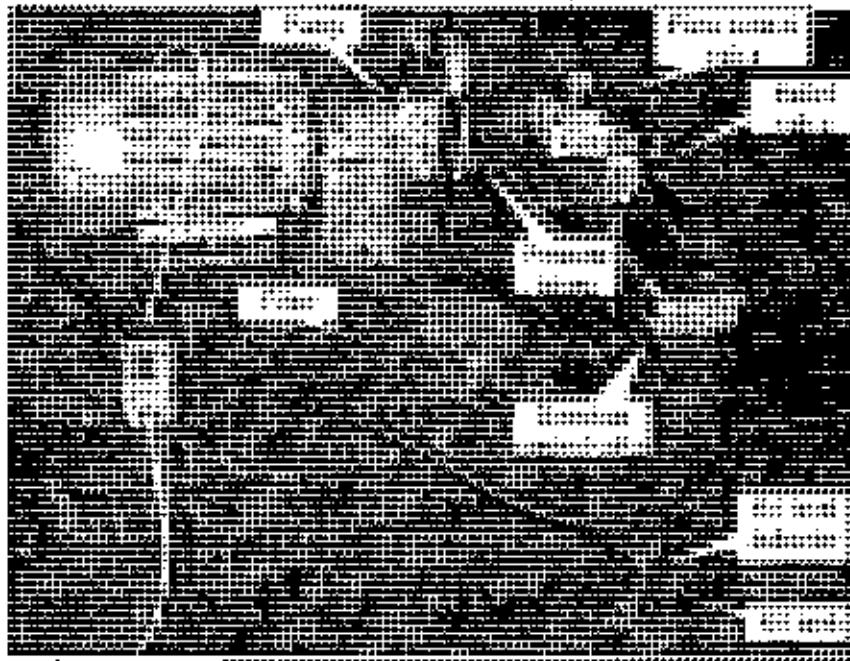
Fig. 4.1 Photographic view of high-pressure coolant system

4.3 Design and Fabrication of the Nozzle

The purpose of a nozzle is to direct cutting fluid to the optimal position to achieve maximum fluid flow at the chip-tool interface. The nozzle also fulfills the purpose of increasing the fluid velocity by contracting the cross-sectional area of the jet stream. A well designed turbulent flow nozzle converts more of the pressure energy in the flow into kinetic energy than does a laminar flow nozzle. A laminar flow nozzle however has the

benefit that the jet stream maintains its coherency for a longer period meaning that turbulent flow nozzles must be positioned as close to the chip-tool contact as possible.

The nozzle has been designed and fabricated so that the nozzle spray pattern, covering area and coolant flow rate can be controlled. The nozzle developed and used and its setting along the tool holder are schematically shown in Fig.4.2 The nozzle tip of 0.50 mm bore diameter was fixed to the tool post and is connected with direction control valve through hydraulic pipe to supply coolant in the form of jet to the cutting zone. A flow control valve is used to control the flow of coolant as required. The jet should impinge at the cutting zone in liquid state only. The expected result of this arrangement is effective cooling with economical coolant dispensing. It is important to properly position coolant delivery nozzle to achieve the following:

i. getting the fluid to the tool/workpiece interface

ii. minimizing mist and odor problems

iii. controlling thermal shock. The tool will be alternately heated and cooled, if the fluid stream does not continually reach the tool

iv. keeping the workpiece constantly in the fluid's flow and

v. moving the chips/ swarf out of the cutting zone. This is one of the most important functions of the fluid, and may require positioning one or more fluid lines just to move chips out of the cutting zone

Nozzle is placed 15.0 mm away from the tool tip to minimize the interference of the nozzle with the flowing chips and to reach quite close to the chip-tool contact zone without avoiding of bulk cooling of the tool and the job, which may cause unfavorable metallurgical changes.

42
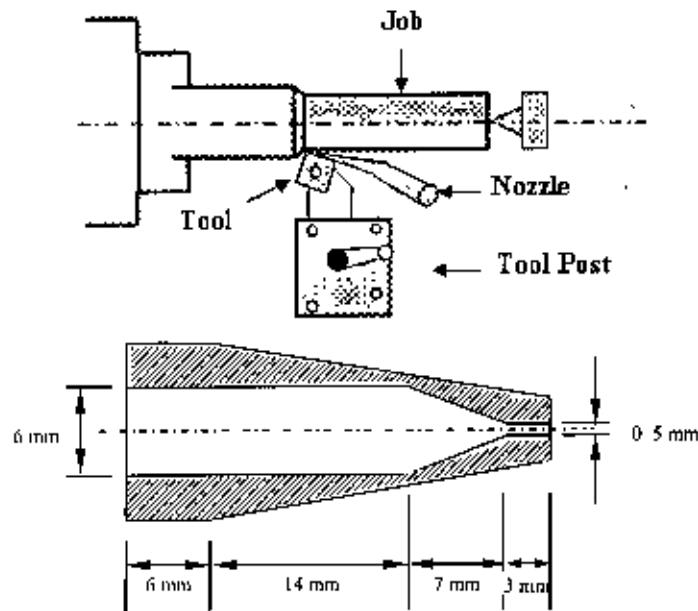
Fig. 4.2 Schematic view of the nozzle used for coolant delivery at the cutting zone

4.4   Experimental Procedure and Conditions

The concept of high-pressure coolant presents itself as a possible solution for high speed machining in achieving slow tool wear while maintaining cutting forces/power at reasonable levels, provided that the high-pressure cooling parameters can be strategically tuned. It has the benefits of a powerful stream that can reach the cutting area, it provides strong chip removal, and in some cases enough pressure to deburr. High-pressure coolant injection technique not only provided reduction in cutting forces and temperature but also reduced the consumption of cutting fluid. The aim of the present work is primarily to explore and evaluate the role of high-pressure coolant on machinability characteristics of commonly used tool-work combination mainly in terms of cutting temperature and chip-forms, which govern productivity, product quality and overall economy.

The machining tests were carried out by straight turning of three different steels (C-60 steel, 17Cr Ni Mo6 steel and 42CrMo4 steel) in a reasonably rigid and powered (10

43

hp) centre lathe (China) at different cutting speeds (V) and feed rates (f) under dry, wet (1:20 soluble oil) and high-pressure coolant environments. Keeping in view less significant role of depth of cut (d) on cutting temperature, saving of work material and avoidance of dominating effect of nose radius on cutting temperature, the depth of cut was kept fixed to only 1.0 mm and 1.5 mm, which would adequately serve the present purpose.

Effectiveness of cooling and the related benefits depend on how closely the high-pressure coolant jet can reach the chip-tool and the work-tool interfaces where, apart from the primary shear zone, heat is generated. The tool geometry is reasonably expected to play significant role on such cooling effectiveness. Keeping these view two different tool configurations (Sandvik) namely SNMG-120408 and SNMM 120408 have been undertaken for the present investigation. The inserts were clamped in a PSBNR-2525 M12 (Sandvik) type tool holder.
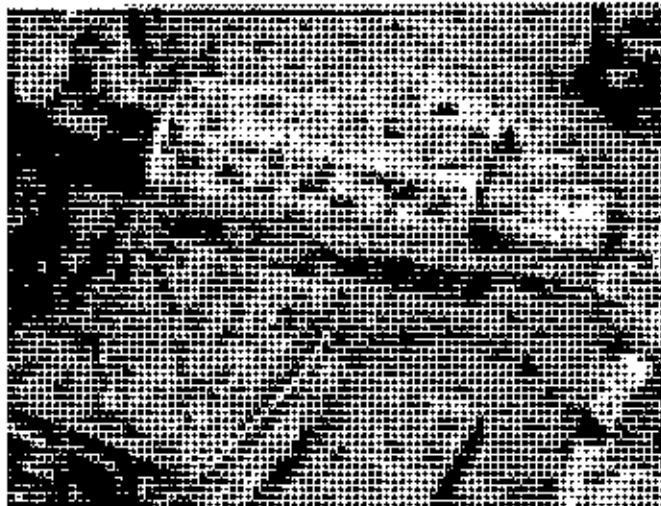
Fig. 4.3   Photographic view of high-pressure coolant delivery nozzle injecting coolant during machining

The positioning of the nozzle tip with respect to the cutting insert has been settled after a number of trials. The final arrangement made and used has been shown in Fig.4.3.

The high pressure coolant jet is directed along the auxiliary cutting edge at an angle 30° to reach at the principal flank and partially under the flowing chips through the in-built groove parallel to the cutting edges. The schematic view of the experimental setup is shown in Fig.4.4. The photographic view of the experimental set-up is shown in Fig.4.5.

1	Coolant tank	6	Pressure gauge	10 Machine tool
2	Foot valve	7	Direction control valve	11 Supply pump
3	High-pressure pump	8	Nozzle	12 Filter
4	Flow control valve	9	Dynamometer	13 Computer
5	Relief valve			
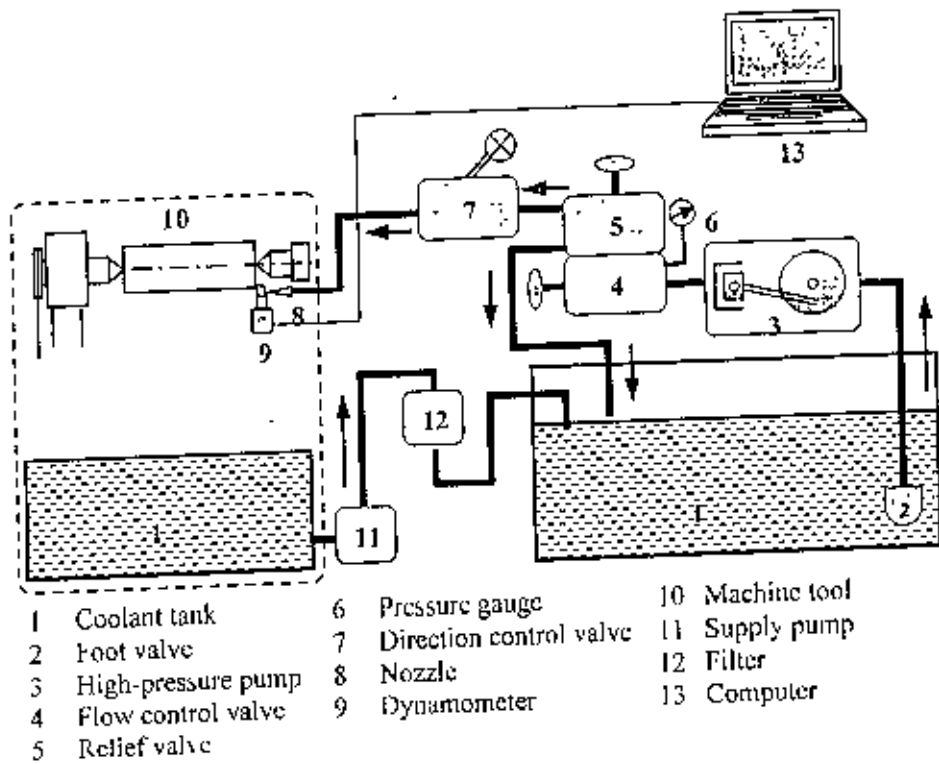
Fig. 4.4 Schematic view of the experimental set-up
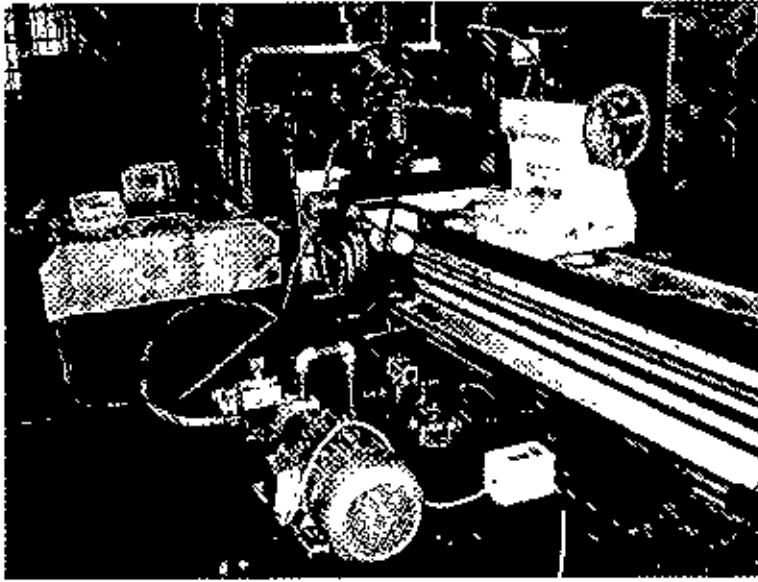
Fig. 4.5 Photographic view of experimental set-up

The ranges of cutting speed and feed rate chosen in the present investigation are representative of the current industrial practice for the tool-work material combination that has been investigated. The conditions under which the machining tests have been carried out are briefly given in Table 4.1.The machining responses have been monitored and studied using sophisticated and reliable equipments and techniques as far as possible. The machining responses studied and evaluated for assessing its machinability characteristics are presented in Table 4.2.

It has already been reported [Paul et al. 2000 and Seah et al. 1995] that use of conventional cutting fluids (wet machining) does not serve the desired purpose in machining steels by carbides, rather reduces tool life and often may cause premature failure of the insert by brittle fracture. However, one of the steels (C-60 steel) undertaken has been machined with conventional method (1:20 soluble oil) in addition to dry and high-pressure coolant (HPC) conditions to see again the relative role of wet machining under the same cutting speed, feed rate and depth of cut, particularly in respect of condition and life of the cutting inserts, surface finish and dimensional deviation.

46

Table 4.1   Experimental conditions

Machine tool	: Lathe (10 hp), China
Work materials	: • C-60 steel (Size: Ø178 X 580 mm, BHN: 195)
	• 17CrNi Mo6 steel (Size: Ø200 X520 mm, BHN: 201)
	• 42CrMo4 steel (Size: Ø220 X 520 mm, BHN: 252)
Cutting insert	: • SNMG 120408 TTS, Sandvik (ISO Specification)
	• SNMM 120408 TTS, Sandvik (ISO Specification)
Tool holder	: PSBNR 2525 M12, Sandvik
Working tool geometry	: -6°, -6°, 6°, 6°, 15°, 75°. 0. 8 mm
Process parameters	
Cutting speed, V	: 93,133, 186, 266 and 193 m/min
Feed rate, f	: 0.10, 0.14. 0.18 and 0 22 mm/rev
Depth of cut, d	: 1.0 mm and 1.50 mm
High pressure coolant (HPC)	: 80 bar, Coolant: 6.0 l/min through external nozzle
Coolant type	: VG-68 (ISO grade)
Environments	: • Dry
	• Wet and
	• High pressure coolant (HPC) condition

Table 4.2   Machining responses investigated

Investigated responses	Work materials						
	C-60 steel			17CrNiMo6 steel		42CrMo4steel	
	Dry	Wet	HPC	Dry	HPC	Dry	HPC
Thermocouple calibration	✓	×	×	✓	×	✓	×
Chips	✓	×	✓	✓	✓	✓	✓
Temperature	✓	×	✓	✓	✓	✓	✓
Cutting forces	✓	×	✓	✓	✓	✓	✓
Tool wear	✓	✓	✓	✓	✓	✓	✓
SEM views of worn out inserts	✓	✓	✓	✓	✓	✓	✓
Tool life	✓	×	✓	✓	✓	✓	✓
Machined surface roughness	✓	✓	✓	✓	✓	✓	✓
Dimensional deviation	✓	✓	✓	✓	✓	✓	✓

4.5   Tool-Work Thermocouple Calibration

Cutting temperature can be measured using direct and indirect techniques [Venkatesh 1987]. Direct methods include the use of temperature sensitive powders [Narutaki and Yamane 1979], infrared measurement [Abrao et al. 1996], the tool-work thermocouple techniques [Stephenson 1993] and embedded thermocouple techniques [Kitagawa et al. 1997] whereas indirect methods mainly include microstructural changes and microhardness changes [Wright and Trent 1973] in the tool materials due to high cutting temperature.

Tool-work thermocouple technique [Stephenson 1993] is simple but quite reliable for measurement of average cutting temperature in machining with continuous chip formation like plain turning. But proper functioning of this technique need care about;

i.   parasitic emf generation by secondary junction

ii.   proper calibration

iii. electrical insulation of the tool and the job

Fig.4.6 shows the calibration technique employed for the tool-work thermocouple used in the present investigation. The thermocouple junction was constructed using a long continuous chip of the concerned work material and a tungsten carbide insert to be used in actual cutting. To avoid generation of parasitic emf, a long carbide rod was used to extend the insert. A graphite block embedded with an electrically heated porcelain tube served as the heat sink. A chromel-alumel thermocouple was used as a reference in the vicinity of the tool-work thermocouple for measuring the temperature of the graphite block. The junction temperature measured by the reference thermocouple was recorded using a digital

temperature readout meter (Eurotherm, UK) while the emf generated by the tool-work thermocouple was recorded by a digital multimeter (Rish Multi, India).
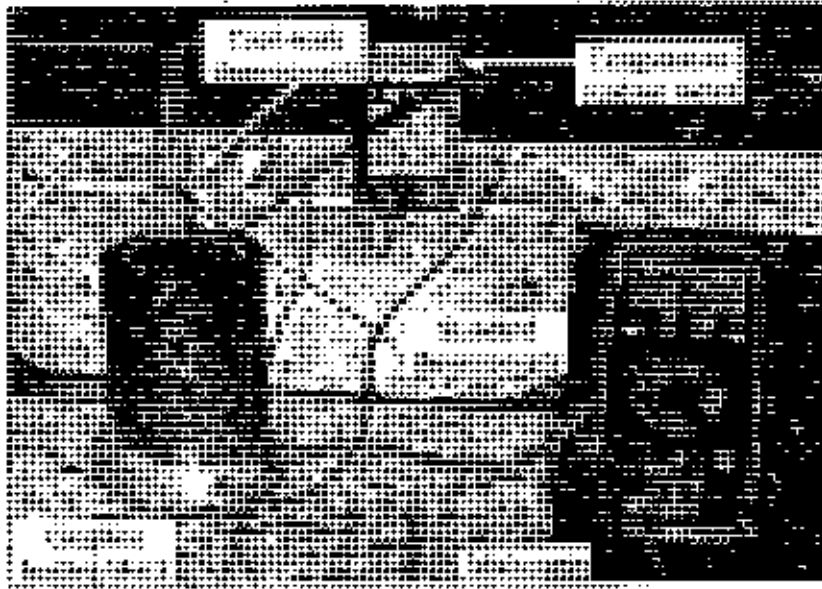
Fig.4.6 Tool-work thermocouple calibration set up

Fig.4.7 shows the calibration curves obtained for the tool-work pair with tungsten carbide (P30 Grade, Sandvik) as the tool material and the different steels undertaken as the work materials. In the present case, almost linear relationships between the temperature and emf have been obtained with correlation coefficients of 0.994. In the present work the average cutting temperature has been measured by tool-work thermocouple technique as indicated in Fig.4.8 taking care of the aforesaid factors.
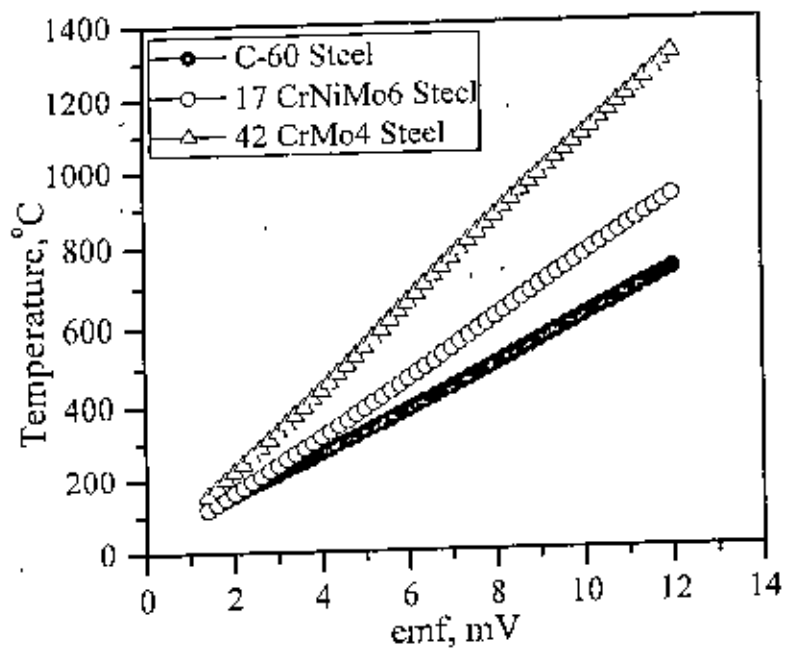
Fig.4.7 Tool-work thermocouple calibration curve
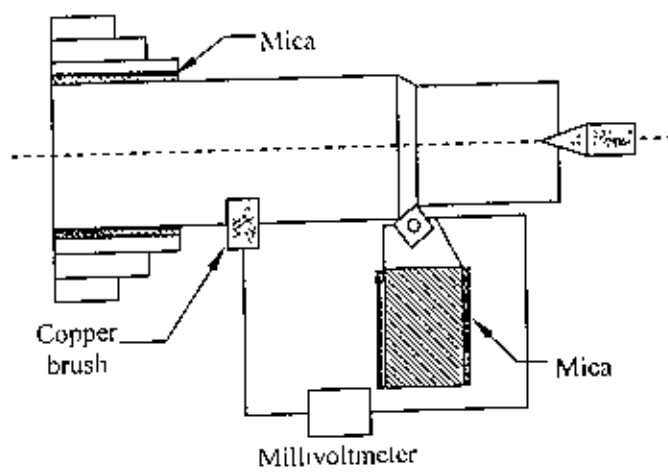
Fig.4.8 Schematic view of the tool-work thermocouple loop

4.6   Experimental Results

4.6.1   Chip Formation

An important machinability index is chip thickness ratio, r_c (ratio of chip thickness before and after cut). For given tool geometry and cutting conditions, the value of chip thickness ratio depends upon the nature of chip-tool interaction. chip contact length, curl radius and form of the chips all of which expected to be influenced by high-pressure coolant in addition to the level of cutting speeds and feed rates. The thickness of the chips was repeatedly measured by a slide caliper to determine the value of chip thickness ratio (ratio of chip thickness before and after cut). The schematic view of the formation of chip is shown in Fig.4.9.
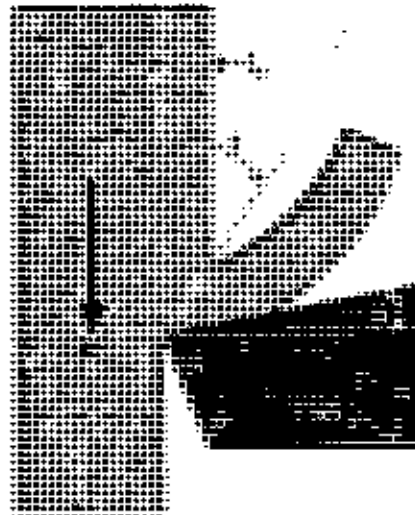
Fig.4.9 Schematic view of the formation of chip

The variation in value of chip thickness ratio with change in tool configuration, cutting speeds and feed rates as well as machining environment evaluated for C-60 steel have been plotted and shown in Fig.4.10. Similar results for other two steels undertaken have been shown in Fig.4.11 and Fig.4.12.

51
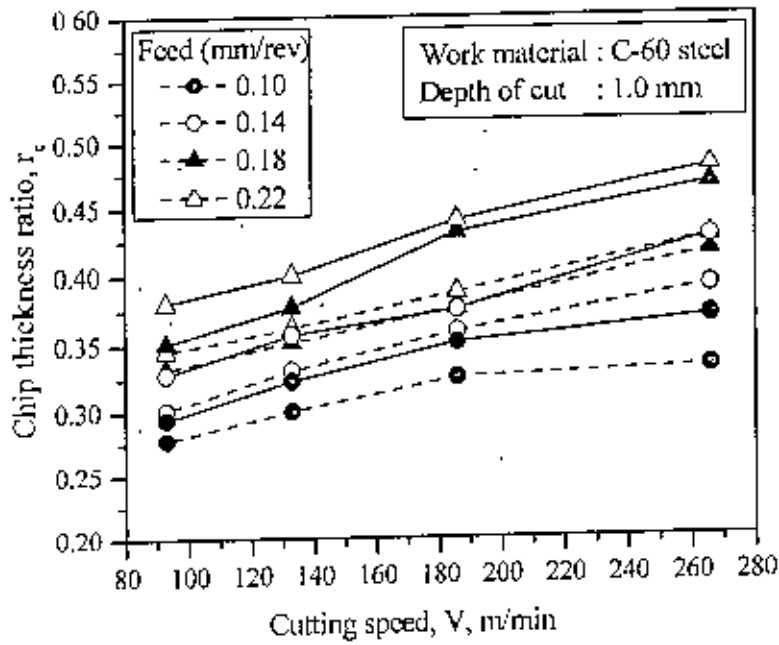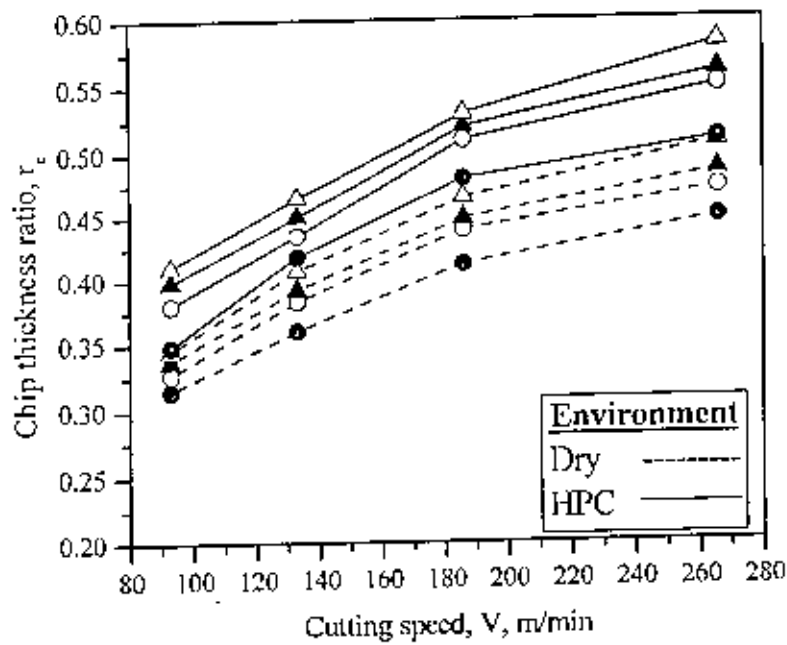
(a) SNMG insert

(b) SNMM insert

Fig.4.10 Variation in chip thickness ratio (r_c) with that of V and f in turning C-60 steel by (a) SNMG and (b) SNMM inserts under Dry and HPC conditions

52
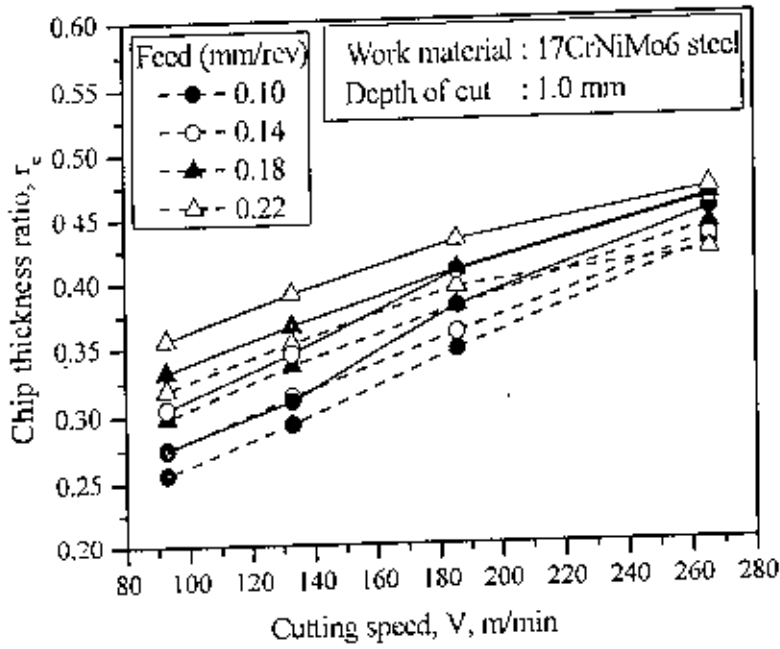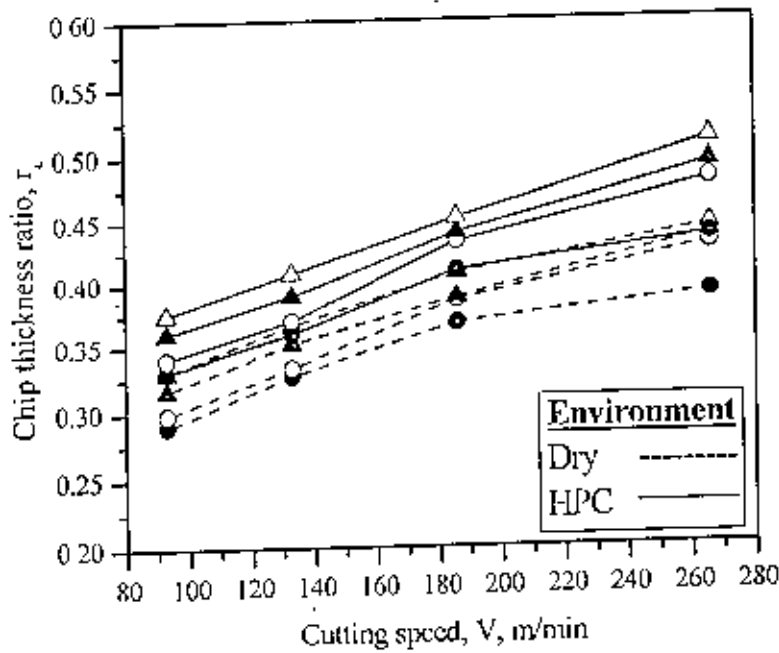
(a) SNMG insert

(b) SNMM insert

Fig.4.11 Variation in chip thickness ratio (r_c) with that of V and f in turning 17CrNiMo6 steel by (a) SNMG and (b) SNMM inserts under Dry and HPC conditions
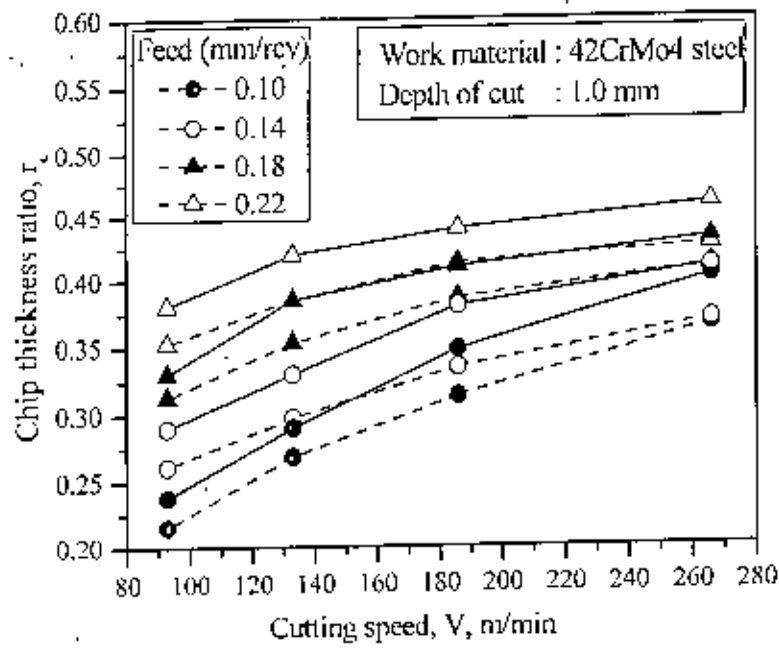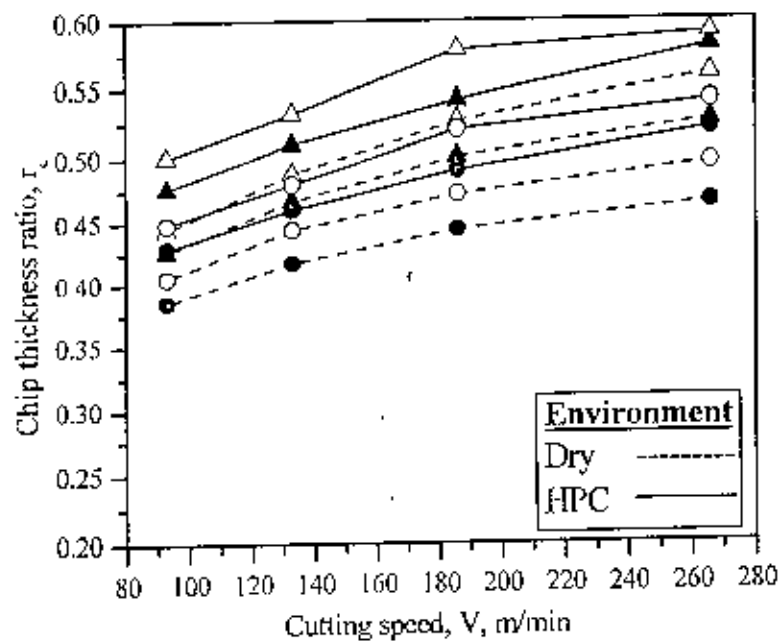
Fig.4.12 Variation in chip thickness ratio (r_c) with that of V and f in turning 42CrMo4 steel by (a) SNMG and (b) SNMM inserts under **Dry** and **HPC** conditions

The machining chips were collected during all the treatments for studying their shape, colour and nature of interaction with the cutting insert at its rake surface. Chips have been visually examined and categorised with respect to their shape and colour. Chip shape and colour for different steels are incorporated in Table 4.3, Table 4.4 and Table 4.5.

Table 4.3   Shape and color of chips produced during turning C-60 steel by SNMG and SNMM inserts under both Dry and HPC conditions

f (mm/rev)	V (m/min)	SNMG 120408				SNMM 120408			
		Dry		HPC		Dry		HPC	
		Shape	Color	Shape	Color	Shape	Color	Shape	Color
0.10	93	■	blue	■	metallic	●	blue	○	metallic
	133	■	blue	■	metallic	●	blue	▲	metallic
	186	■	blue	■	metallic	●	blue	○	metallic
	266	■	blue	■	metallic	▲	blue	●	metallic
0.14	93	■	blue	■	metallic	○	blue	■	metallic
	133	■	blue	■	metallic	●	blue	■	metallic
	186	■	blue	■	metallic	●	blue	■	metallic
	266	■	blue	■	metallic	●	blue	■	metallic
0.18	93	■	blue	■	metallic	◙	blue	■	metallic
	133	■	blue	■	metallic	■	blue	■	metallic
	186	■	blue	■	metallic	■	blue	■	metallic
	266	■	blue	■	metallic	■	blue	■	metallic
0.22	93	■	blue	■	metallic	◙	blue	■	metallic
	133	■	blue	■	metallic	■	blue	■	metallic
	186	■	blue	■	metallic	■	blue	■	metallic
	266	■	blue	■	metallic	■	blue	■	metallic

Chip shape	Loose arc	■	Snarled ribbon	●	Snarled tubular	◙
	Short washer	□	Long washer	○	Long ribbon	▲

55

Table 4.4 Shape and color of chips produced during turning 17CrNiMo6 steel by SNMG and SNMM inserts under both **Dry** and **HPC** conditions

f (mm/rev)	V (m/min)	SNMG 120408				SNMM 120408			
		Dry		HPC		Dry		HPC	
		Shape	Color	Shape	Color	Shape	Color	Shape	Color
0.10	93	◙	blue	■	metallic	●	blue	○	metallic
	133	◙	blue	■	metallic	■	blue	■	metallic
	186	○	blue	●	metallic	●	blue	■	metallic
	266	●	blue	■	metallic	●	blue	■	metallic
0.14	93	◙	blue	▫	metallic	▫	blue	■	metallic
	133	◙	blue	■	metallic	■	blue	▫	metallic
	186	■	blue	■	metallic	▪	blue	■	metallic
	266	■	blue	■	metallic	■	blue	▪	metallic
0.18	93	○	blue	■	metallic	■	blue	▪	metallic
	133	■	blue	■	metallic	■	blue	■	metallic
	186	■	blue	■	metallic	▪	blue	■	metallic
	266	■	blue	■	metallic	▪	blue	■	metallic
0.22	93	■	blue	■	metallic	○	blue	▪	metallic
	133	■	blue	■	metallic	■	blue	■	metallic
	186	▫	blue	■	metallic	■	blue	■	metallic
	266	■	blue	▪	metallic	▫	blue	■	metallic
Chip shape		Loose arc	.	▪	Snarled ribbon		●	Snarled tubular	◙
		Short washer		▫	Long washer		○	Long ribbon	▲

56

Table 4.5 Shape and color of chips produced during turning 42CrMo4 steel by SNMG and SNMM inserts under both Dry and HPC conditions

f (mm/rev)	V (m/min)	SNMG 120408				SNMM 120408			
		Dry		HPC		Dry		HPC	
		Shape	Color	Shape	Color	Shape	Color	Shape	Color
0.10	93	■	blue	■	metallic	●	blue	■	metallic
	133	●	blue	■	metallic	●	blue	▲	metallic
	186	●	blue	■	golden	●	blue	▲	metallic
	266	●	blue	■	golden	○	blue	◙	golden
0.14	93	■	blue	■	golden	●	blue	▲	metallic
	133	■	blue	■	metallic	●	blue	▲	metallic
	186	■	blue	●	golden	●	blue	●	metallic
	266	■	blue	■	golden	■	blue	●	golden
0.18	93	■	blue	■	golden	●	blue	●	metallic
	133	■	blue	■	metallic	●	blue	□	metallic
	186	■	blue	■	golden	●	blue	▲	metallic
	266	■	blue	■	golden	○	blue	□	golden
0.22	93	■	blue	■	golden	■	blue	▲	metallic
	133	■	blue	■	metallic	○	blue	■	metallic
	186	■	blue	■	golden	○	blue	○	metallic
	266	■	blue	■	golden	■	blue	■	golden
Chip shape		Loose arc		■	Snarled ribbon		●	Snarled tubular	◙
		Short washer		□	Long washer		○	Long ribbon	▲

The actual form and color of the chips produced by the different steels during machining steels by the SNMG and SNMM type inserts at different V–f combinations under both dry and high-pressure coolant conditions are shown in Fig.4.13, Fig.4.14, Fig.4.15, Fig.4.16, Fig.4.17 and Fig.4.18 respectively.

Cutting speed, V (m/min)	Feed rates, f (mm/rev)							
	0.10		0.14		0.18		0.22	
	Environment							
	Dry	HPC	Dry	HPC	Dry	HPC	Dry	HPC
93								
133								
186								
266								

Fig.4.13 Shape and color of chip during turning of C-60 steel by SNMG insert under Dry and HPC conditions [8.1 mega pixel]

Cutting speed, V (m/min)	Feed rates, f (mm/rev)							
	0.10		0.14		0.18		0.22	
	Environment							
	Dry	HPC	Dry	HPC	Dry	HPC	Dry	HPC
93								
133								
186								
266								

Fig.4.14 Shape and color of chip during turning of C-60 steel by SNMM insert under Dry and HPC conditions [8.1 mega pixel]

Cutting speed, V (m/min)	Feed rates, f (mm/rev)							
	0.10		0.14		0.18		0.22	
	Environment							
	Dry	HPC	Dry	HPC	Dry	HPC	Dry	HPC
93								
133								
186								
266								

Fig.4.15 Shape and color of chip during turning of 17CrNiMo6 steel by SNMG insert under Dry and HPC conditions [8.1 mega pixel]

Cutting speed, V (m/min)	Feed rates, f (mm/rev)							
	0.10		0.14		0.18		0.22	
	Environment							
	Dry	HPC	Dry	HPC	Dry	HPC	Dry	HPC
93								
133								
186								
266								

Fig.4.16 Shape and color of chip during turning of 17CrNiMo6 steel by SNMM insert under Dry and HPC conditions [8.1 mega pixel]

Cutting speed, V (m/min)	Feed rates, f (mm/rev)							
	0.10		0.14		0.18		0.22	
	Environment							
	Dry	HPC	Dry	HPC	Dry	HPC	Dry	HPC
93								
133								
186								
266								

Fig.4.17 Shape and color of chip during turning of 42CrMo4 steel by SNMG insert under Dry and HPC conditions [8.1 mega pixel]

Cutting speed, V (m/min)	Feed rates, f (mm/rev)							
	0.10		0.14		0.18		0.22	
	Environment							
	Dry	HPC	Dry	HPC	Dry	HPC	Dry	HPC
93								
133								
186								
266								

Fig.4.18 Shape and color of chip during turning of 42CrMo4 steel by SNMM insert under Dry and HPC conditions [8.1 mega pixel]

4.6.2   Cutting Temperature

High production machining associated with high speed and feed rate inherently generate high heat as well as high cutting zone temperature. The cutting temperature if not controlled properly, cutting tools undergo severe flank wear and notch wear, loose sharpness of the cutting edge either wearing or become blunt by welded built-up edge and weaken the product quality. In normal cutting condition all such heat sources produce maximum temperature at the chip-tool interface, which substantially influence the chip formation mode; cutting forces, tool life and product quality. High production machining needs to increase the process parameters further for meeting up the growing demand and cost competitiveness. Cutting temperature is increased with the increase in process parameter as well as with the increase in hardness and strength of the work material. Therefore, attempts are made to reduce this detrimental cutting temperature

The average cutting temperature was measured under all the machining conditions undertaken by simple but reliable tool-work thermocouple technique with proper calibration. The evaluated role of high-pressure coolant on average chip-tool interface temperature in turning three different steels by two types of inserts at different V–f combinations in compare to dry condition have been shown in Fig.4.19, Fig.4.20 and Fig.4.21

61
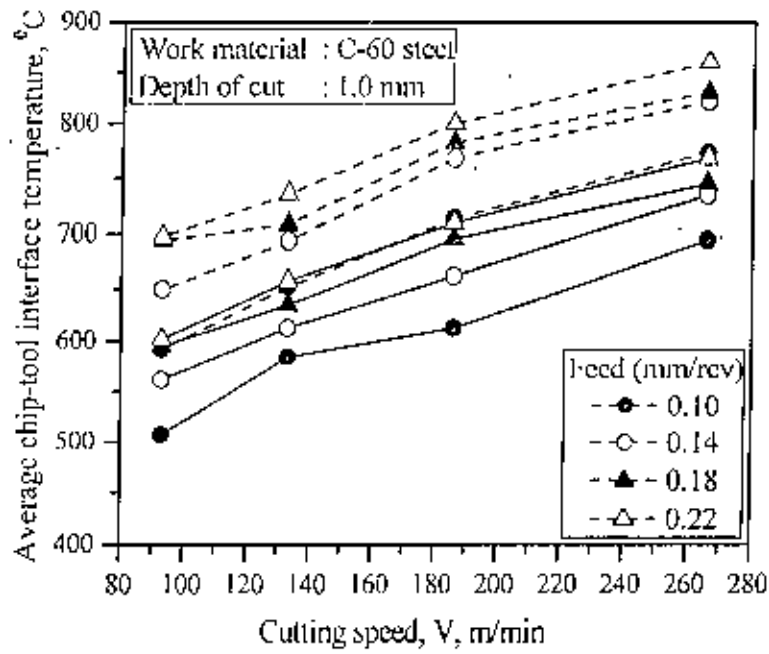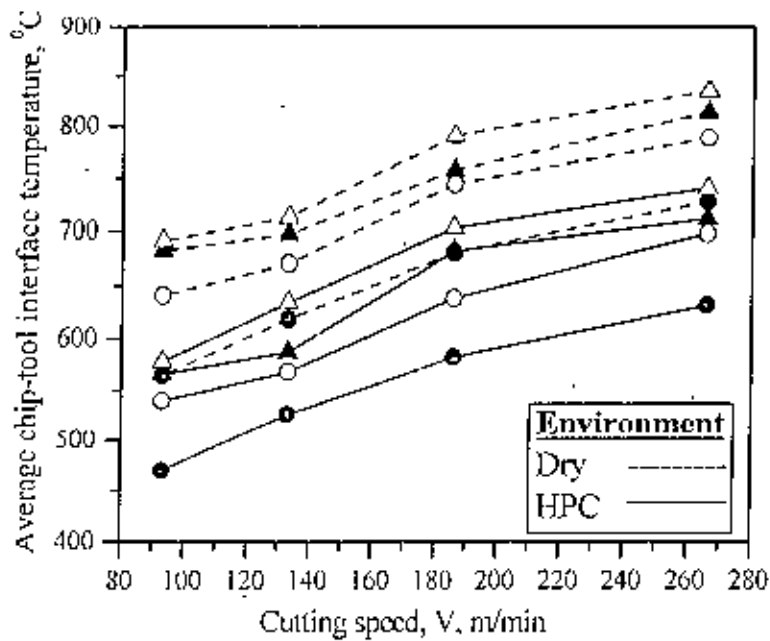
(a) SNMG insert

(b) SNMM insert

Fig.4.19 Variation in temperature (θ) with that of V and f in turning C-60 steel by (a) SNMG and (b) SNMM inserts under Dry and HPC conditions
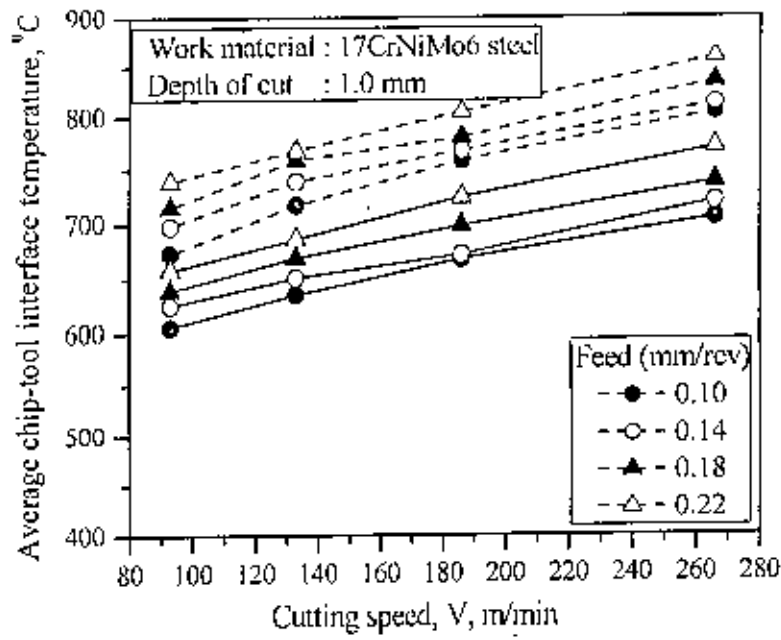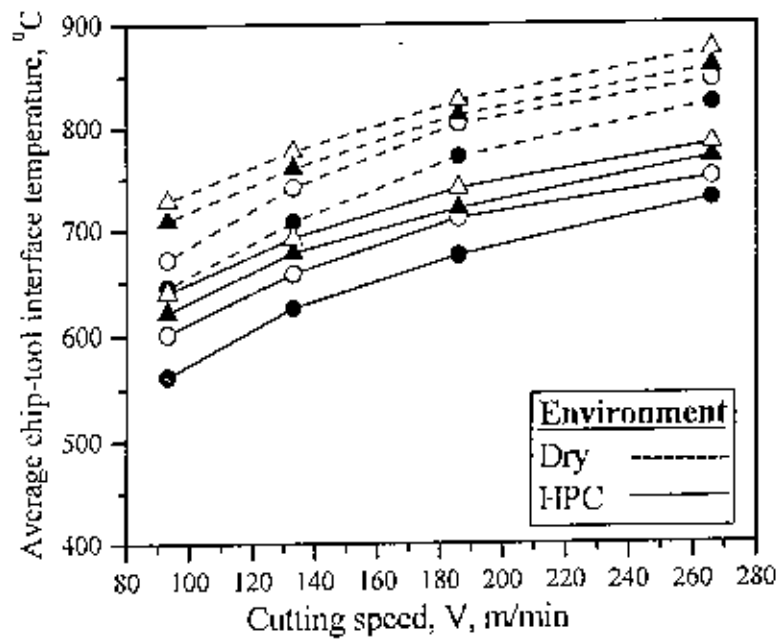
(a) SNMG insert

(b) SNMM insert

Fig.4.20 Variation in temperature (θ) with that of V and f in turning 17CrNiMo6 steel
by (a) SNMG and (b) SNMM inserts under Dry and HPC conditions
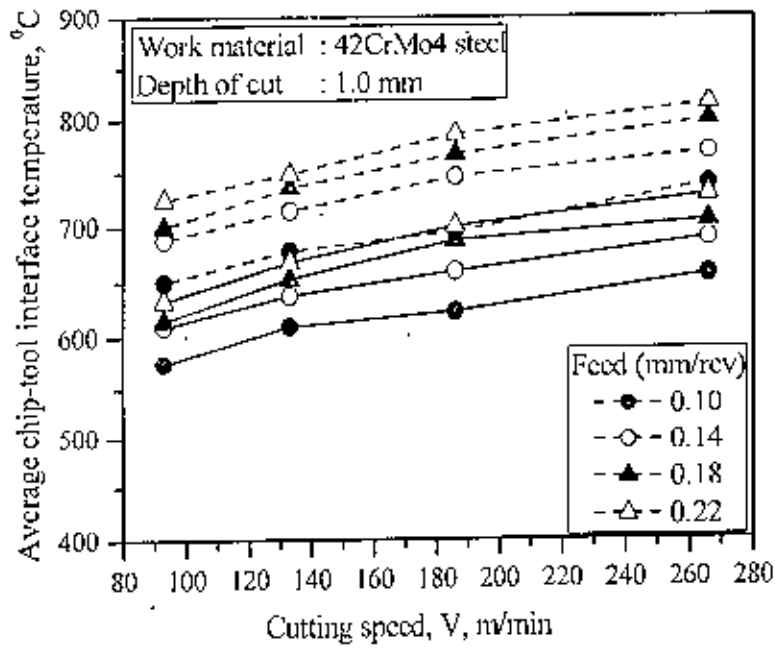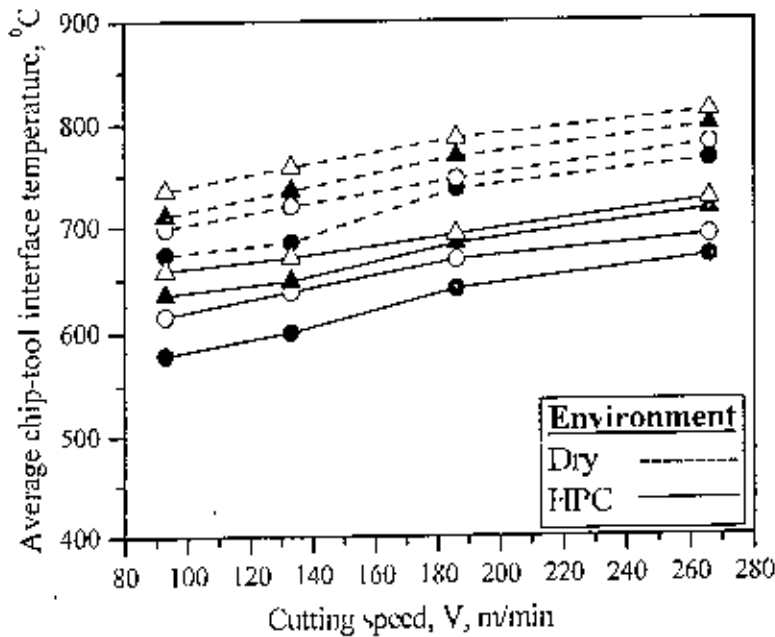
(a) SNMG insert

(b) SNMM insert

Fig.4.21 Variation in temperature (θ) with that of V and f in turning 42CrMo4 steel by (a) SNMG and (b) SNMM inserts under Dry and HPC conditions

4.6.3 Cutting Forces

Cutting forces are generally resolved into components in mutual perpendicular directions for convenience of measurement, analysis, estimation of power consumption and for the design of Machine-Fixture-Tool-Work systems. In turning by single point tools like inserts, the single cutting force generated is resolved into three components namely, tangential force or main cutting force, F_c, feed force, F_f and transverse force, F_t. Each of those interrelated forces has got specific significance.

In the present work, the magnitude of F_c and F_f have been monitored by dynamometer (Kistler) for all the combinations of steel specimen, tool configuration, cutting speeds, feed rates and environments undertaken. The effect of high-pressure coolant on F_c that have been observed while turning C-60 steel specimen by the carbide inserts, (a) SNMG and (b) SNMM under different V and f have been graphically shown in Fig. 4.22. The similar results obtained while machining 17CrNiMo6 steel and 42CrMo4 steel are shown in Fig. 4.23 and Fig. 4.24 respectively.
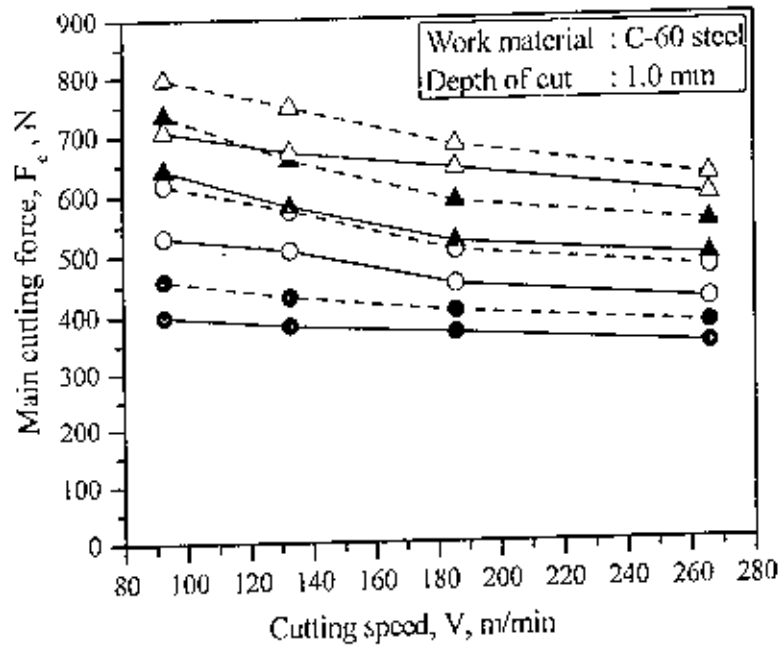
(a) SNMG insert
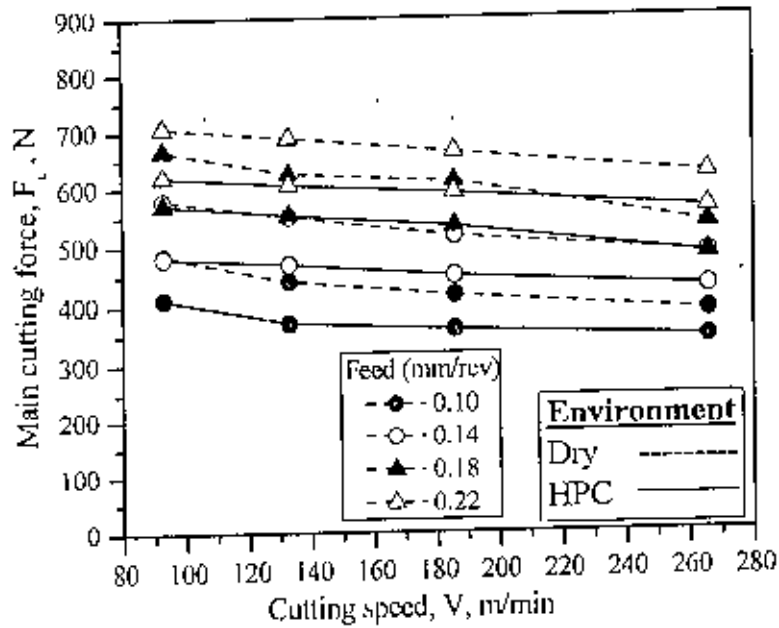
(b) SNMM insert

Fig 4.22 Variation in main cutting force (F_c) with that of V and f in turning C-60 steel by (a) SNMG and (b) SNMM inserts under Dry and HPC conditions

66
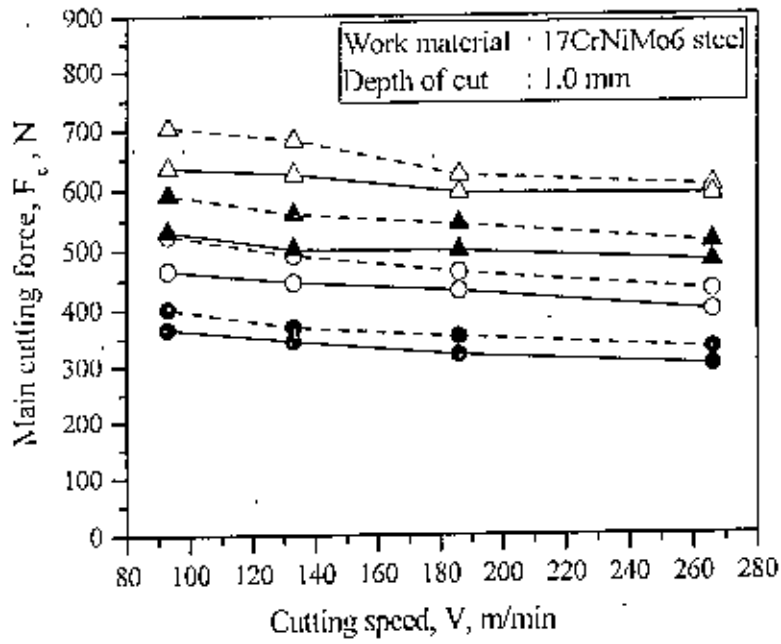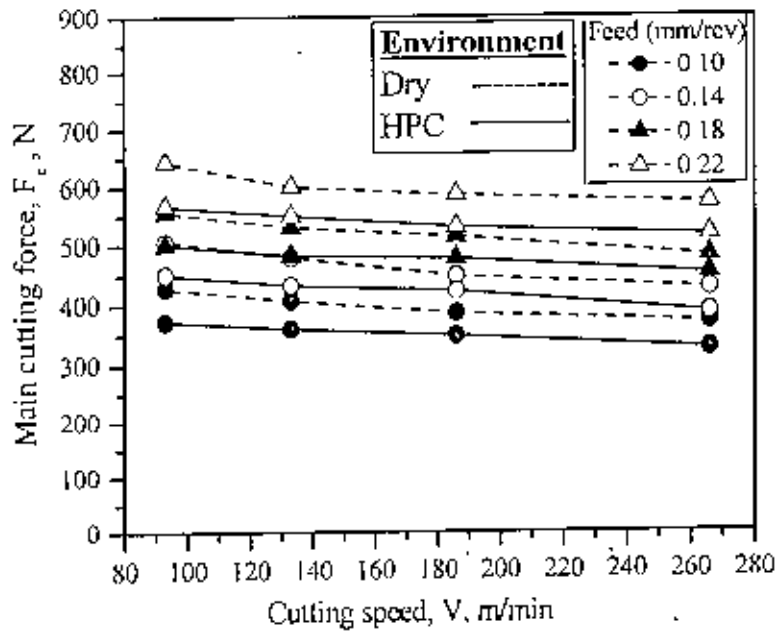
(a) SNMG insert

(b) SNMM insert

Fig.4.23 Variation in main cutting force (F_c) with that of V and f in turning 17CrNiMo6 steel by (a) **SNMG** and (b) **SNMM** inserts under **Dry** and **HPC** conditions
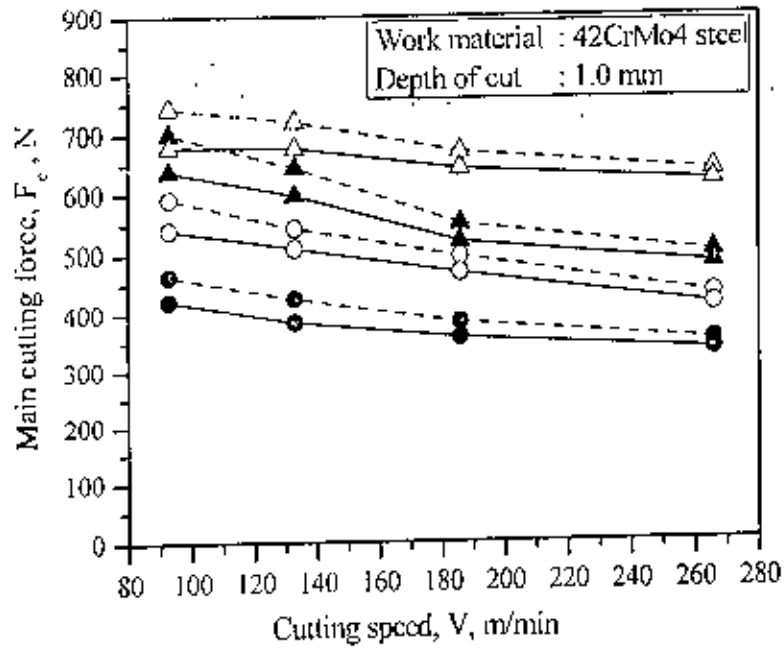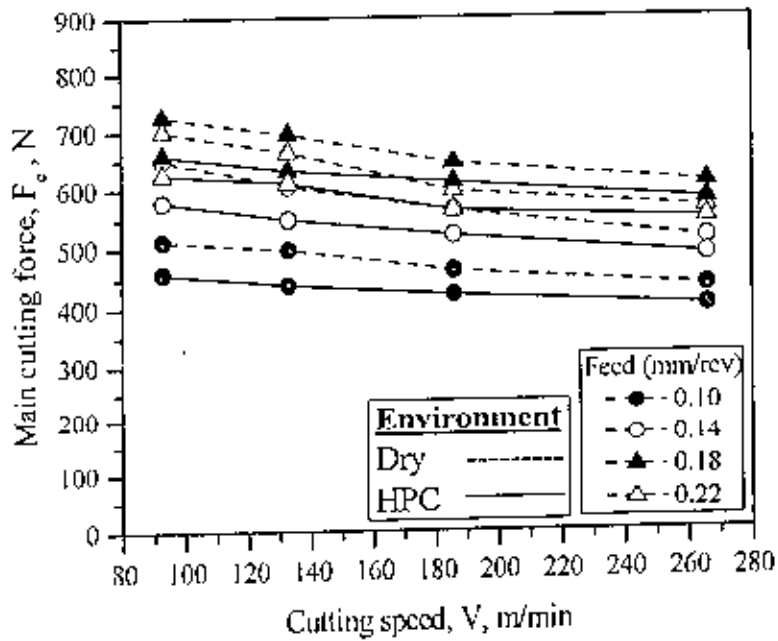
(a) SNMG insert

(b) SNMM insert

Fig.4.24 Variation in main cutting force (F_c) with that of V and f in turning 42CrMo4 steel by (a) SNMG and (b) SNMM inserts under Dry and HPC conditions

The effects of high pressure coolant on feed force, Ft, recorded for the three different steels under different machining conditions have been shown in Fig.4.25, Fig.4.26 and Fig. 4.27.
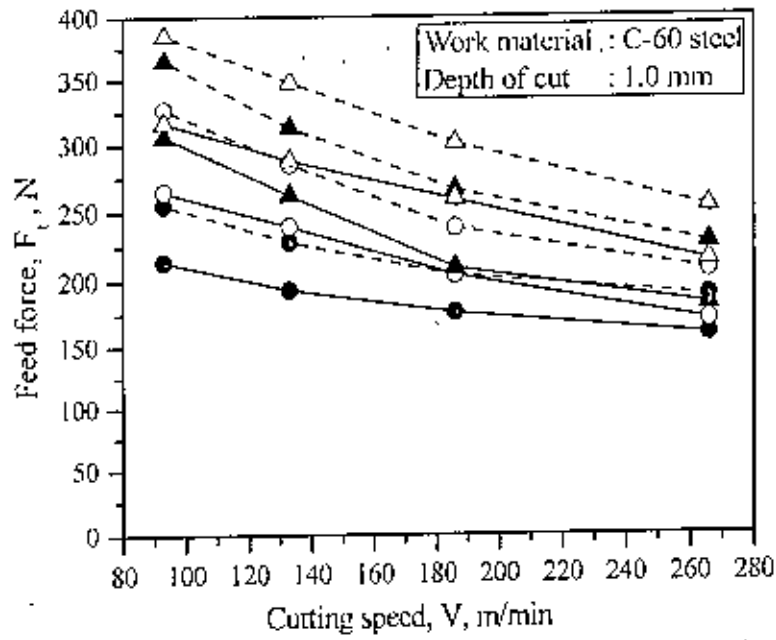
(a) SNMG insert
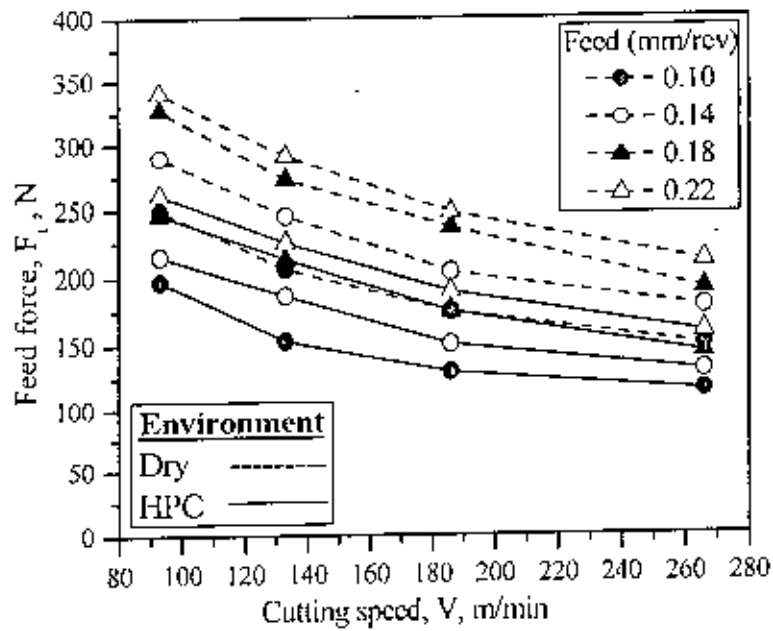
(b) SNMM insert

Fig 4.25 Variation in feed force (F_t) with that of V and f in turning C-60 steel by (a)SNMG and (b) SNMM inserts under Dry and HPC conditions
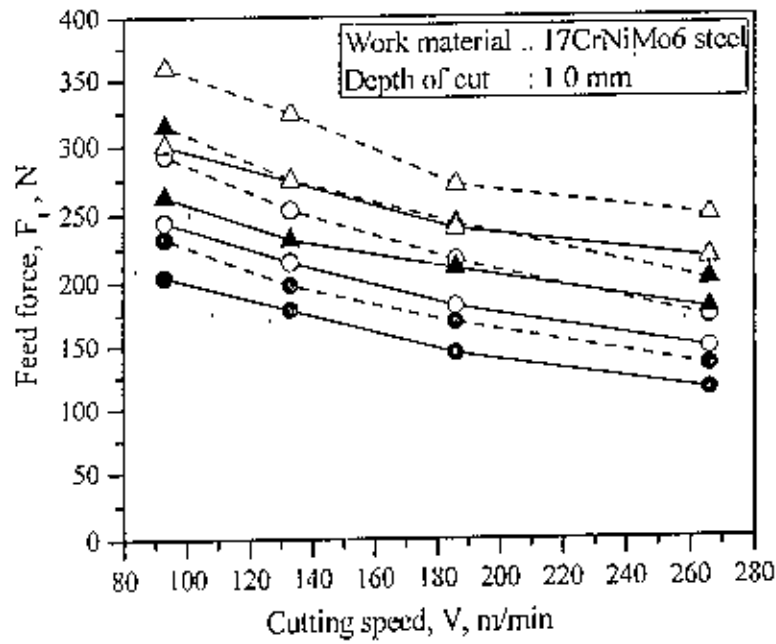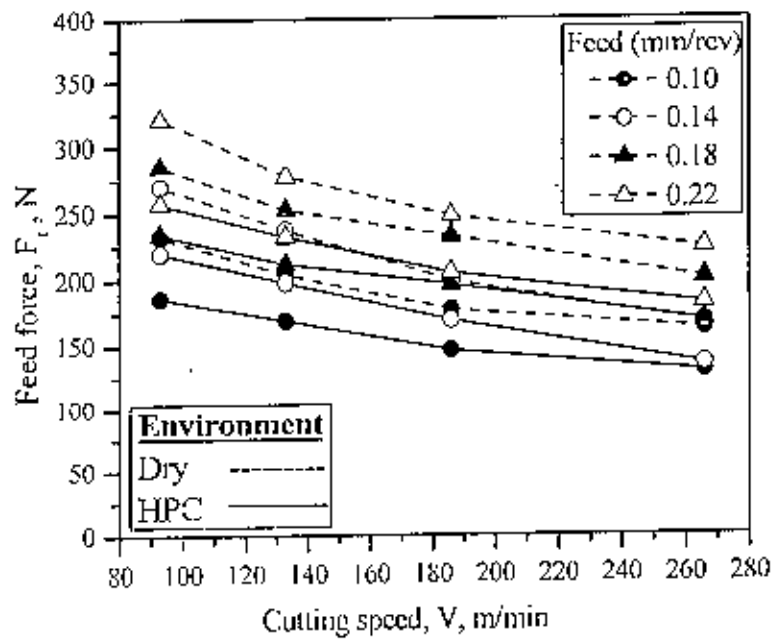
(a) SNMG insert

(b) SNMM insert

Fig.4.26 Variation in feed force (F_t) with that of V and f in turning 17CrNiMo6 steel by (a) SNMG and (b) SNMM inserts under **Dry** and **HPC** conditions
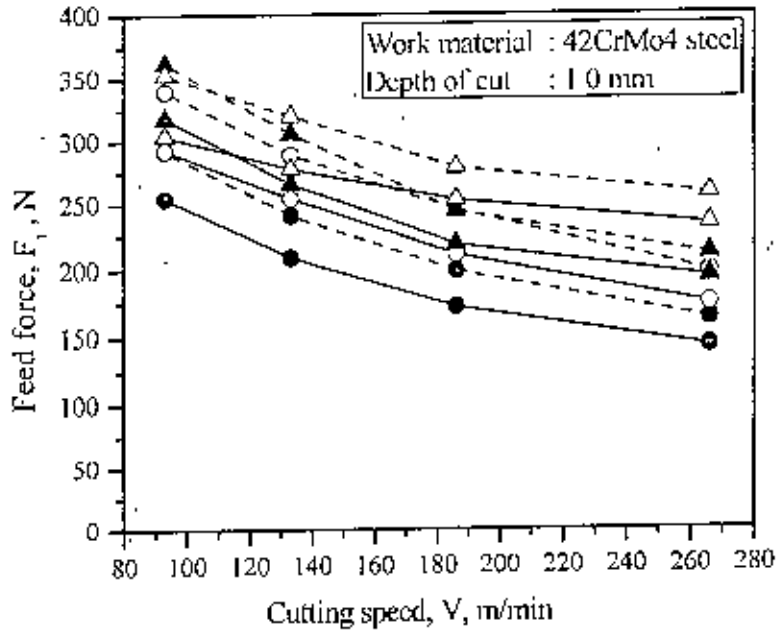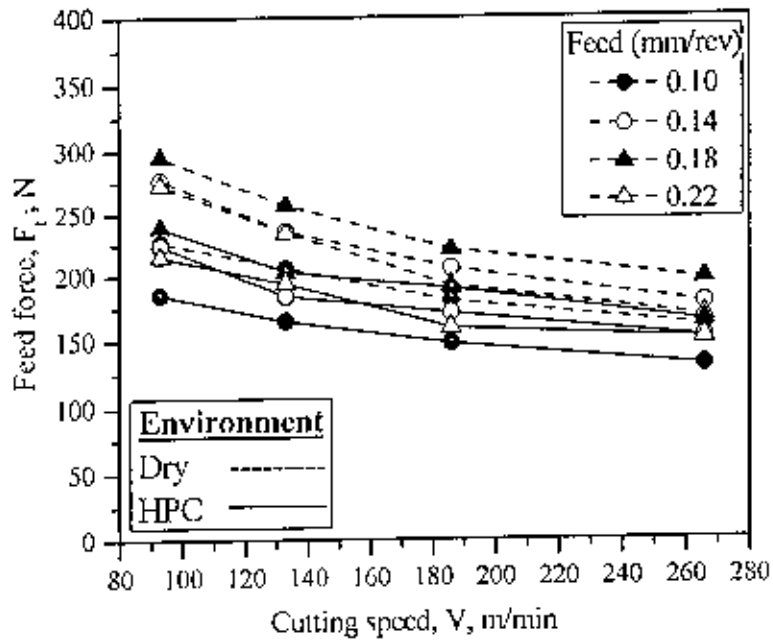
(a) SNMG insert

(b) SNMM insert

Fig 4.27 Variation in feed force (F_i) with that of V and f in turning **42CrMo4 steel** by (a)
SNMG and (b) **SNMM** inserts under **Dry** and **HPC** conditions

4.6.4 Tool Wear

The cutting tool in conventional machining. particular in continuous chip formation process like turning. generally fails by gradual wear by abrasion, adhesion. diffusion. chemical erosion, galvanic action etc. depending upon the tool-work material and machining condition. Tool wear initially starts with a relatively faster rate due to what is called break-in wear caused by attrition and microchipping at the sharp cutting edges.

Cutting tools also often fail prematurely, randomly and catastrophically by mechanical breakage and plastic deformation under adverse machining conditions caused by intensive pressure and temperature and/or dynamic loading at the tool tips particularly if the tool material lacks strength, hot hardness and fracture toughness However, in the present investigations with the tools and work materials and the machining conditions undertaken, the tool failure mode has been mostly gradual wear. The geometrical pattern of tool wear that is generally observed in turning by carbide inserts is schematically shown in Fig.4.28. The major features that characterize flank wear and crater wear are also indicated in the figure.

VB= Average flank wear
VN= Notch wear
VM= Maximum flank wear
VS= Average auxiliary flank wear
VSN= Maximum auxiliary flank wear
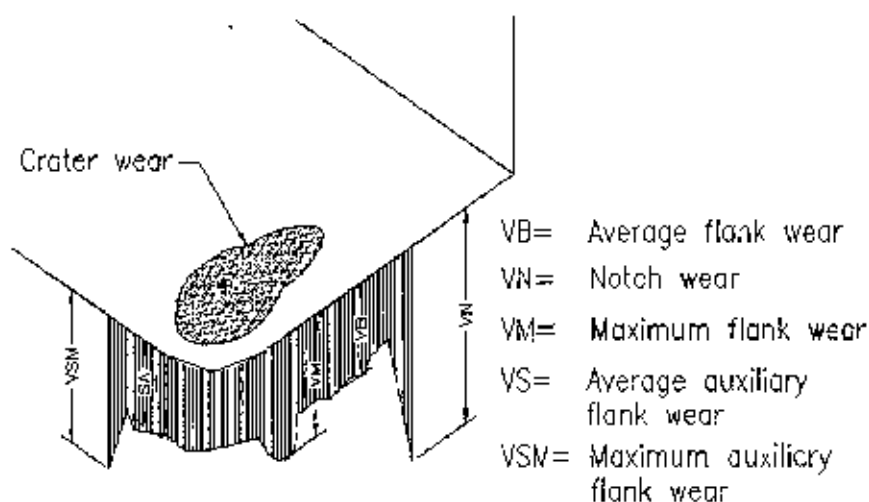
Fig. 4.28 Schematic view of general pattern of wear

Again, the life of the tools, which ultimately fail by systematic gradual wear, is generally assessed at least for R&D work, by the average value of the principal flank wear (*VB*), which aggravates cutting forces and temperature and may induce vibration with progress of machining. The pattern and extent of wear (*VS*) of the auxiliary flank affects surface finish and dimensional accuracy of the machined parts. Growth of tool wear is sizeably influenced by the temperature and nature of interactions of the tool-work interfaces, which again depend upon the machining conditions for given tool-work pairs.

However, tool rejection criteria for finishing operation were employed in this investigation. The values established in accordance with ISO Standard 3685 for tool life testing. A cutting tool was rejected and further machining stopped based on one or a combination of rejection criteria [**Ezugwu et al. 2005**]:

i.	Average Flank Wear	≥	0.3 mm
ii.	Maximum Flank Wear	≥	0.4 mm
iii.	Nose Wear	≥	0.3 mm
iv.	Notching at the depth of cut line	≥	0.6 mm
v.	Average surface roughness value	≥	1.6 µm
vi.	Excessive chipping (flanking) or catastrophic fracture of cutting edge.		

Therefore, attempts should be made to reduce the rate of growth of flank wear (*VB*) in all possible ways without much sacrifice in MRR.

During machining under each condition, the cutting insert was withdrawn at regular intervals and then the salient features like. *VB*, *VS* etc. were measured under metallurgical microscope (Carl Zesis, Germany) fitted with micrometer of least count 1µm.

It has already been mentioned that C-60 steel has been machined also under wet condition in addition to dry and high pressure cooling conditions to see again [Dhar et al. 2001] the actual effect of such conventional cutting fluid application on condition and performance of carbide tools in continuous machining of steel. The growth of average flank wear, VB with machining time observed while turning C-60 steel by the two different types of inserts at moderately high cutting speed, feed and depth of cut under dry, wet and high-pressure coolant environment have been shown in Fig. 4.29.

The growth of principal flank wear, VB with progress of machining recorded while turning the other two steels undertaken, by SNMG and SNMM type inserts at the same cutting speed, feed rate and depth of cut under dry and high-pressure coolant conditions have been shown in Fig. 4.30 and Fig. 4.31 respectively.
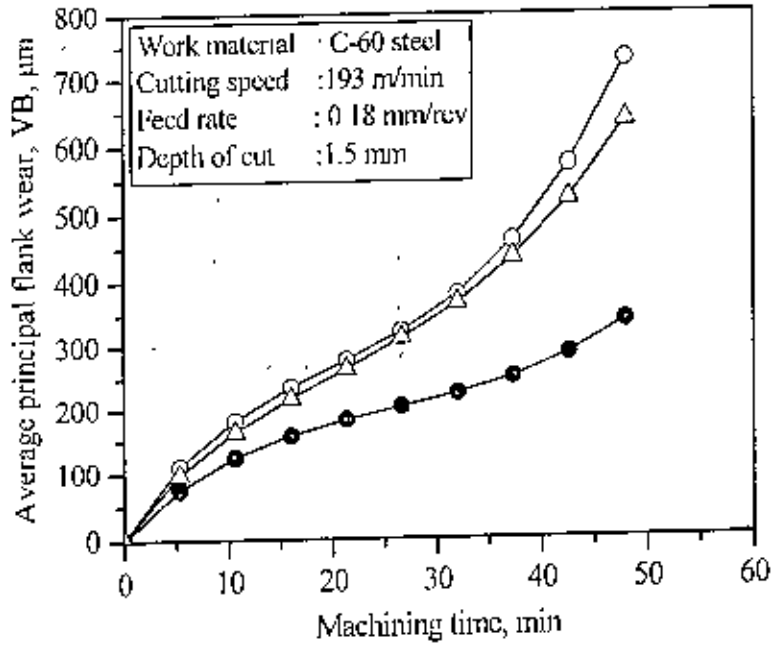
(a) SNMG insert
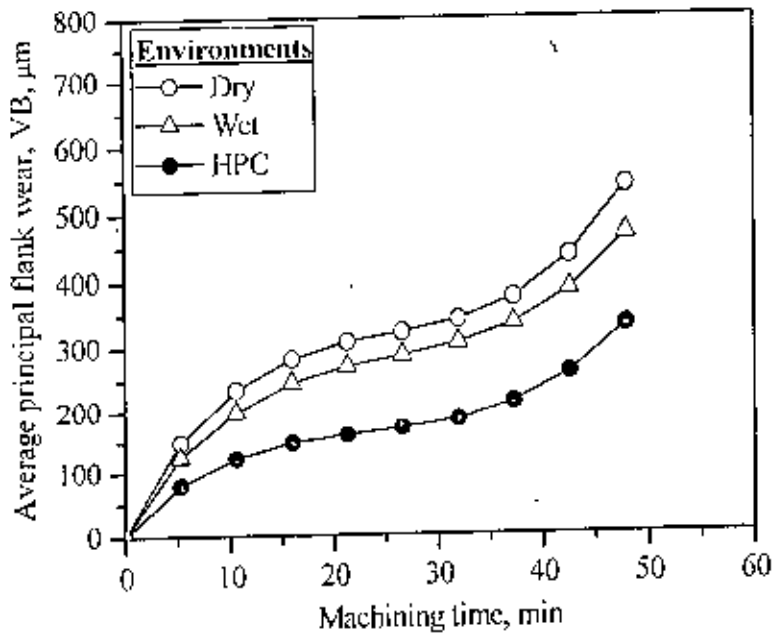
(b) SNMM insert

Fig.4.29 Growth of average principal flank wear (*VB*) with machining time in turning C-60 steel by (a) SNMG and (b) SNMM inserts under **Dry, Wet** and **HPC** conditions

75
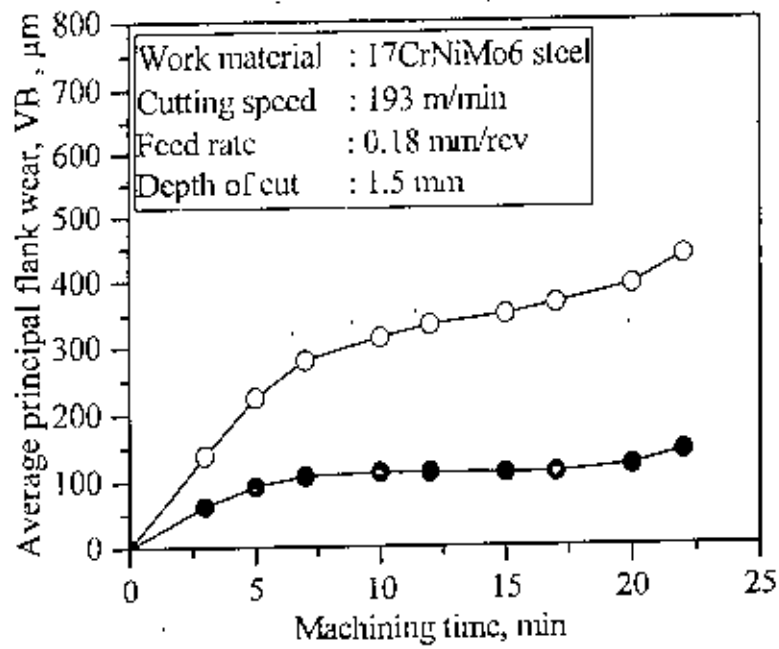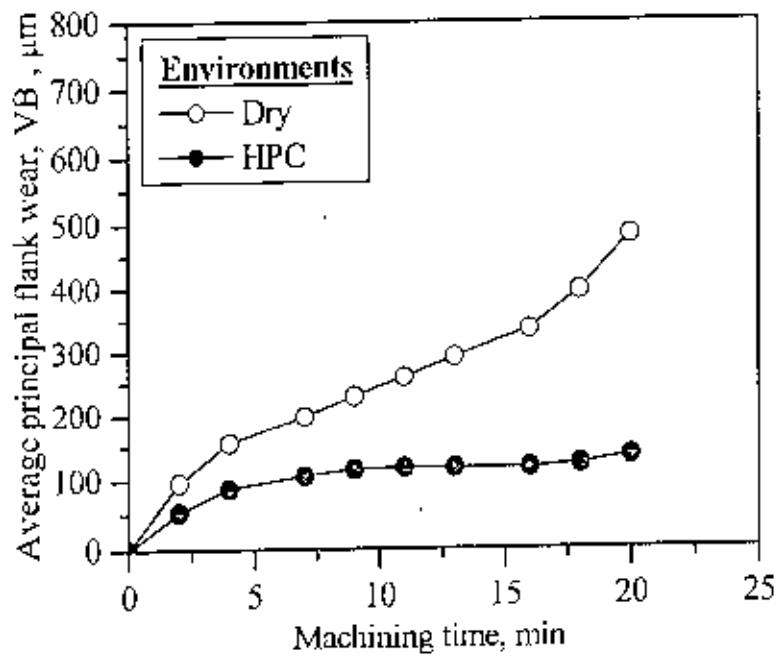
Fig.4 30 Growth of average principal flank wear (*VB*) with machining time in turning 17CrNiMo6 steel by (a) SNMG and (b) SNMM inserts under Dry and HPC conditions
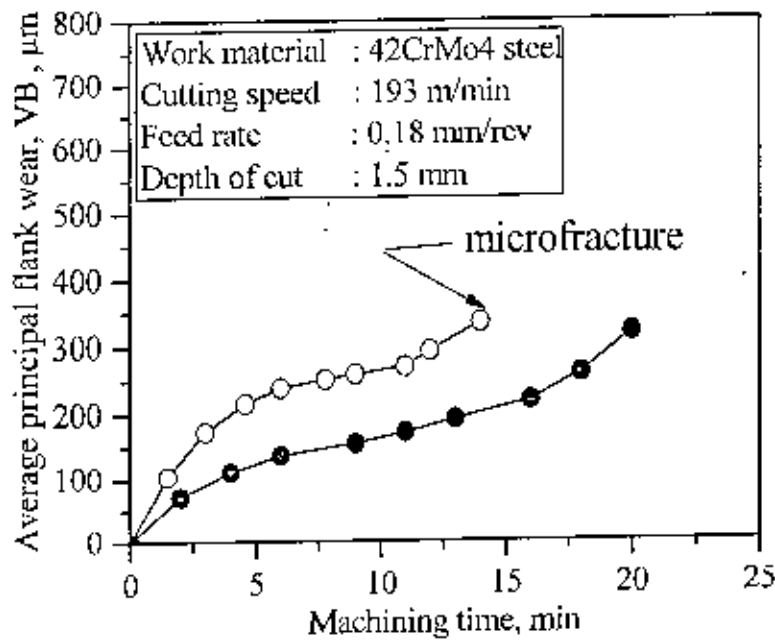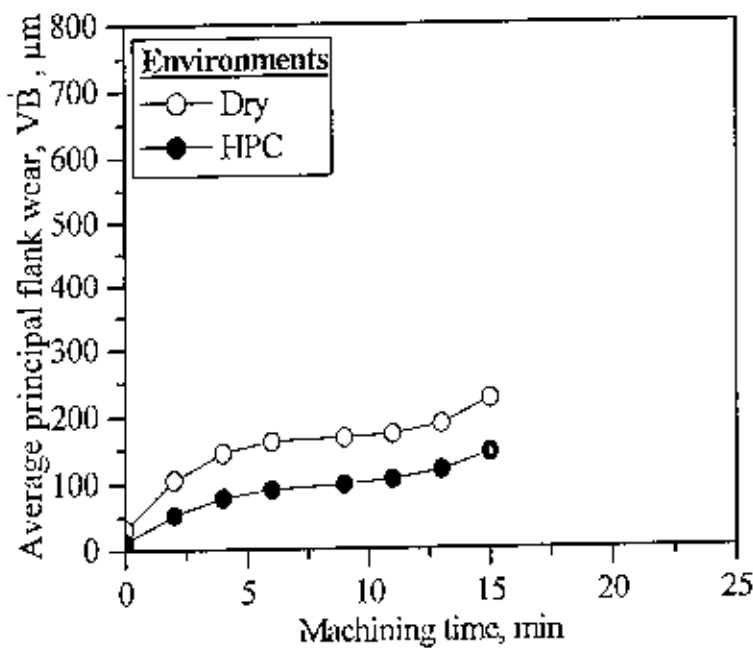
(a) SNMG insert

(b) SNMM insert

Fig.4.31 Growth of average principal flank wear (*VB*) with machining time in turning 42CrMo4 steel by (a) SNMG and (b) SNMM inserts under Dry and HPC conditions

The growth of average auxiliary flank wear. *VS* with machining time observed while turning C-60 steel, 17CrNiMo6 Steel and 42CrMo4 steel by the two different types

of inserts under previous conditions and environments have been shown in Fig.4.32, Fig.4.33 and Fig.4.34 respectively.
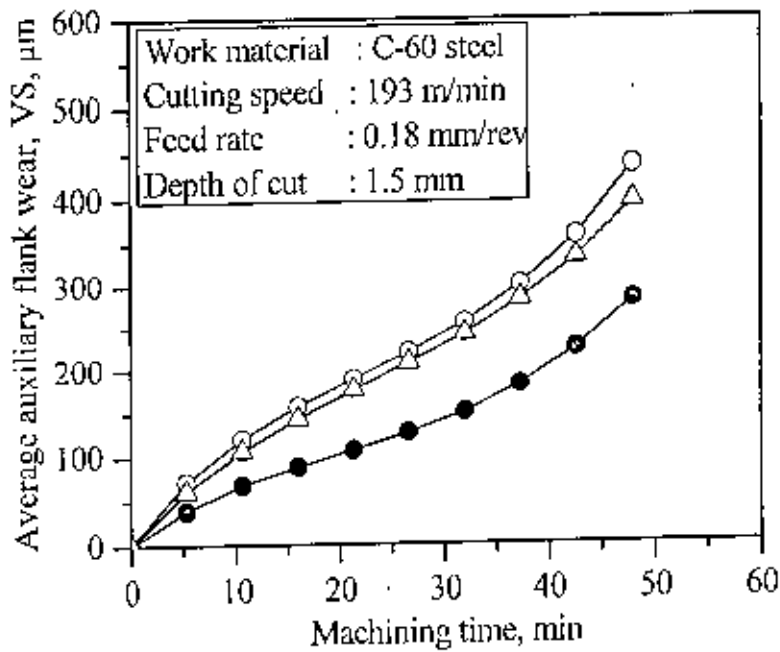
(a) SNMG insert

(b) SNMM insert

Fig.4.32 Growth of average auxiliary flank wear (*VS*) with machining time in turning C-60 steel by (a) SNMG and (b) SNMM inserts under Dry, Wet and HPC conditions
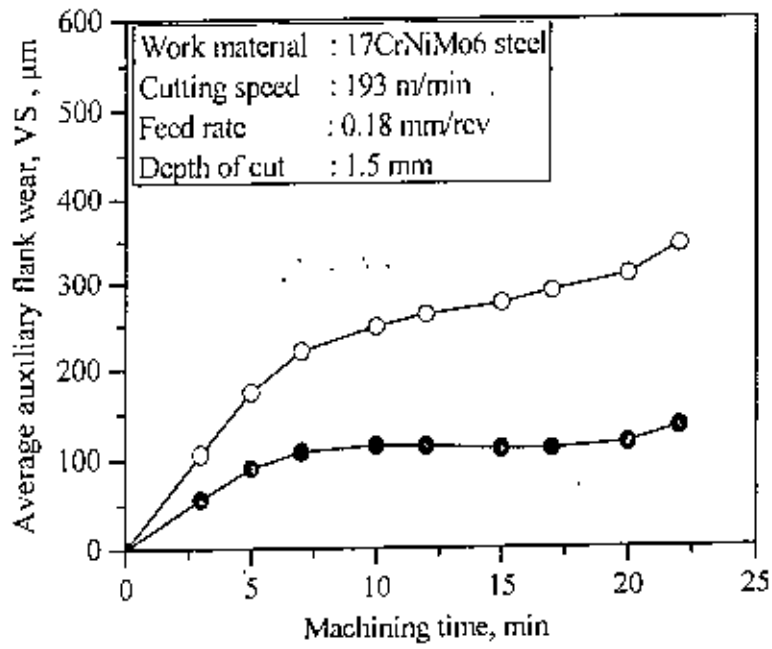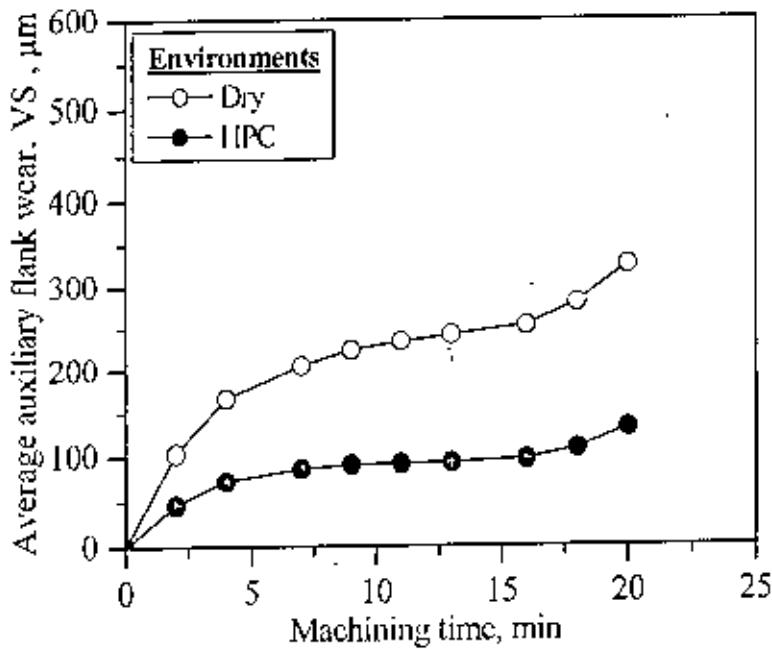
(a) SNMG insert

(b) SNMM insert

Fig 4.33 Growth of average auxiliary flank wear (*VS*) with machining time in turning 17CrNiMo6 steel by (a) SNMG and (b) SNMM inserts under Dry and HPC conditions
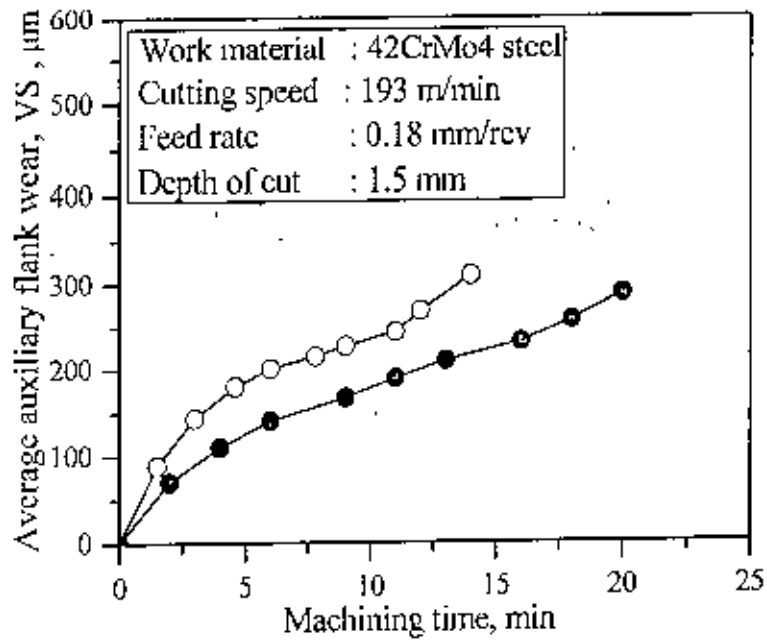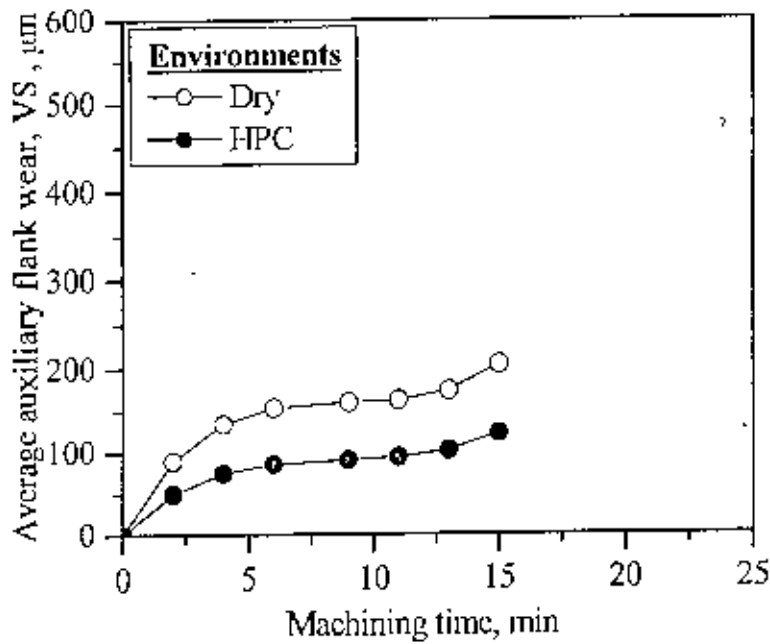
(a) SNMG insert

(b) SNMM insert

Fig.4.34 Growth of average auxiliary flank wear (VS) with machining time in turning 42CrMo4 steel by (a) SNMG and (b) SNMM inserts under Dry and HPC conditions

4.6.5 Scanning Electron Microscopy (SEM) Views of Worn out Inserts

The pattern and extent of wear that developed at the different surfaces of the tool tips after being used for machining different steels over reasonably long period have been observed under Scanning Electron Microscope (Philips XL 30, Belgium) to see the actual effects of different environments on wear of the carbide inserts of present two configurations. Fig.4.35 and Fig.4.36 show the scanning electron microscopy (SEM) views of the worn out insert (SNMG 120408) after being used at V=193 m/min, f=0.18 mm/rev and d =1.50 mm for 48 min. under dry, wet and high-pressure coolant condition. Fig.4.37 and Fig.4.38 show the pattern and extent of wear and fracture the SNMM insert attained after 48 min. of dry, wet and high-pressure coolant machining of the C-60 steel under the same machining condition. The SEM views of worn out inserts (SNMG and SNMM) being used for machining 17CrNiMo6 steel and 42CrMo4 steel under dry and HPC conditions are shown in Fig. 4.39, Fig. 4.40, Fig. 4.41, Fig. 4.42, Fig. 4.43, Fig. 4.44, Fig. 4.45 and Fig. 4.46.
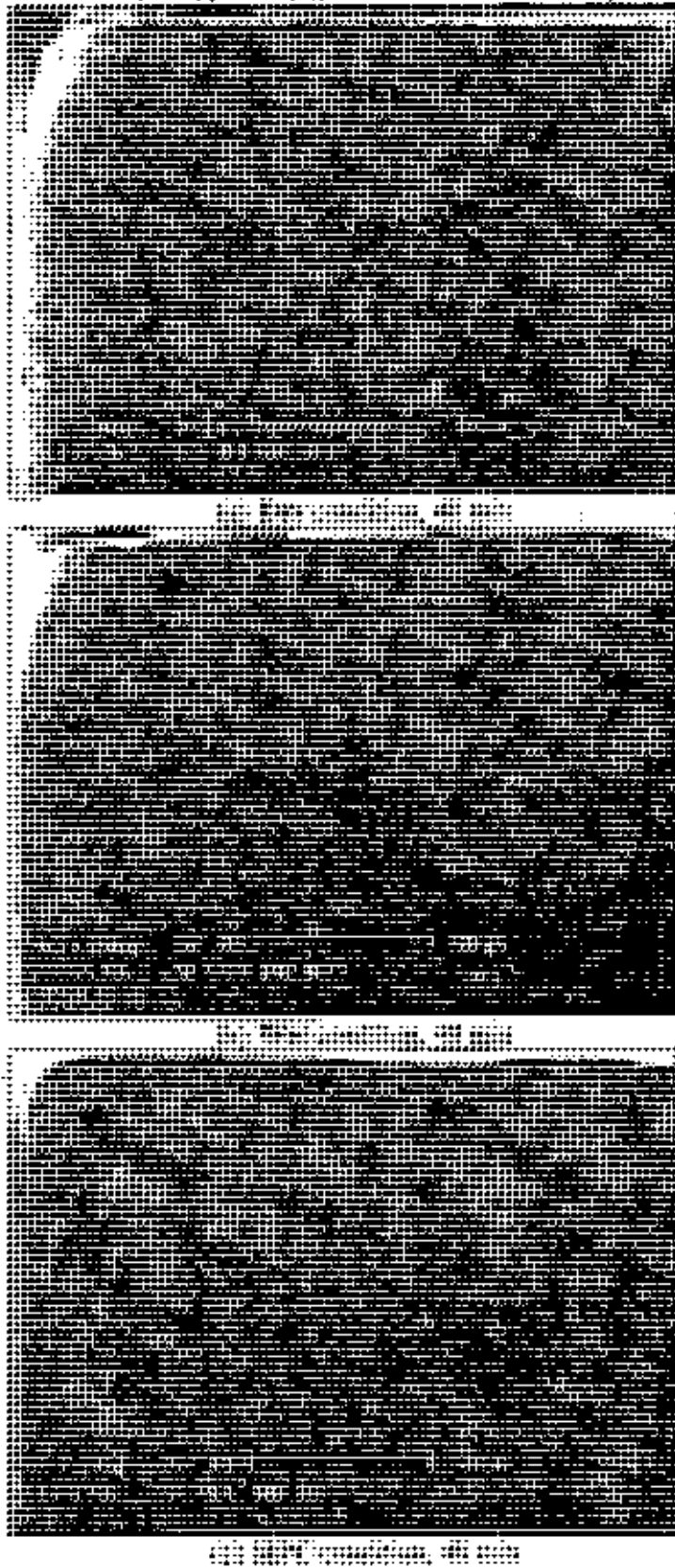
Fig.4.35 SEM ▓▓▓▓ ▓▓ ▓▓▓▓▓▓ ▓▓▓▓ ▓▓ ▓▓▓ ▓▓▓ ▓▓ ▓▓▓▓▓ ▓▓▓▓ after machining
C-60 steel under (a) **Dry,** (b) Wet and (c) **HPC** conditions
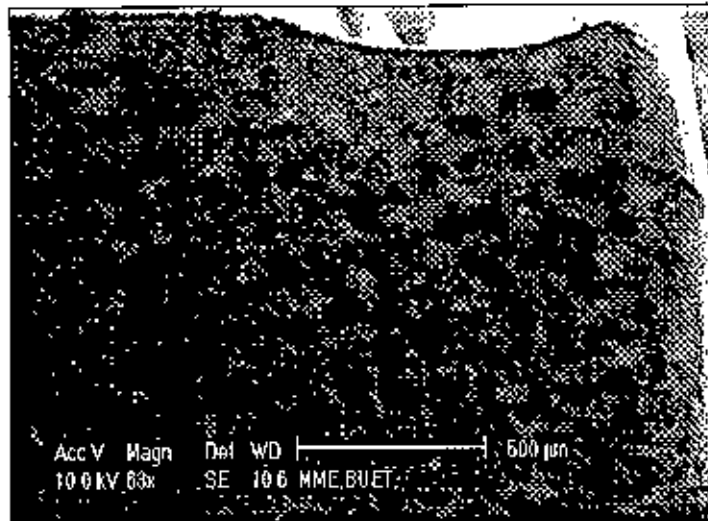
(a) **Dry** condition. 48 min
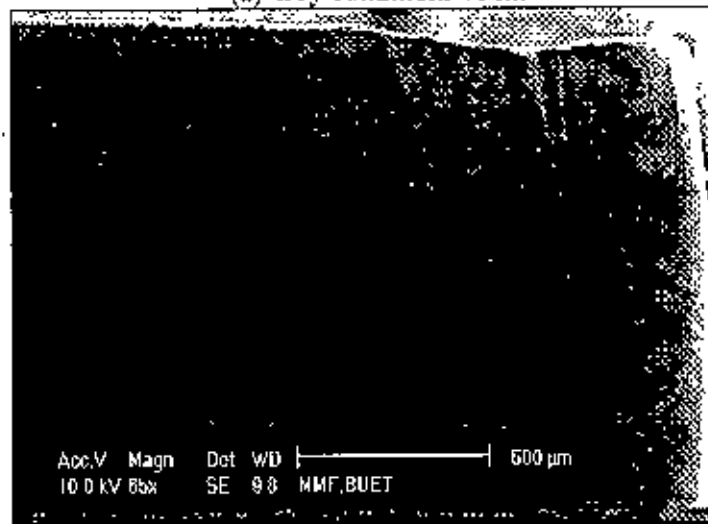
(b) **Wet** condition, 48 min
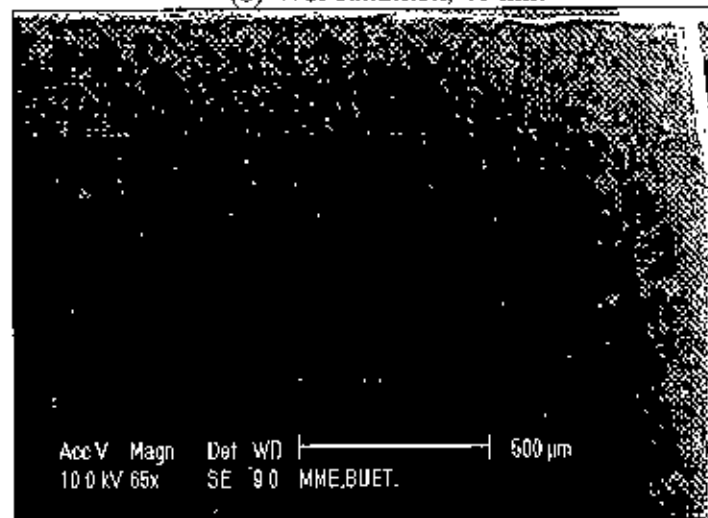
(c) **HPC** condition. 48 min

Fig.4.36 SEM views of **auxiliary flank** of worn out tip of **SNMG** insert after machining **C-60 steel** under (a) **Dry**, (b) **Wet** and (c) **HPC** conditions

83
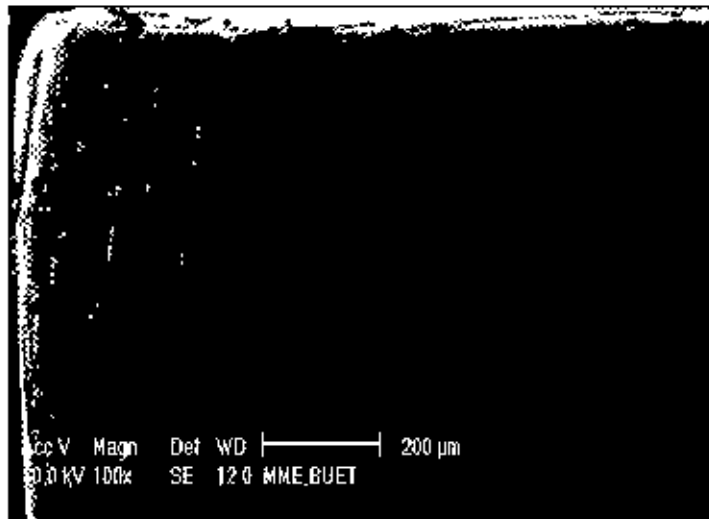
(a) Dry condition, 48 min
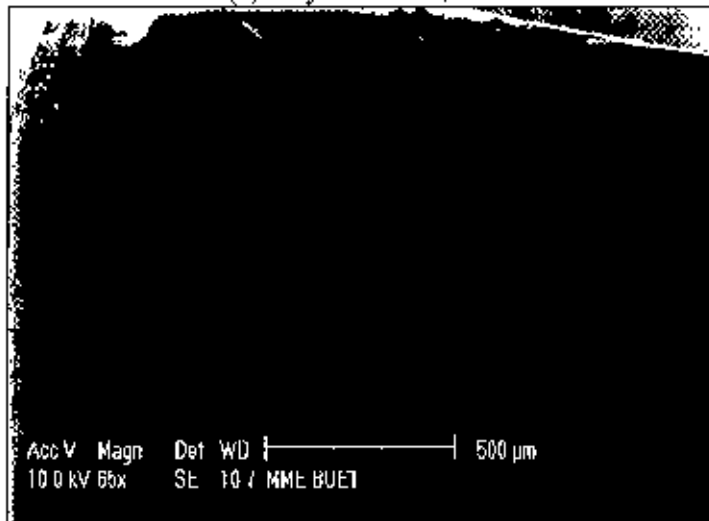
(b) Wet condition, 48 min
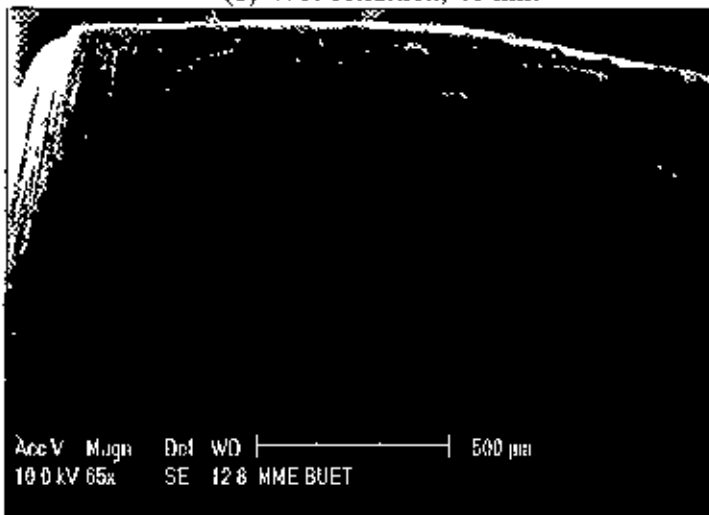
(c) HPC condition, 48 min

Fig.4 37 SEM views of **principal flank** of worn out tip of **SNMM** insert after machining
C-60 steel under (a) **Dry**, (b) **Wet** and (c) HPC conditions
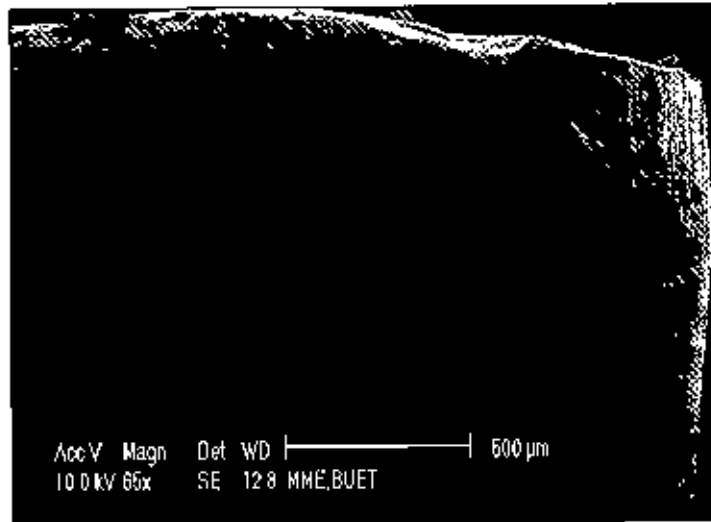
(a) **Dry** condition, 48 min
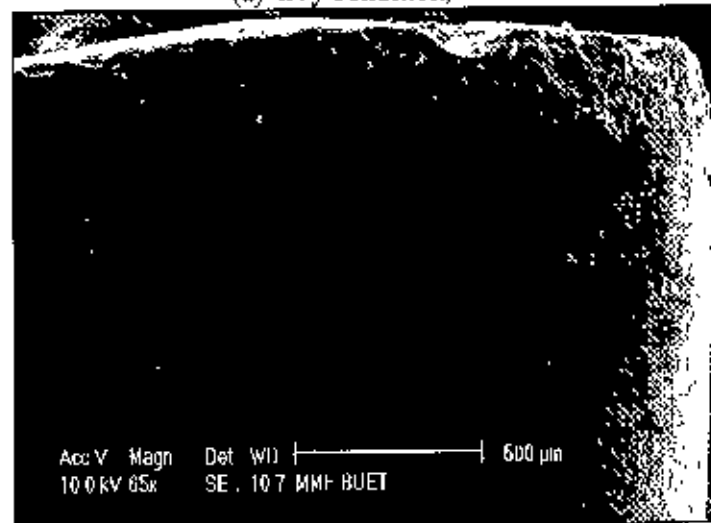
(b) **Wet** condition, 48 min
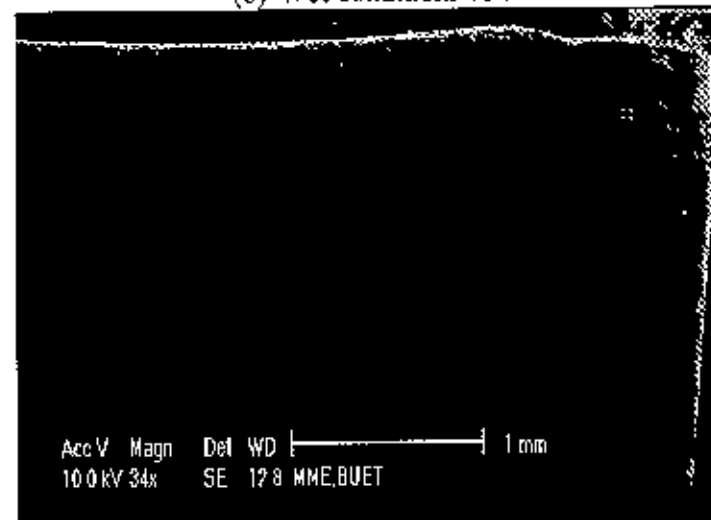
(c) **HPC** condition, 48 min

Fig.4.38 SEM views of **auxiliary** worn out tip of **SNMM** insert after machining **C-60** steel under (a) **Dry**, (b) **Wet** and (c) **HPC** conditions

85

(a) **Dry** condition, 22 min

(b) **HPC** condition, 22 min

Fig.4.39 SEM views of **principal flank** of worn out tip of **SNMG** insert after machining
17CrNiMo6 steel under (a) **Dry** and (b) **HPC** conditions
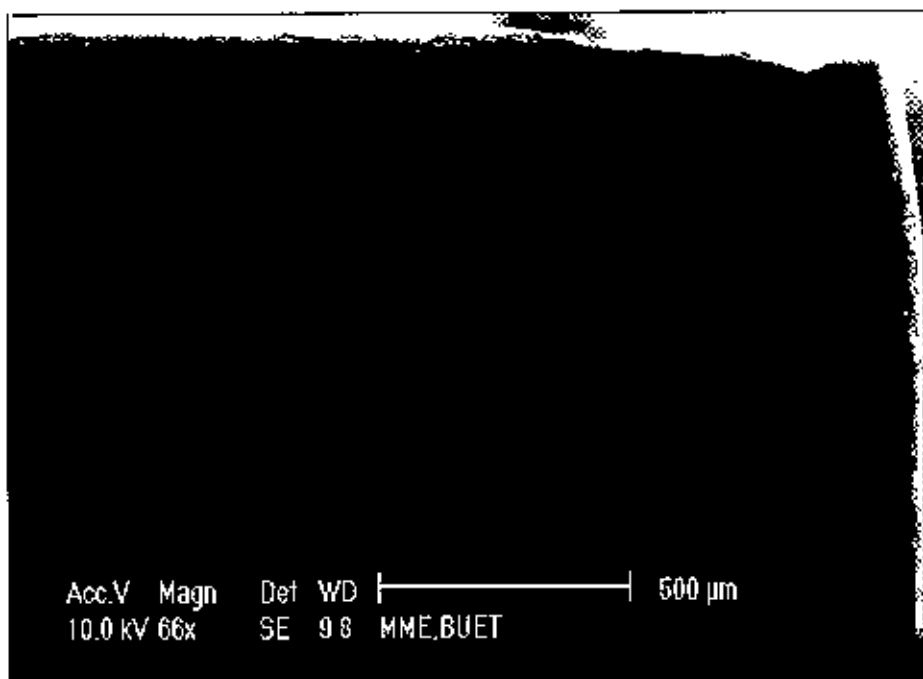
(a) **Dry** condition, 22 min
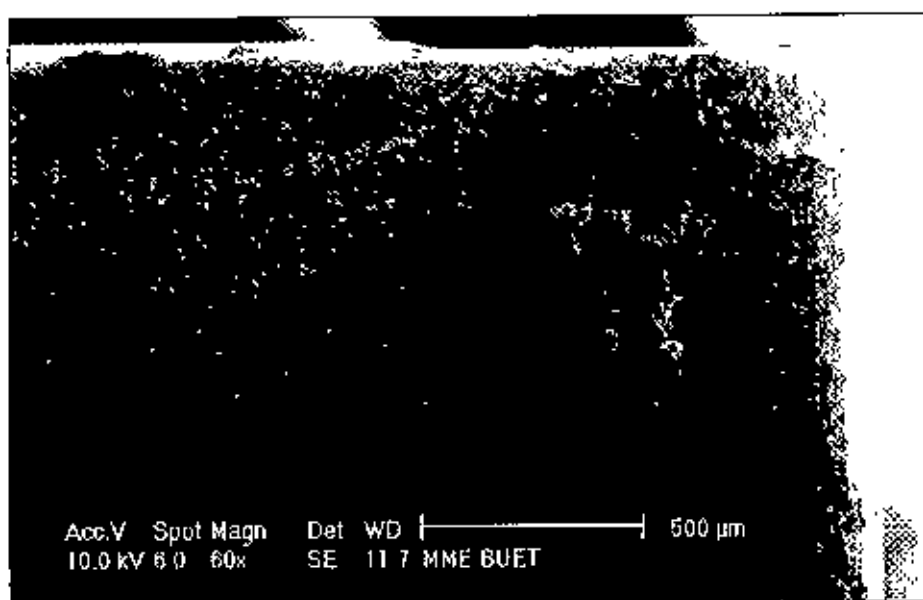
(b) **HPC** condition, 22 min

Fig.4.40 SEM views of **auxiliary flank** of worn out tip of **SNMG** insert after machining **17CrNiMo6 steel** under (a) **Dry** and (b) **HPC** conditions
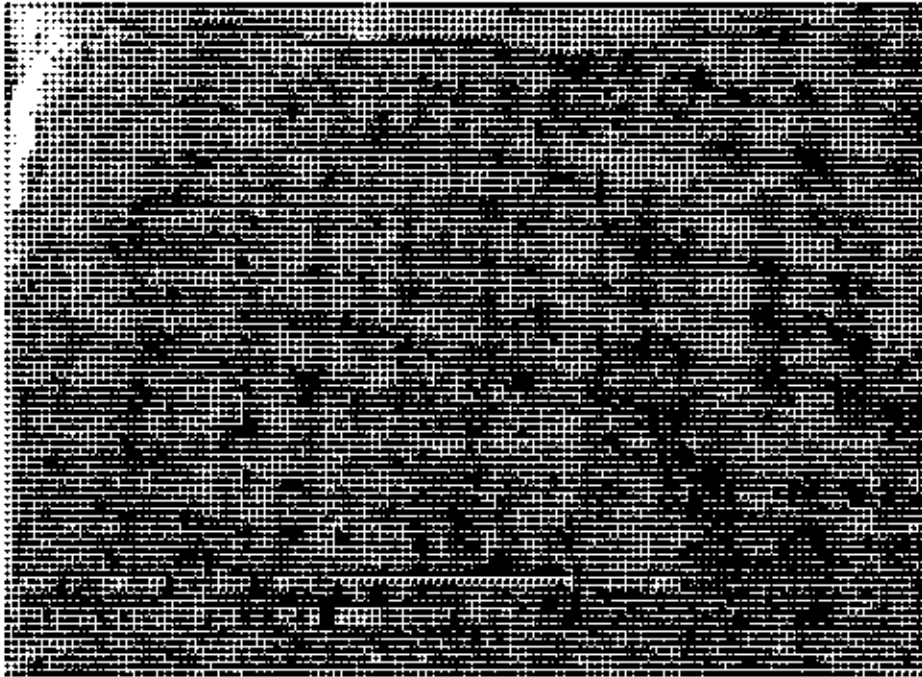
(a) **Dry** condition, 20 min

(b) **HPC** condition, 20 min

Fig.4.41 SEM views of **principal flank** of worn out tip of **SNMM** insert after machining
17CrNiMo6 steel under (a) **Dry** and (b) **HPC** conditions
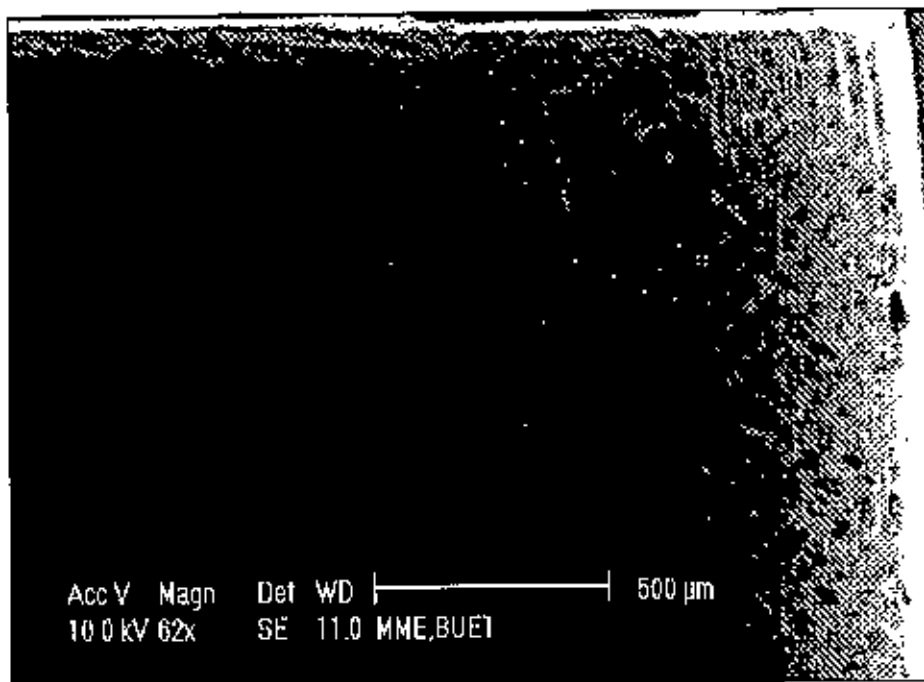
(a) **Dry** condition. 20 min

(b) **HPC** condition, 20 min

Fig.4.42 SEM views of **auxiliary flank** of worn out tip of **SNMM** insert after machining **17CrNiMo6 steel** under (a) **Dry** and (b) **HPC** conditions

(a) **Dry** condition, 14 min
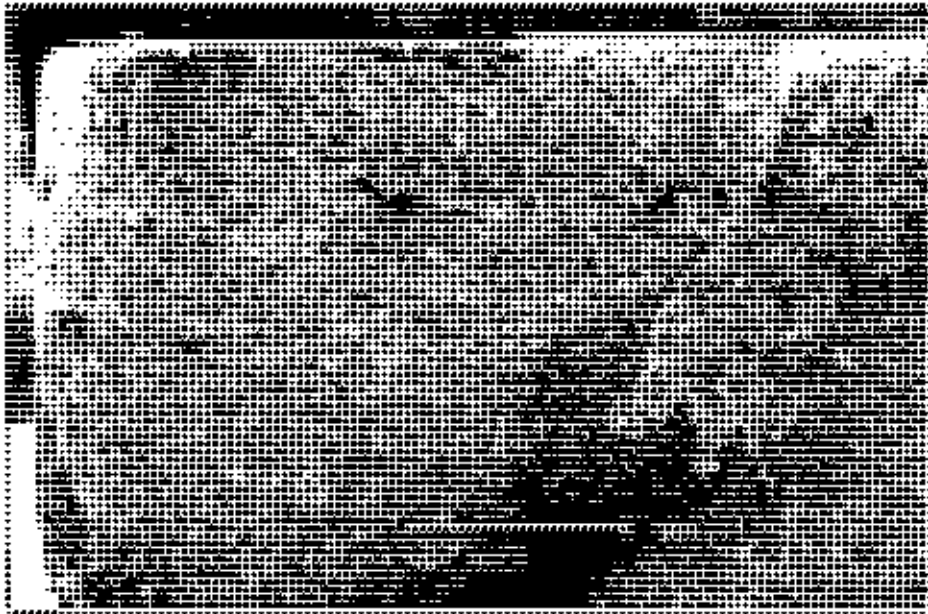
(b) **HPC** condition, 20 min

Fig 4.43 SEM views of **principal flank** of worn out tip of **SNMG** insert after machining
42CrMo4 steel under (a) **Dry and** (b) **HPC** conditions

Acc V   Magn   Det   WD ├──────────────┤ 500 μm
10 0 kV 64x   SE   12.7   NME.BUET
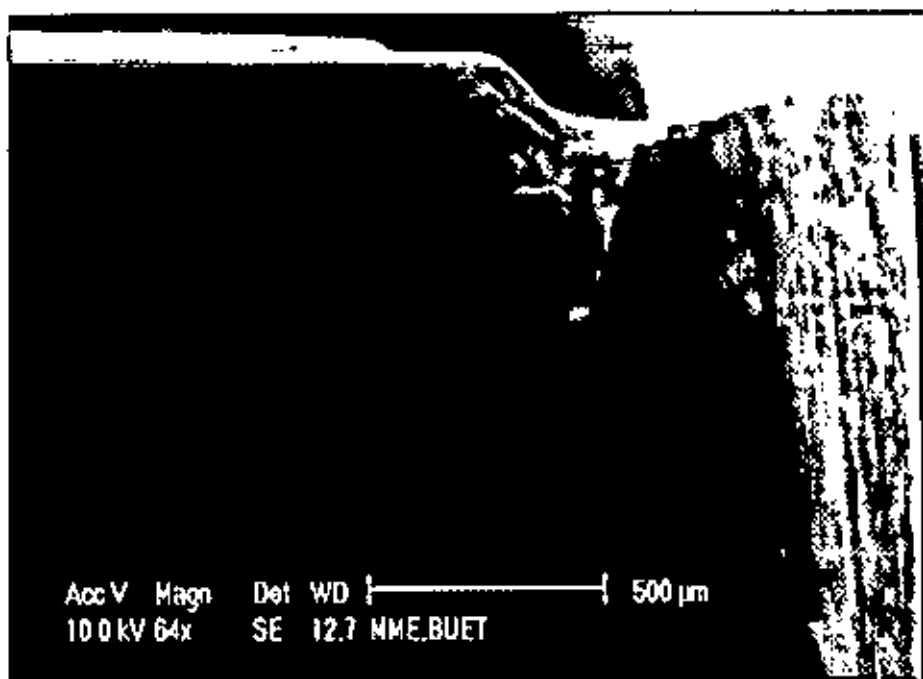
(a) Dry condition. 14 min

(b) HPC condition, 20 min

Fig.4.44   SEM views of auxiliary flank of worn out tip of SNMG insert after machining
42CrMo4 steel under (a) Dry and (b) HPC conditions
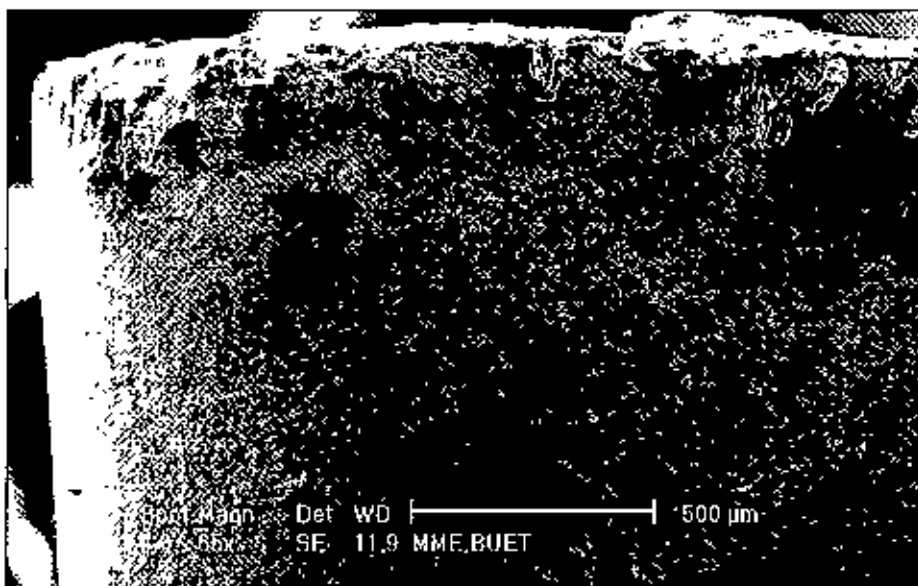
(a) **Dry** condition, 15 min

(b) **HPC** condition, 15 min

Fig.4.45 SEM views of **principal flank** of worn out tip of **SNMM** insert after machining **42CrMo4 steel** under (a) **Dry** and (b) **HPC** conditions

(a) **Dry** condition, 15 min

(b) **HPC** condition, 15 min

Fig.4.46 SEM views of auxiliary flank of worn out tip of **SNMM** insert after machining **42CrMo4 steel** under (a) **Dry** and (b) **HPC** conditions

4.6.6 Tool Life

The effect of application of high-pressure coolant over dry conditions on tool life in turning C-60 steel by SNMG and SNMM inserts at different V-f combination is briefly shown in Table 4.6.

Table 4.6   Tool life of **SNMG** and **SNMM** insert at $VB=300\mu m$

Cutting speed (m/min)	Feed rate (mm/rev)	SNMG insert		SNMM insert	
		Tool life (min)		Tool life (min)	
		Dry	HPC	Dry	HPC
133	0.14	59	91	35	84
	0.18	45	73	29	67
	0.22	41	67	23	50
152	0.14	44	71	30	62
	0.18	35	53	24	50
	0.22	30	42	17	31
186	0.14	40	53	25	50
	0.18	24	42	19	40
	0.22	21	36	12	22

The effects of high-pressure coolant over dry condition on tool life in machining C-60 steel by SNMG and SNMM inserts at different V-f combination have been evaluated by regression analysis based on (i) only limiting flank wear and (ii) overall tool failure using the limited experimental data. The results are shown in Fig.4.47 and Fig 4.48 respectively.
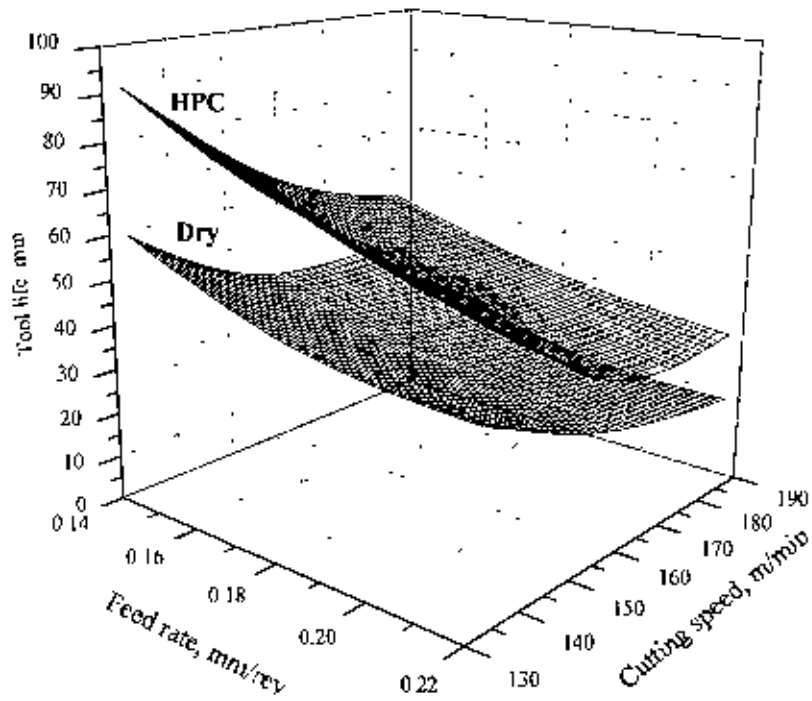
Fig.4.47 Effect of dry and HPC on tool life of SNMG insert while machining C-60 steel evaluated by regression analysis of the experimental data and based on limiting flank wear criteria $VB = 300$ μm
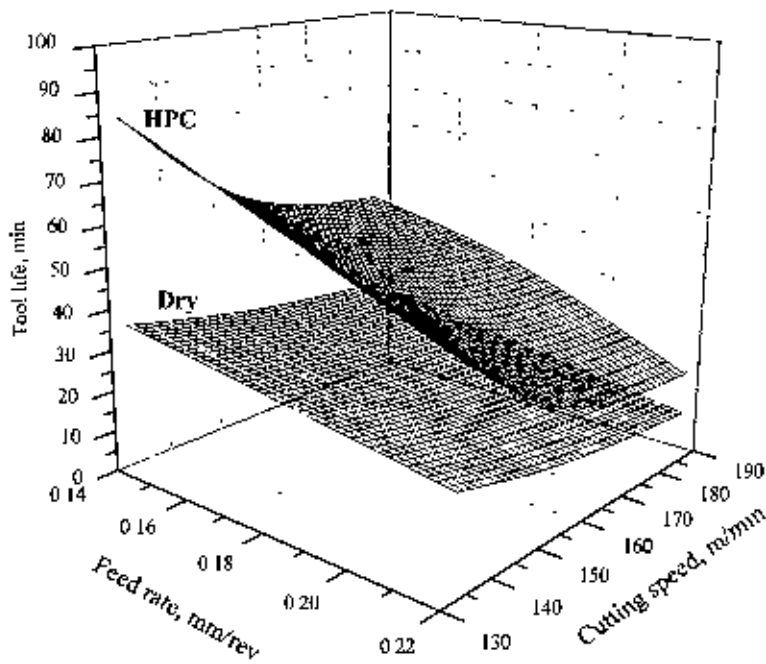
Fig.4.48 Effect of dry and HPC on tool life of SNMM insert while machining C-60 steel evaluated by regression analysis of the experimental data and based on limiting flank wear criteria $VB = 300$ μm

4.6.7 Surface Roughness

Surface roughness is another important index of machinability which is substantially influenced by the machining environment for given tool-work pair and speed-feed conditions.

Surface roughness has been measured at two stages; one, after a few seconds of machining with the sharp tool while recording the cutting temperature and forces and second, with the progress of machining while monitoring growth of tool wear with machining time.

The surface roughness attained after 45 seconds of machining of C-60 steel, 17CrNiMo6 steel and 42CrMo4 steel by the sharp (a) SNMG and (b) SNMM inserts at various V-f combinations under dry and HPC conditions are shown in Fig. 4.49, Fig. 4.50 and Fig. 4.51 respectively.
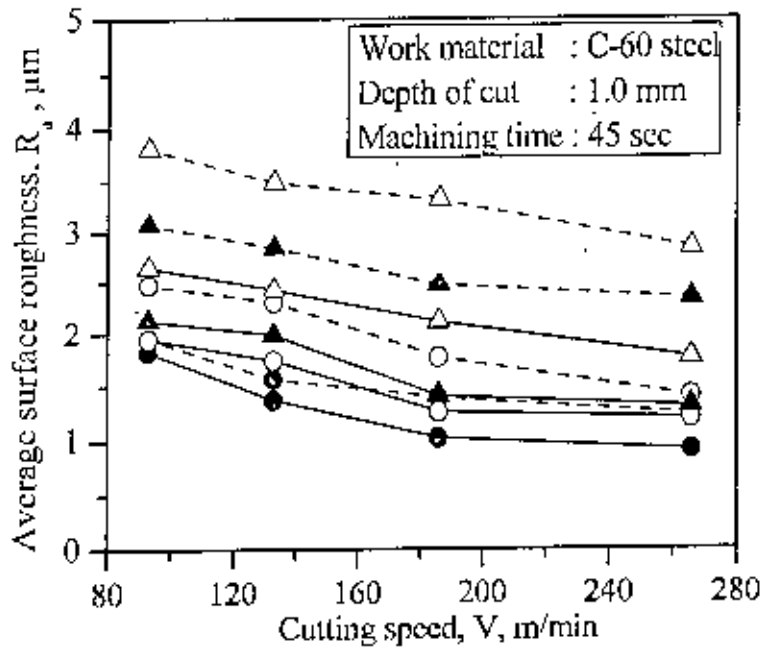
(a) SNMG insert
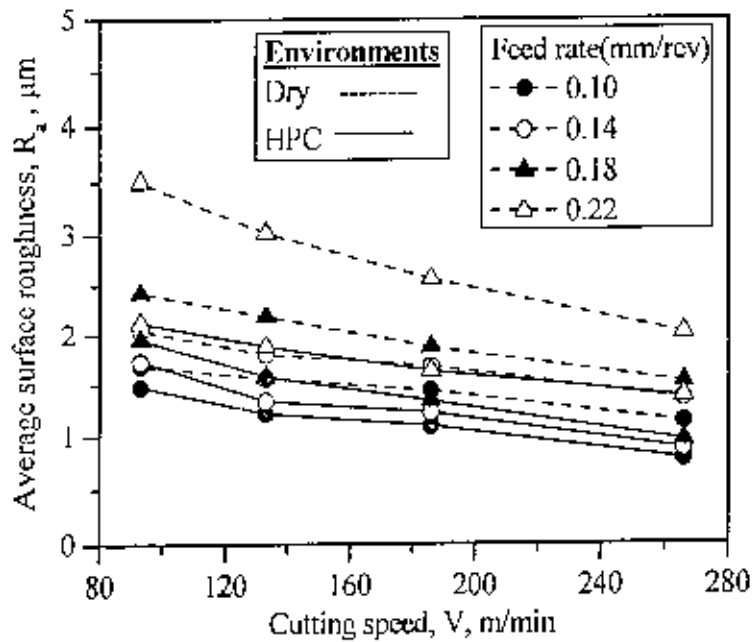
(b) SNMM insert

Fig.4.49 Variation in surface roughness (Ra) with that of V and f in turning C-60 steel by (a) SNMG and (b) SNMM inserts under Dry and HPC conditions

97
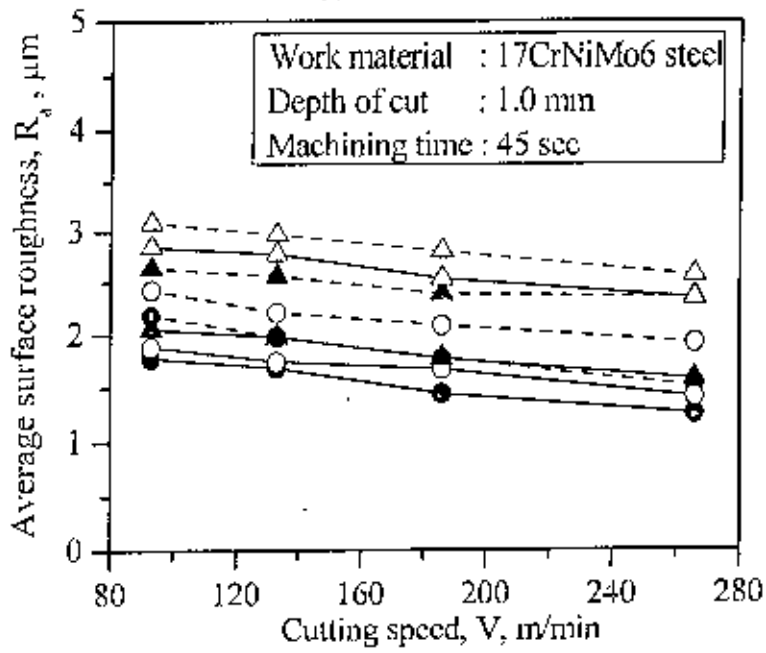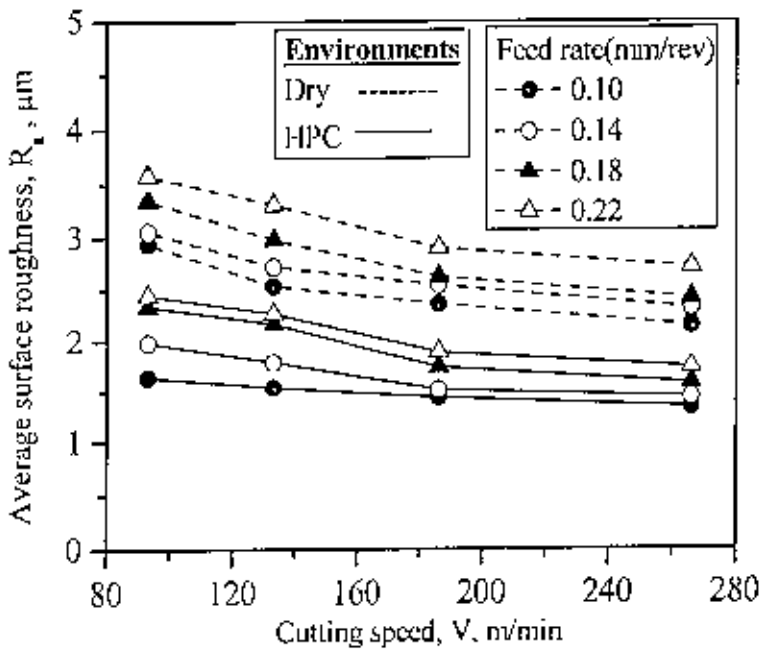
(a) SNMG insert

(b) SNMM insert

Fig.4.50 Variation in **surface roughness** (*Ra*) with that of *V* and *f* in turning 17CrNiMo6

steel by (a) **SNMG** and (b) **SNMM** inserts under **Dry** and **HPC** conditions

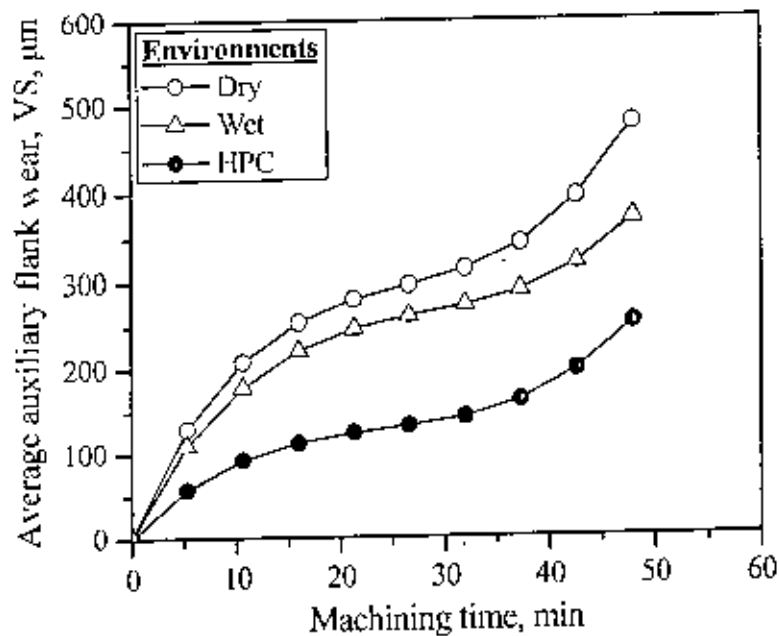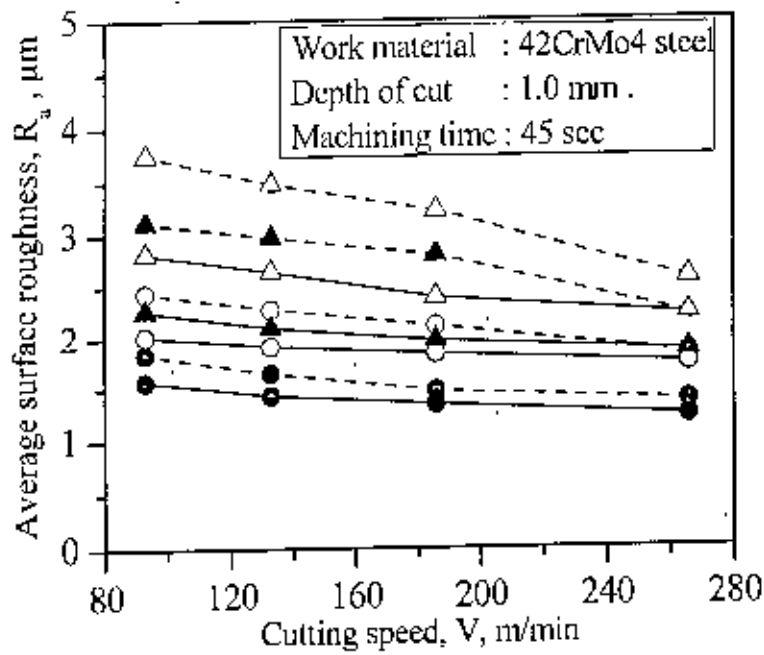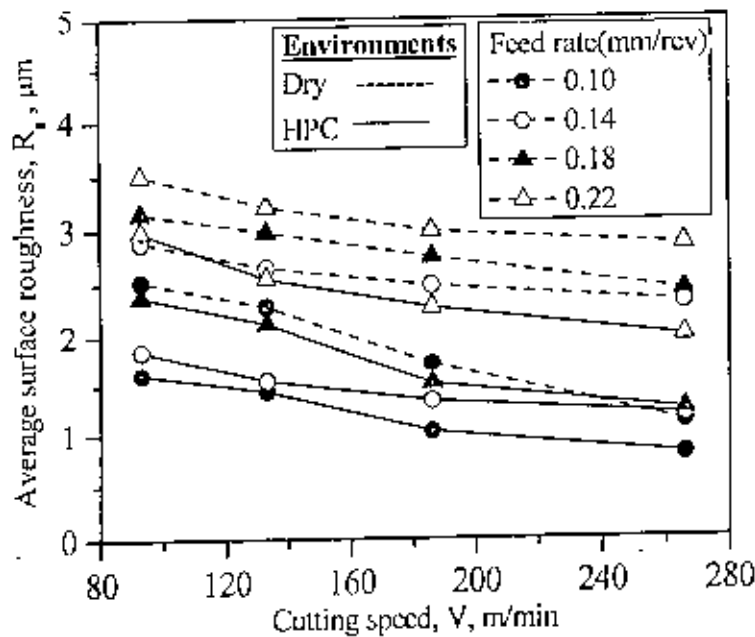(a) SNMG insert

(b) SNMM insert

Fig.4.51 Variation in **surface roughness (Ra)** with that of V and f in turning **42CrMo4 steel** by (a) **SNMG** and (b) **SNMM** inserts under **Dry** and **HPC** conditions

The variation of surface roughness observed with progress of machining of C-60 steel by two types of inserts at a particular set of V-f and d under dry, wet and HPC

conditions have been shown in Fig. 4.52. Similarly the variation in surface roughness with the time observed for the other two steels being machined under dry and HPC conditions are shown in Fig. 4.53 and Fig. 4.54.
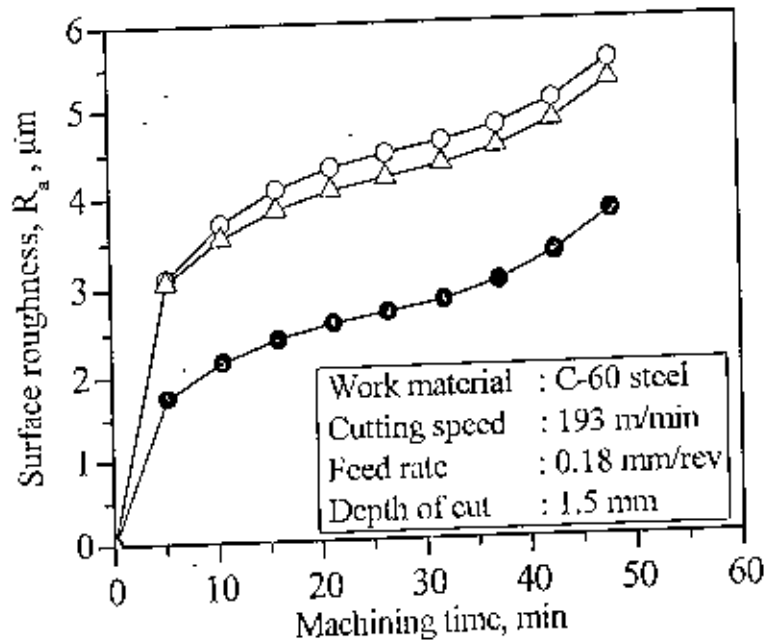
(a) SNMG insert
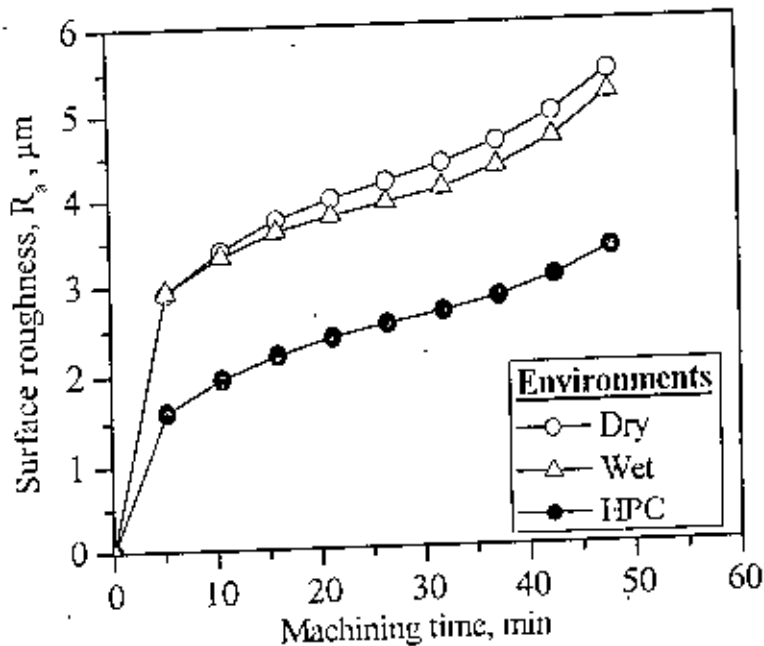
(b) SNMM insert

Fig.4.52 **Surface roughness** (*Ra*) developed with progress of machining of C-60 steel by (a) SNMG and (b) SNMM inserts under **Dry, Wet and HPC** conditions
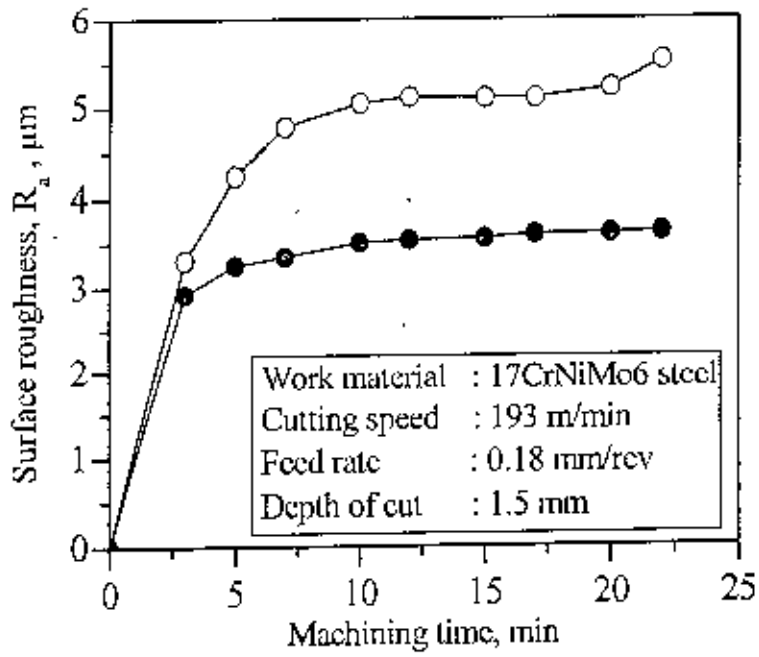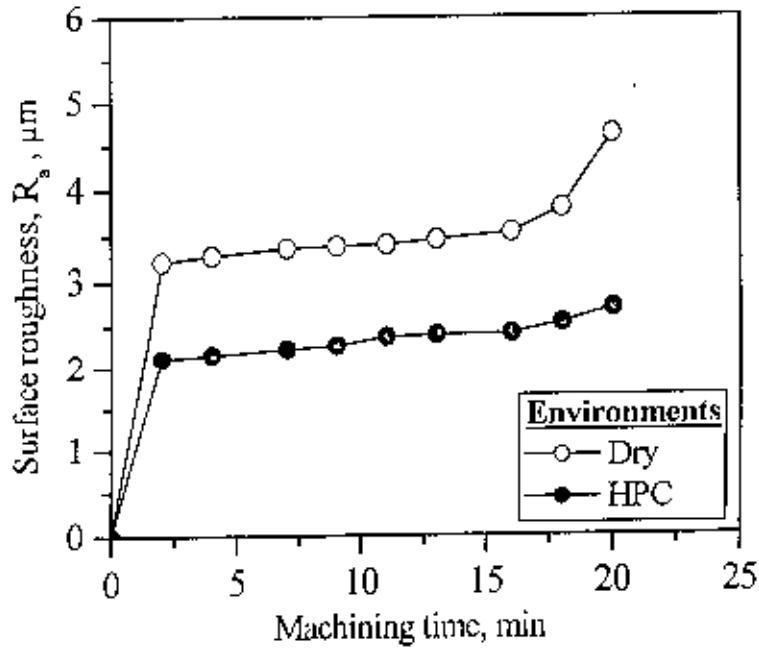
(a) SNMG insert

(b) SNMM insert

Fig.4.53 **Surface roughness** (*Ra*) developed with progress of machining of 17CrNiMo6 steel by (a) **SNMG** and (b) **SNMM** inserts under **Dry** and **HPC** conditions
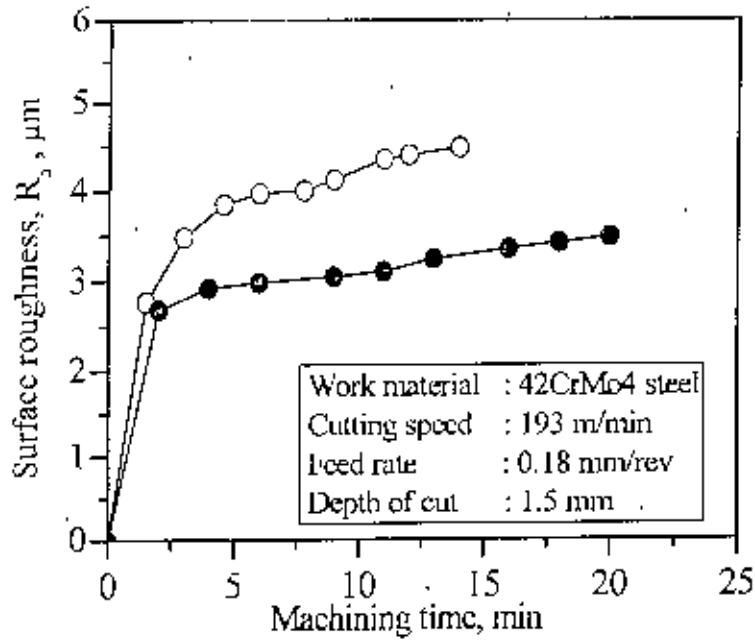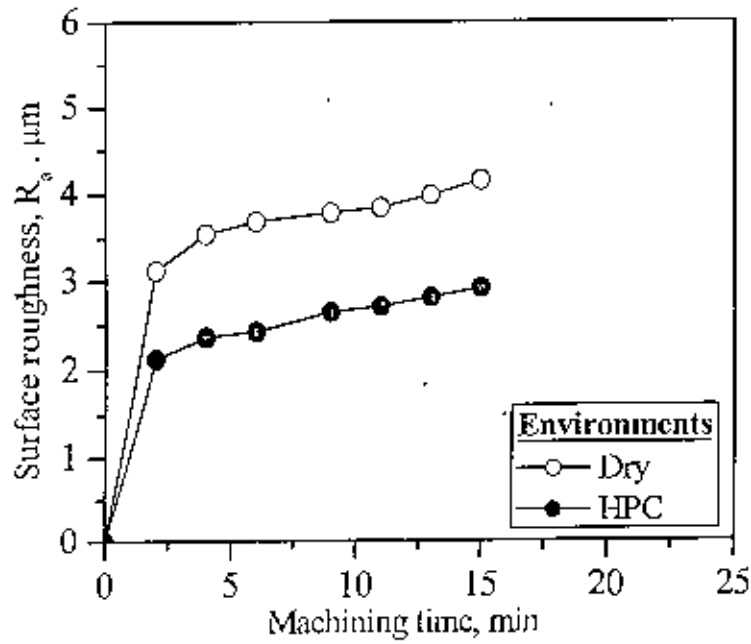
(a) SNMG insert

(b) SNMM insert

Fig.4.54 Surface roughness (*Ra*) developed with progress of machining of 42CrMo4 steel by (a) SNMG and (b) SNMM inserts under Dry and HPC conditions

4.6.8 Dimensional Deviation

During straight turning in a centre lathe, the diameter of the machined part is generally form to

i. increase along length of cut due to gradual wear of the tool tip

ii. decrease due to thermal expansion and subsequent cooling of the job if the job temperature rises significantly during machining

iii. increase due to system compliance of the Machine-Fixture-Tool-Work (M-F-T-W) system under the action of cutting forces.

The order of dimensional deviation possible due to thermal expansion of the job even under dry machining and due to compliance of the M-F-T-W system were calculated for the steel specimens being machined under the present condition and the values appear to be extremely small (less than 1 μm) compared to that possible due to wear of the tool. Therefore, in the present study, the dimensional deviations are considered to be mainly due to wear of the tool tips.

The variation in diameter of the job was preciously measured along its axis after one full pass of the machining over 500 mm length with full depth at reasonably high cutting speed and feed rate suitable for the tool-work combination. This has been done for all the tool-work-environment combination undertaken keeping the initial diameter and length of the steel rods same and uniform as per as possible.

The gradual increase in dimensional deviation on diameter observed along the length of cut on C-60 steel after one full pass of machining with SNMG and SNMM inserts at cutting speed of 193 m/min, 1.50 mm depth of cut and 0.18 mm/rev feed rate

103

under dry and HPC conditions have been shown in Fig. 4.55. Similar observation made on the 17CrNiMo6 steel and 42CrMo4 steel are shown in Fig. 4.56 and Fig. 4.57 respectively.
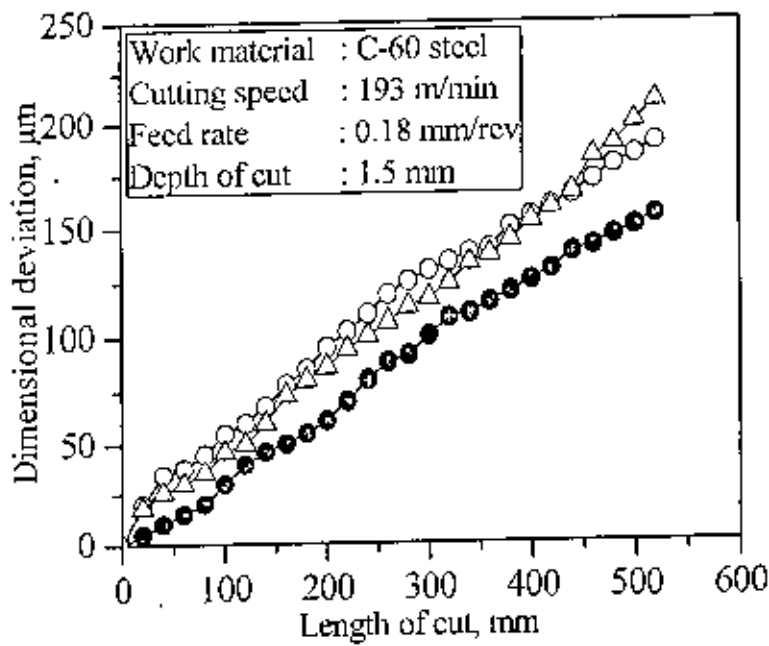
(a) SNMG insert
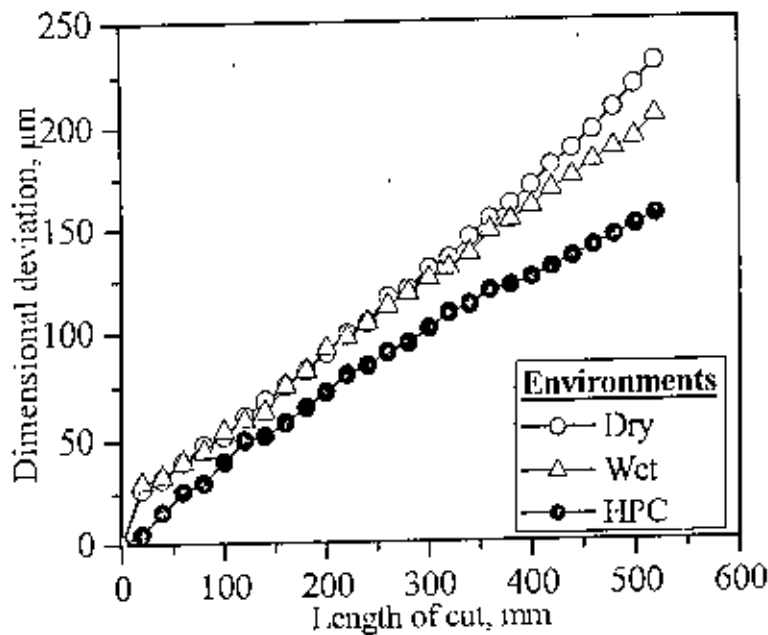
(b) SNMM insert

Fig.4.55 Dimensional deviation observed after one full pass turning of C-60 steel by (a) SNMG and (b) SNMM inserts under Dry, Wet and HPC conditions
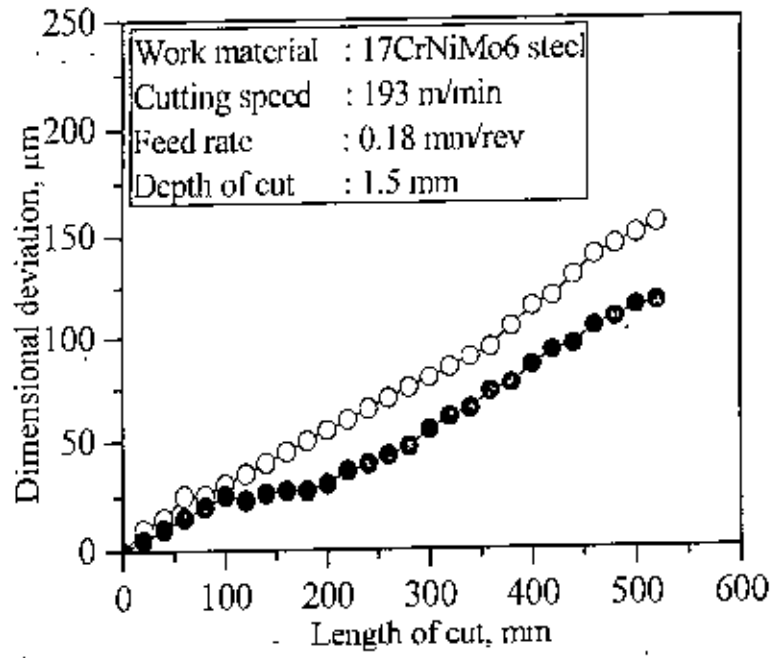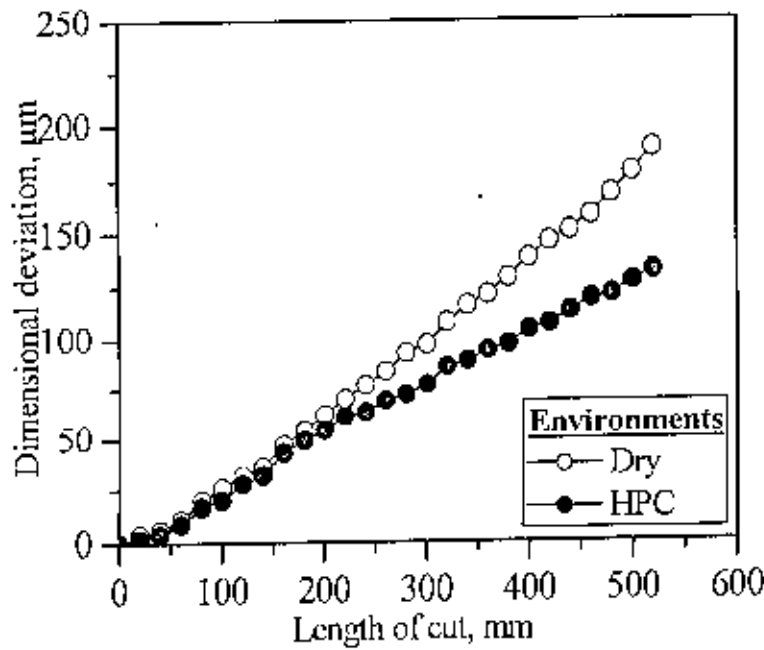
(a) SNMG insert

(b) SNMM insert

Fig.4.56 Dimensional deviation observed after one full pass turning of 17CrNiMo6 steel
by (a) SNMG and (b) SNMM inserts under Dry and HPC conditions
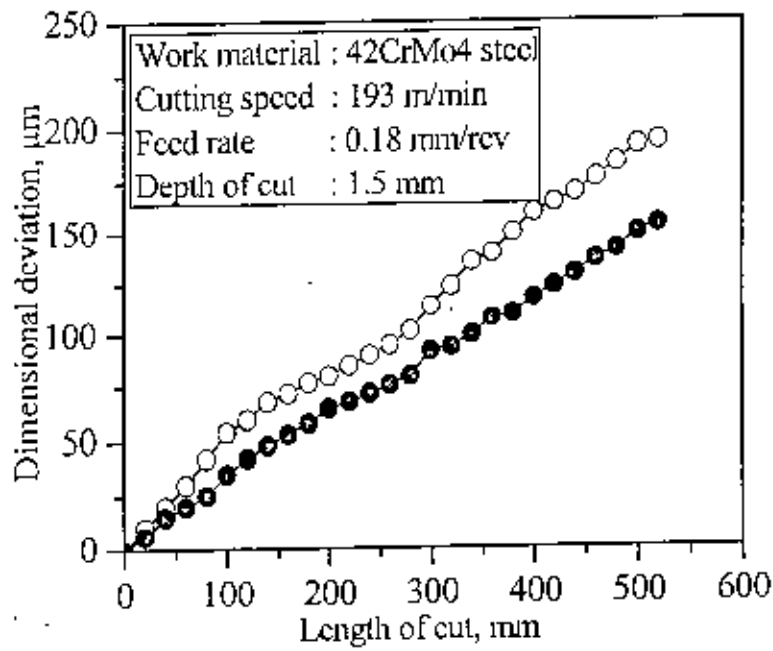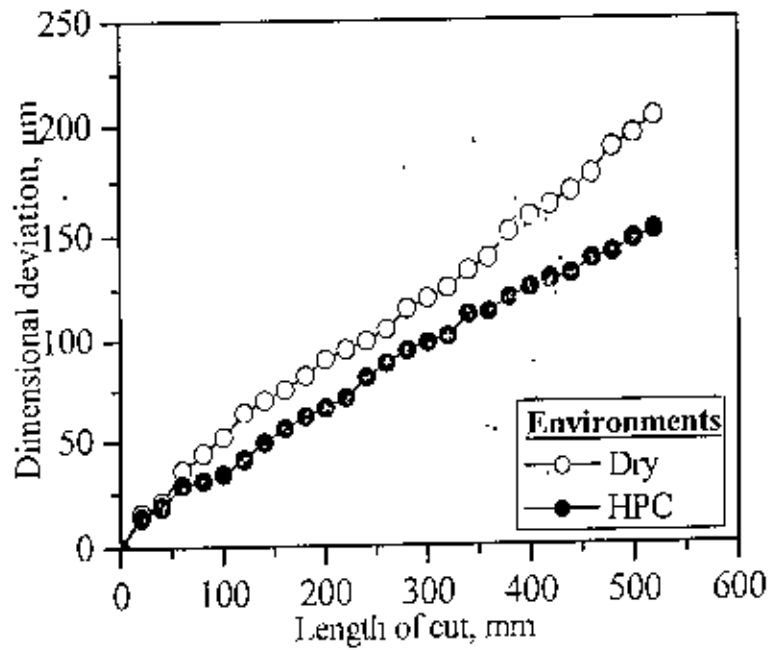
(a) SNMG insert

(b) SNMM insert

Fig.4.57 Dimensional deviation observed after one full pass turning of 42CrMo4 steel by (a) SNMG and (b) SNMM inserts under Dry and HPC conditions

Chapter-5

Modeling of Cutting Temperature

5.1   Introduction

Earlier researchers [Hahn 1951; Loewen and Shaw 1954; Weiner 1955] used Jeager's model of moving heat sources and blok's partition principle to estimate average temperature at the shear plane and at the chip-tool interface. However, these models could not take into account variation in thermal properties of work and tool material with temperature, the elasto-plastic nature of chip-tool interaction, work-tool interaction at the wear land in flank etc. Temperature distribution on the tool-chip interface was attributed to the primary heat source (due to shear deformation in the shear zone) and secondary heat source (due to friction on the tool-chip interface) as specified in a moving oblique heat source model or a stationary square heat source model. For example, the heat generated by the friction on the tool-chip interface was considered as a moving heat source for any fixed point on the chip, while it was considered as a stationary heat source for any fixed point on the tool. Huang and Liang [2003] extended the heat source method to the application of worn tools. Unfortunately, those studies focused primarily on dry cutting conditions only. For machining under wet cutting conditions, the research pursued either experimental observations or finite element method simulations [Childs et al. 1988; Li 1995; Dhar et al. 2002]. It was generally found that a small reduction of the cutting temperature required a large increase of the coolant flow rate [Li 1995].

The objective of this chapter is to model the cutting temperature for high-pressure coolant machining. The analysis of cutting temperatures in dry turning has been well documented in the literature. However, the effect of the cutting at high pressure has not yet been fully understood. In this study, the high-pressure coolant is applied at the chip-tool interface along the rake surface through an external nozzle. The heat source method is utilized to model the contributions of different heat sources and heat losses. The heat losses are considered in a two dimensional cutting model in which the cooling effect occurs on the tool rake face. The cooling-effected area can then be specified by the tool insert thickness in length and the width of cut in width. The temperature in the chip is attributed to the primary heat source due to plastic shearing and the secondary heat source due to friction. The temperature in the tool is attributed to the secondary heat source, and the heat loss due to cooling on the tool rake face due to the high-pressure coolant jet, while the rubbing heat source is also considered when the tool is worn. For a worn tool, the temperature on the interface between the tool flank face and the workpiece has to be estimated to calculate the heat partition factors on the tool-workpiece interface [**Huang and Liang 2003**]. On the other hand, for a new tool, its flank face and the workpiece have a point contact. Therefore, the cutting temperature at the tool tip can be calculated according to the heat distribution on the tool-chip interface. The temperature change in the workpiece is caused by the primary heat source, the rubbing heat source, and heat the loss due to cooling. The proposed model is verified by experimental data of turning C-60 steel under high-pressure coolant condition. The measured cutting forces are transferred to the equivalent cutting forces and feed forces in orthogonal cutting according to the tool insert geometry [**Oxley 1989**]. The obtained forces are the inputs to estimate the heat source intensities. The temperatures are measured by a tool work thermocouple for comparison with model predictions.

5.2   Temperature on Sharp Tool under HPC Condition

In this study, fluid is applied through an external nozzle of 0.50 mm diameter along the auxiliary cutting edge, as shown in Fig.5.1. The opening aims at the tool flank, thus the cooling effect is modeled as a heat loss at the gap between the tool flank and the workpiece surface below it.
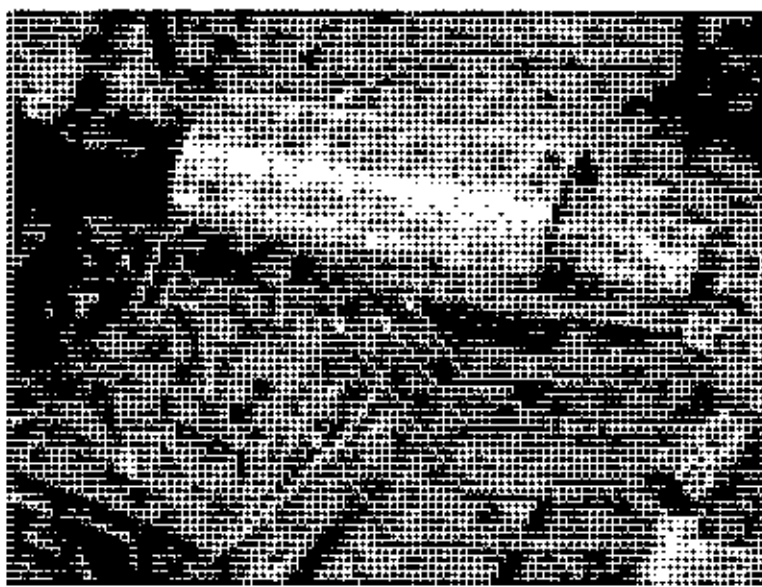
Fig. 5.1 Nozzle and the thermocouple location

The temperature distribution on the tool-chip interface for sharp tool edges in dry machining can be calculated with an analytical model, as proposed by Komanduri and Hou [2001]. It is believed that the temperature rise in dry machining is caused by the primary heat source at the shear plane and the secondary heat source at the tool-chip interface. In high-pressure coolant (HPC) machining, three heat sources/losses are considered (i) the primary heat source due to shear deformation (ii) the secondary heat source due to friction. and (iii) the heat loss due to high-pressure coolant, as shown in Fig.5.2.
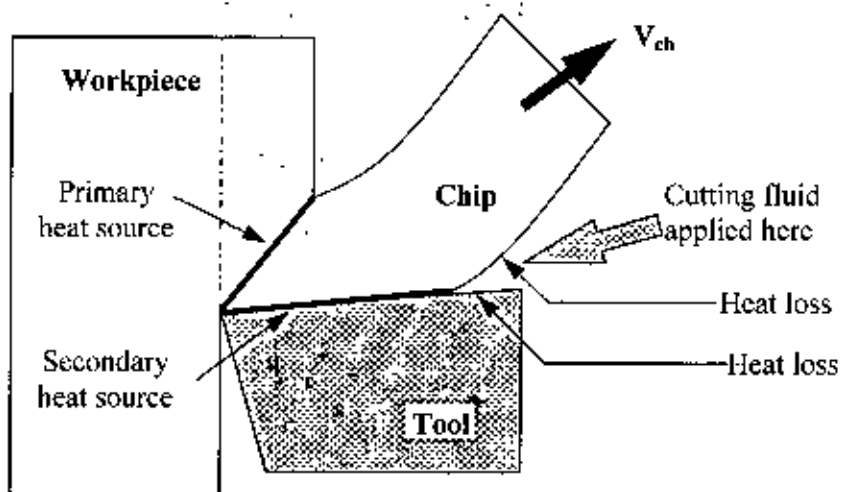
Fig. 5.2 Heat sources and heat loss for the 2D model under HPC condition

5.2.1 Temperature Rise on the Chip-tool Interface in Chip

Fig.5.3 shows [Hahn 1951] schematically the shear band heat source moving obliquely at an angle φ with a speed V_m in an infinite medium with a heat liberation intensity of q_{pl} (J/cm^2 s). The band heat source is infinitely long of width $2l$. A moving coordinate system is considered with its oX axis along the width of the plane of the moving band heat source and its origin o coinciding with the mid point. The location of point M is expressed by the coordinates in the moving coordinate system at time t.
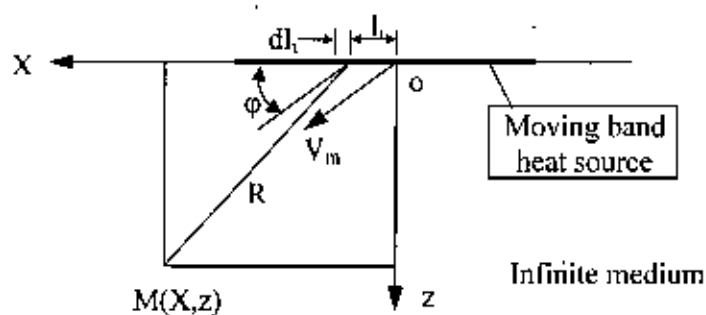
Fig. 5.3 Schematic of Hahn's model of a band heat source moving obliquely in an infinite medium [Hahn 1951]

The moving band heat source is considered as a combination of infinitely small differential segments dl_t, each of which is considered as an infinitely long moving line heat

source. Thus the solution for an infinitely long moving line heat source in an infinite medium [**Jaeger 1942**] can be used for calculating the temperature rise at any point M caused by a differential segment dl_i.

$$\theta_M = \frac{q_l}{2\pi\lambda} e^{-\frac{XV_m}{2a}} K_o\left(\frac{RV_m}{2a}\right) \quad \ldots\ldots\ldots\ldots\ldots\ldots\ldots\ldots\ldots\ldots\ldots\ldots\ldots\ldots[5.1]$$

where,

θ_M	=	Temperature rise at point M, °C
q_l	=	Heat liberation intensity of a moving line heat source, J/cm-s
λ	=	Thermal conductivity, J/cm s °C
V_m	=	Velocity of a moving plane heat source, cm/s
a	=	Thermal diffusivity, cm²/s
K_o	=	Modified Bessel function of the second kind of order zero
R	=	Distance between the moving line heat source and the point M, where the temperature rise is concerned, cm
X, z	=	The coordinates of the point where the temperature rise is concerned in the moving coordinate system, cm

For continuous chip formation in orthogonal machining, the shear plane heat source is moving in a semi-infinite medium with the work surface and the chip surface being the boundaries of a semi-infinite media. Thus, Hahn's oblique moving heat source solution should be modified with consideration for the effect of the boundaries and the use of appropriate image heat sources. Temperature rise in the chip is attributed to both the primary heat source and the secondary heat source. The effect of the primary heat source is considered as this heat source is moving in a continuous chip flow. The back side of the chip is assumed to be adiabatic. Then, the primary heat source and the imaginary heat source are symmetric with respect to the back side of the chip. The schematic of the imaginary chip and the heat sources is shown in Fig.5.4. The upper boundary of the semi-infinite body can be considered adiabatic for many practical cases involving machining

dry, i.e., without chanced cooling. For an adiabatic boundary, an image heat source (a mirror image of the primary heat source with respect to the boundary surface) with the same heat liberation intensity should be considered as shown in the Fig.5.4. A moving coordinate system is used for the analysis of the thermal effect caused by the oblique moving band heat source, where ox is the abscissa and oz is the ordinate of the system. The origin of the system coincides with the upper end of the oblique moving band heat source and moves together with it with the same velocity and in the same direction.
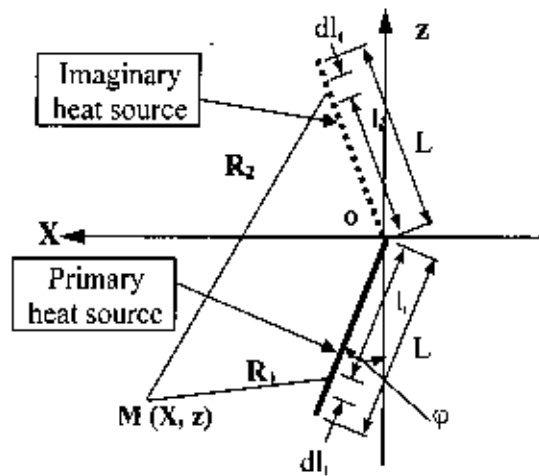
Fig. 5.4   Schematics of the moving heat source model of the primary heat source for chip

The temperature rise at any point $M(X, z)$ is due to the combined effect of the primary and image heat source. Each of these heat sources can be considered as a combination of numerous infinitesimal segments dl_i, with each again as an infinitely long moving line heat source. Thus, the temperature rise at any point M caused by the segmental moving line heat source dl_i can be calculated using Equation (5.1). For any one of the segmental moving line heat source dl_i (Fig.5.3), $q_i = q_{pl}\, dl_i$; the distance between point M and the primary segmental line heat source, R_i, is $\sqrt{[X - l_i \sin(\varphi - \alpha)]^2 + [z - l_i \cos(\varphi - \alpha)]^2}$; the distance between point M and the image source, R_2, is $\sqrt{[X - l_i \sin(\varphi - \alpha)]^2 + [z + l_i \cos(\varphi - \alpha)]^2}$; and the projection of these

distances on the *X-axis* (direction of the motion) is *[X-l₁ sin (φ-α)]*. Thus, the temperature rise at any point *M* caused by a segmental moving line heat source *dl*, including its image heat source is given by

$$d\theta_M = \frac{q_{pl}\,dl_1}{2\pi\,\lambda}\,e^{-\frac{[X-l_1'\sin(\varphi\cdot\alpha)]\,V_m}{2a}}\left[K_o\left(\frac{V_m R_1}{2\,a}\right)+K_o\left(\frac{V_m R_2}{2a}\right)\right]\quad\ldots\ldots\ldots\ldots[5.2]$$

The total temperature rise at any point *M* caused by the complete oblique moving band heat source including its image heat source of equal intensity is given by

$$\theta_M = \frac{q_{pl}}{2\pi\,\lambda}\int_{l_1=0}^{L}e^{-\frac{[X-l\sin(\varphi\cdot\alpha)]\,V_m}{2a}}\left[K_o\left(\frac{V_m R_1}{2\,a}\right)+K_o\left(\frac{V_m R_2}{2a}\right)\right]dl_1\quad\ldots\ldots\ldots\ldots[5.3]$$

Thus, the temperature rise in the chip due to primary heat source can be calculated from Equation (5.3) and is given by

$$\theta_{c-p} = \frac{q_p}{2\pi\,\lambda}\int_{l_1=0}^{L}e^{-\frac{[X-l_1\sin(\varphi-\alpha)]V_r}{2a}}\left[K_o\left(\frac{V_c R_1}{2\,a}\right)+K_o\left(\frac{V_c R_2}{2a}\right)\right]dl_1\quad\ldots\ldots\ldots\ldots[5.4]$$

where,

θ_{c-p}	=	Temperature rise in the chip due to the primary heat source, °C
q_p	=	Heat intensity of the primary heat source, J/cm-s
L	=	Length of the shear plane, cm
V_c	=	Chip velocity, cm/s
a	=	Thermal diffusivity of the chip, cm²/s
K_o	=	Modified Bessel function of the second kind of order zero
φ	=	Shear angle, degree
α	=	Rake angle, degree

The above equation is valid only in the region of the chip physically removed, not the imaginary chip as depicted by the dash lines since there is not any material in the imaginary region.

113

The effect of the secondary heat source is also considered as a continuous chip flow with an imaginary heat source, as shown in Fig.5.5. The interface frictional heat source relative to the chip is a band heat source moving with a velocity V_m. Considering the heat partition fraction for the chip to be B, the heat liberation rate Bq of the moving band heat source is considered totally transferred into the chip. Thus, the interface boundary is considered as adiabatic and the solution used should be for a semi-infinite medium. Since the heat source is entirely on the boundary surface, the solution for a semi infinite medium will be twice that for an infinite medium.

The chip thickness, t_c in metal cutting is considerably small. Hence, the boundary effect of the upper surface of the chip cannot be neglected. For this, an image heat source which is a mirror image of the chip-tool interface heat source with respect to the upper boundary surface of the chip and located at a distance of $2t_c$ from the primary interface frictional heat source as shown in Fig.5.5 should be considered. The liberation rate of the image heat source will be the same as the primary heat source when the upper surface is considered adiabatic.
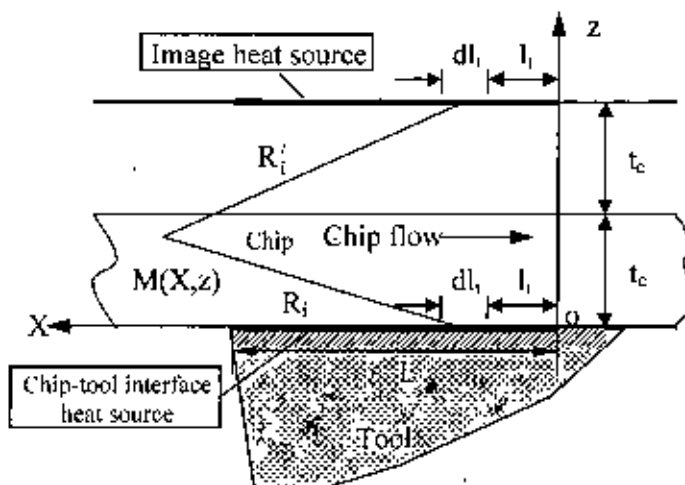
Fig. 5.5   Schematic of the moving heat source model of the secondary heat source for chip

The first objective in the analysis is to determine the temperature rise at any point $M(X, z)$ in the chip side caused by the interface frictional moving heat source including its image heat source. Referring to Fig.5.5, the tool-chip interface heat source of length L can be considered as a combination of a series of differential segments of width dl_t. Each segment can be considered as an infinitely long moving-line heat source. Thus, the semi-infinite solution of an infinitely long moving-line heat source given in the following [**Rosenthal 1946**] is used as a starting point.

$$\theta = \frac{q_l}{\pi \hat{\lambda}} e^{\frac{-XV_m}{2a}} K_0\left(\frac{RV_m}{2a}\right) \quad \ldots\ldots\ldots\ldots\ldots\ldots\ldots\ldots\ldots\ldots\ldots [5.5]$$

Using the above solution [**Rosenthal 1946**], the differential temperature rise at any point $M(X, z)$ caused by the differential segmental line heat source [the one located at a distance l_t from the origin o of the coordinate system used as shown in Fig.5.5] including its image line heat source is given by

$$d\theta_M = \frac{q_{pl} dl_t}{\pi \lambda} e^{\frac{-(X-l_t)V_m}{2a}} \left[K_0\left(\frac{R_l V_m}{2a}\right) + K_0\left(\frac{R_l' V_m}{2a}\right) \right] \quad \ldots\ldots\ldots\ldots [5.6]$$

The total temperature rise at any point $M(X, z)$ in the chip caused by the entire moving interface frictional heat source, including its image source, is given by

$$\theta_M = \frac{q_{pl}}{\pi \lambda} \int_{l_t=0}^{L} e^{\frac{-(X-l_t)V_m}{2a}} \left[K_0\left(\frac{R_l V_m}{2a}\right) + K_0\left(\frac{R_l' V_m}{2a}\right) \right] dl_t \quad \ldots\ldots\ldots\ldots [5.7]$$

Thus, the temperature rise in the chip due to entire moving interface frictional heat source can be calculated from Equation (5.7) and is given by

$$\theta_{c\text{-}s} = \frac{q_s}{\pi \lambda} \int_{l_t=0}^{l_t} B_1(x) e^{\frac{(X-l_t)V_c}{2a}} \left[K_0\left(\frac{R_l V_c}{2a}\right) + K_0\left(\frac{R_l' V_c}{2a}\right) \right] dl_t \quad \ldots\ldots\ldots [5.8]$$

115

where,

$\theta_{c\text{-}s}$ =   Temperature rise in the chip due to the secondary heat source, °C

q_s =   Heat intensity of the secondary heat source, J/cm-s

B_l =   Fraction of secondary heat source transfer into the chip

R_l = $\sqrt{(X - l_l)^2 + z^2}$

R'_l = $\sqrt{(X - l_l)^2 + (2t_c - z)^2}$

The above equations [Equation (5.4) and (5.8)] are valid only in the region of the chip removed. Considering both the primary heat source and the secondary heat source, the temperature rise in the chip is $\theta_{c\text{-}p} + \theta_{c\text{-}s}$.

5.2.2   Temperature Rise on the Chip-tool Interface in Tool

Fig.5.6 is a schematic of the heat transfer model of the frictional heat source at the tool-chip interface on the tool side. The interface frictional heat source relative to the tool is a stationary rectangular heat source of length, L_c and width w. Considering the heat partition fraction for the tool to be $(1\text{-}B)$, the heat liberation rate $(1\text{-}B)q$ of the stationary rectangular heat source is considered totally transferred into the tool. Thus, the interface boundary is considered as adiabatic and the solution used should be for a semi-infinite medium. Also, as the heat source is on the boundary surface, the semi-infinite solution is obtained by multiplying by two of the value for the solution of an infinite medium.

The clearance face of the tool should also be considered as an adiabatic boundary. Thus, the mirror image heat source of the primary stationary rectangular heat source with respect to the clearance surface should also be considered as shown in Fig.5.6. The heat liberation rate of the imaginary heat source is the same as that of the primary heat source.
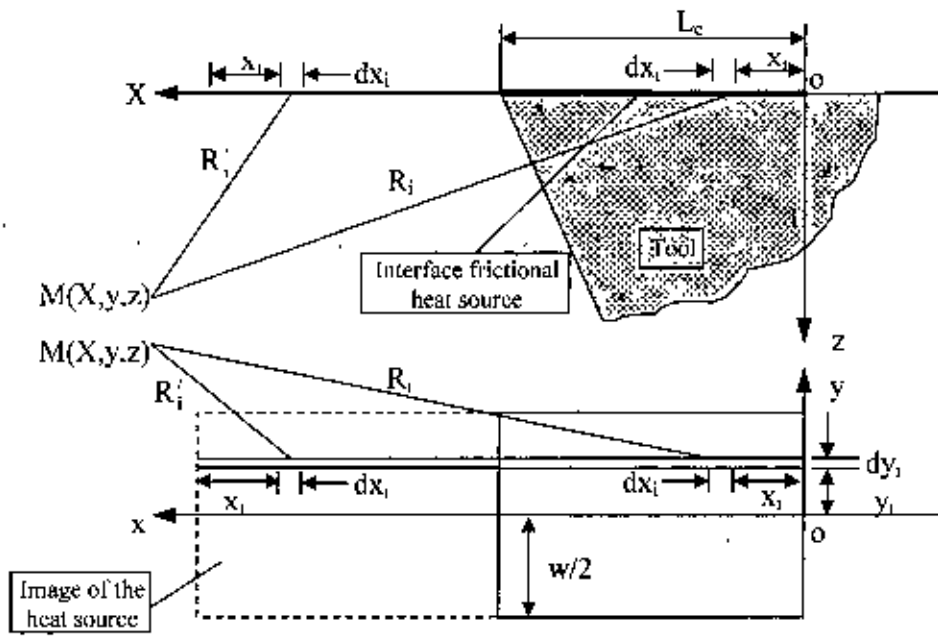
Fig. 5.6   Schematic of the stationary heat source model of the secondary heat source for the tool

The second objective in the analysis is to determine the temperature rise at any point $M(X, y, z)$ in the tool caused by the interface frictional stationary heat source including its image heat source. Referring to Fig.5.6, the tool-chip interface heat source of length L together with its image source can be considered as a combination of a series of differential segmental line heat source of width dy_i. Each segmental line can be considered as a combination of a series of elementary segments of length dx_i and each in turn can be considered as a point heat source continuously liberating heat. The rate of heat liberation of such a point heat source q_{pt} is given by

$$q_{pt} = \frac{q_0 dx_i dy_i}{L_c w} = q_{pl} dx_i dy_i \quad \text{...[5.9]}$$

Where, q_0 is the heat liberation rate of a rectangular heat source in J/s. So, for a uniform rectangular heat source, the heat liberation intensity q_{pl} is given by $q_0/L_c w$ in

117

J/cm^2-s. In this analysis, consider elementary solutions of the one-dimensional diffusion equation

$$\frac{\partial^2 \theta}{\partial x^2} = \frac{1}{\lambda}\frac{\partial \theta}{\partial t} \quad\dots\dots\dots\dots[5.10]$$

Now considering the expression

$$\theta = \frac{1}{\sqrt{t}}e^{\left(-\frac{x^2}{4\lambda t}\right)} \quad\dots\dots\dots\dots[5.11]$$

For this function it is readily seen that

$$\frac{\partial^2 \theta}{\partial x^2} = \frac{x^2}{4\lambda^2 t^{5/2}}e^{\left(-\frac{x^2}{4\lambda t}\right)\left(\frac{1}{2\lambda t^{3/2}}\right)} \quad\dots\dots\dots\dots[5.12]$$

$$\frac{\partial \theta}{\partial t} = \frac{x^2}{4\lambda t^{5/2}}e^{-\frac{x^2}{4\lambda t}} - \frac{1}{2t^{\frac{3}{2}}}e^{-x^2/4\lambda t} \quad\dots\dots\dots\dots[5.13]$$

showing that function (5.11) is a solution of Equation (5.10). It shows immediately that

$$\frac{1}{2\sqrt{\pi\lambda t}}e^{-\frac{(x-\xi)^2}{4\lambda t}} \quad\dots\dots\dots\dots[5.14]$$

where ξ is an arbitrary real constant, is also a solution. Further more if the function $\phi(x)$ is bounded for all real values of x, then it is possible that the integral

$$\frac{1}{2\sqrt{\pi\lambda t}}\int_{-\alpha}^{\alpha}\phi(\xi)e^{\left(-\frac{(x-\xi)^2}{4\lambda t}\right)}d\xi \quad\dots\dots\dots\dots[5.15]$$

Thus the Poisson integral

$$\theta(x,t) = \frac{1}{2\sqrt{\pi\lambda t}}\int\phi(\xi)e^{\left(-\frac{(x-\xi)^2}{4\lambda t}\right)}d\xi \quad\dots\dots\dots\dots[5.16]$$

118

is the solution of initial value problem. Now considering the Fourier equation of heat conduction

$$\frac{\partial^2 \theta}{\partial x^2} + \frac{\partial^2 \theta}{\partial y^2} + \frac{\partial^2 \theta}{\partial z^2} = \frac{1}{\lambda}\frac{\partial \theta}{\partial t} \qquad \dots\dots\dots\dots\dots\dots[5.17]$$

This equation is satisfied by solution of the type

$$\theta(x,y,z,t) = \frac{1}{8(\pi \lambda T)^{3/2}} e^{\left(\frac{-\left((x-x')^2+(y-y')^2+(z-z')^2\right)}{4\lambda T}\right)} \qquad \dots\dots\dots\dots\dots\dots[5.18]$$

where heat liberation intensity is unity. If q be the strength of an instantaneous point source of heat liberating at x', y', z' at time T=0. Then

$$\theta = \frac{q}{8(\pi \lambda T)^{3/2}} e^{\left(\frac{-\left((x-x')^2+(y-y')^2+(z-z')^2\right)}{4\lambda T}\right)} \qquad \dots\dots\dots\dots\dots\dots[5.19]$$

Generally instantaneous point heat source solution is taken as fundamental. By integrating with respect to time with a given rate of heat liberation continuous point heat source solution is obtained. For a continuous point heat source, when heat is liberated at a rate of $\phi(T)\rho C$ per unit time, from $T = 0$ to $T = T''$ at a location x', y', z', the temperature rise at x, y, z at time T is

$$\theta = \frac{1}{8(\pi \lambda(T-T'))^{3/2}} \int_0^t \phi(T')e^{\left(\frac{-\left((x-x')^2+(y-y')^2+(z-z')^2\right)}{4\lambda(T-T')}\right)} dt$$

$$= \frac{1}{8(\pi\lambda)^{3/2}} \int_0^t \phi(T') e^{-\frac{R^2}{4\lambda(T-T')}} \frac{dT'}{(T-T')^{3/2}} \qquad \dots\dots\dots\dots\dots\dots[5.20]$$

where $R^2 = -\left((x-x')^2 + (y-y')^2 + (z-z')^2\right)$.

If the rate of heat liberation is constant

$$\theta = \frac{q}{4(\pi\lambda)^{3/2}}\frac{\sqrt{\pi\lambda}}{R}erfc\frac{R}{\sqrt{4\lambda T}} = \frac{q}{4\pi\lambda R}erfc\frac{R}{\sqrt{4\lambda T}} \qquad \dots\dots\dots\dots\dots\dots[5.21]$$

119

For steady state distribution when $T \to \alpha$, $\theta = \dfrac{q}{4\pi\lambda R}$. So the steady state distribution of

stationary heat source is $\theta = \dfrac{q}{4\pi\lambda R}$. The temperature of the semi infinite solid would be

two times of this solution. Hence, the steady state solution of stationary heat source

$$\theta = \frac{q_{pl}}{2\pi\lambda R} \quad \text{..[5.22]}$$

Using this solution, the differential temperature rise at any point $M(X, y, z)$ caused

by one of the differential elementary point heat source [located at (x_i, y_i) in the coordinate

system used] including its related image point heat source is given by

$$d\theta_M = \frac{q_{pl}}{2\pi\lambda}\left(\frac{1}{R_i} + \frac{1}{R'_i}\right)dx_i dy_i \quad \text{..[5.23]}$$

The total temperature rise at any point $M(x, y, z)$ in the tool caused by the whole

stationary rectangular interface frictional heat source including its image source, is given

by

$$\theta_M = \frac{q_{pl}}{2\pi\lambda} \int\limits_{x_i=a}^{L} \int\limits_{y_i=-\frac{w}{2}}^{+\frac{w}{2}} \left(\frac{1}{R_i} + \frac{1}{R'_i}\right)dx_i dy_i \quad \text{..................................[5.24]}$$

Thus, the temperature rise in the tool due to whole stationary rectangular interface

frictional heat source including its image source can be calculated from Equation (5.24)

and is given by

$$\theta_{t-s} = \frac{q_s}{2\pi\lambda_t} \int\limits_{x_i=0}^{l_c} \int\limits_{y_i=-\frac{w}{2}}^{+\frac{w}{2}} [1-B_i(x_i)]\left(\frac{1}{R_i} + \frac{1}{R'_i}\right)dy_i dx_i \quad \text{............................[5.25]}$$

where,

$\theta_{t\text{-}s}$ = Temperature rise in the tool due to the secondary heat source. $^{\circ}$C

λ_t = Thermal conductivity of the tool insert, J/cm s $^{\circ}$C

L_c = Contact length, cm

w = Width of cut, cm

B_t = Fraction of the secondary heat source transferred into the chip

R_t = $\sqrt{(x-x_t)^2+(y-y_t)^2+z^2}$

R_t' = $\sqrt{(x-2L+x_t)^2+(y-y_t)^2+z^2}$

As high-pressure coolant jet is applied on the tool-rake face, the affected region on the tool rake face acts as a heat sink. It is assumed that the affected region has an area of the chip-tool contact length, L_c, by the width of cut, w (Fig.5.6). The heat loss is stationary with respect to the tool. The relative location of the imaginary heat loss is similar to that of the imaginary heat source in Fig.5.6. Thus, the temperature change in the tool due to heat loss including its image source can be calculated from Equation (5.25) and is given by

$$\theta_{t\text{-}hl} = \frac{q_{hl}}{2\pi\,\lambda_t} \int\limits_{x_t=0}^{L_c} \int\limits_{y_t=-\frac{w}{2}}^{+\frac{w}{2}} \left(\frac{1}{R_t}+\frac{1}{R_t'}\right)dy_t\,dx_t \qquad\dots\dots\dots\dots\dots\dots[5.26]$$

where,

$\theta_{t\text{-}hl}$ = Temperature change in the tool due to the heat loss. $^{\circ}$C

q_{hl} = Heat intensity of the heat loss due to high-pressure coolant, J/cm-s

R_t = $\sqrt{(x-x_t)^2+(y-y_t)^2+z^2}$

R_t' = $\sqrt{(x-2L+x_t)^2+(y-y_t)^2+z^2}$

In machining with high-pressure coolant jet cooling, part of the heat generated is removed by the coolant flowing over the exposed surfaces of the cutting region. In the

cooling processes the rate of removing heat by the coolant depends on the thermal conductivity of the coolant, coolant pressure and coolant temperature gradient at the cooled surface, the latter depending on the flow field in the coolant. The overall effect of the cooling actions can be described using a heat transfer coefficient, $\bar{h}$ defined by

$$q_{hl} = \bar{h}\left(\theta_r - \theta_o\right) \quad \dots\dots\dots\dots\dots\dots\dots\dots\dots\dots\dots\dots\dots\dots\dots\dots\dots\dots[5.27]$$

where,

q_{hl} = Heat intensity of the heat loss due to high-pressure coolant, J/cm-s

$\bar{h}$ = Average heat transfer coefficient, W/m^2-°C

θ_r = Average tool rake face temperature, °C

θ_o = Ambient temperature, °C

For forced convection heat transfer, a simplified form representing the heat transfer coefficient is usually used:

$$Nu = f(Re, Pr, Generic\ shape) \quad \dots\dots\dots\dots\dots\dots\dots\dots\dots\dots\dots\dots\dots\dots\dots[5.28]$$

where,

Nu = Nusselt number, $\dfrac{\bar{h}D}{\lambda_c}$

Re = Reynolds number, $\dfrac{\rho U_i D}{\mu}$

Pr = Prandtl number, $\dfrac{C_p \mu}{\lambda_c}$

$l\ and\ v$ = characteristic length and velocity

λ_c = Thermal conductivity of the coolant

ρ = Density of the coolant

μ = Viscosity of the coolant

C_p = Specific heat of the coolant

122

In the case of jet impinging on a surface (Fig.5.7) the heat transfer coefficient, h, depends also on other parameters: normalized jet nozzle-to-plane spacing L/D; jet inclination angle, α_j; displacement of the stagnation point from the geometric centre of the jet on the impingement surface, E; normalized distance from the stagnation point to a point considered on the impingement surface, r/D; jet Reynolds number $Re_j = \rho U_j D / \mu$. Which latter is based on the diameter of the nozzle, D, and the jet velocity at the exit plane of the nozzle, U_j.
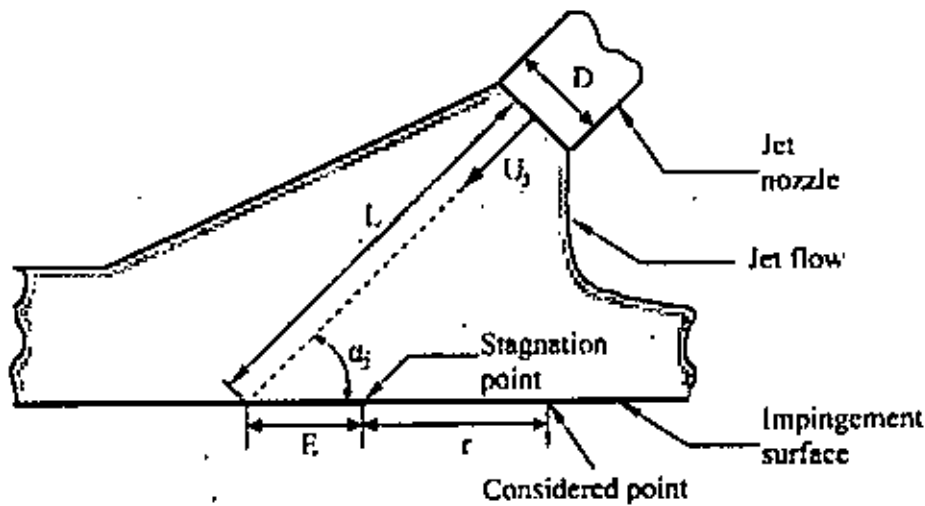
Fig. 5.7 Schematic view of the jet impinging on a flat surface

In the present study, the experimental work presented by Goldstein and Frankchett [1988] on heat transfer from a flat surface to an oblique air jet is considered for determining the heat transfer coefficient in overhead-jet cooling. Goldstein and Frankchett [1988] proposed a correlation equation for the local Nusselt numbers in the form

$$\frac{Nu}{Re_j^{0.7}} = A \, e^{\left[-(B + C \cos\phi)\left(\frac{r}{D}\right)^n \right]} \quad \text{...[5.29]}$$

where, D is the diameter of the jet nozzle, and, r and ϕ are cylindrical coordinates for correlation of contours of constant Nu. For two dimensional problems, r is the distance from the stagnation point on the cooled surface, whilst ϕ is determined according to

$$\phi = \begin{cases} 0 & \text{along the side of surface with } \alpha_j < \dfrac{\pi}{2} \\ \pi & \text{along the side of surface with } \alpha_j > \dfrac{\pi}{2} \end{cases} \quad \ldots\ldots\ldots\ldots\ldots\ldots\ldots[5.30]$$

The coefficients of the correlation of Equation (5.29) are shown in Table 5.1, where E is the displacement of the stagnation point as described in Fig.5.7. Good agreement between the Nusselt numbers calculated from Equation (5.29) and the experimental values was shown by Goldstein and Franchett [1988]. Unfortunately Equation (5.29) is based on experimental data for air jets only. However, since the main difference in heat transfer between air and liquid jets results from the physical properties of the two media, it is contented that Equation (5.29) can be modified for liquid jets, this modification can be achieved by adding the prandtl number, Pr, to the correlation.

Table 5.1   Correlation coefficient [Li 1996]

α_j	A			B	C	E		
	L/D=4	L/D=6	L/D=10			L/D=4	L/D=6	L/D=10
90^0	0.159	0.155	0.123	0.37	0.0	0.0	0.0	0.0
60^0	0.163	0.152	0.115	0.4	0.12	0.8	0.6	0.9
45^0	0.161	0.146	0.107	0.47	0.23	1.2	1.0	1.5
30^0	0.136	0.124	0.091	0.54	0.34	1.5	1.4	1.9

Prandtl does not appear in Equation (5.29), because for air $Pr \approx 0.7$ and $Pr^{1/3}$ (note that $Nu \propto Pr^{1/3}$) is close to unity. Therefore, Equation (5.29) may be rewritten with prandtl included

$$\frac{Nu}{Re_j^{0.7}} = \overline{A}\, Pr^{\frac{1}{3}}\, e^{\left[-(B+C\cos\phi)\left(\frac{r}{D}\right)^m\right]} \quad \ldots\ldots\ldots\ldots\ldots\ldots\ldots\ldots\ldots[5.31]$$

where $\overline{A}$ is a coefficient corresponding to A in Equation (5.29). From comparison of Equation (5.29) and Equation (5.31)

$$\overline{A} \, Pr^{\frac{1}{3}} = A \quad \cdots\cdots\cdots\cdots\cdots\cdots\cdots\cdots\cdots\cdots\cdots\cdots\cdots\cdots\cdots\cdots\cdots [5.32]$$

hence,

$$\overline{A} = \frac{A}{Pr^{\frac{1}{3}}} = 1.122\,A \quad \cdots\cdots\cdots\cdots\cdots\cdots\cdots\cdots\cdots\cdots\cdots\cdots\cdots [5.33]$$

where the value of Pr for air was taken at the temperature used in Goldstein and Franchett's experiments [1988], i.e. $Pr = 0.708$. Substituting Equation (5.33) into Equation (5.31) the modified form of Equation (5.29) is obtained.

$$Nu = \frac{\overline{h}\,D}{\lambda_c} = 1.122\,A\,Pr^{\frac{1}{3}}\,Re_j^{0.7}\,e^{\left[-(B+C\cos\phi)\left(\frac{r}{D}\right)^w\right]} \quad \cdots\cdots\cdots [5.34]$$

where the coefficients A, B, C and D are the same as those shown in Table 5.1. With the modified equation, Equation (5.34), the local Nusselt number for both air jets and liquid jets can be predicted if the relevant value for Pr is provided. Since Pr is composed entirely of the physical properties of the coolant and is a function of temperature, its value is determined according to the average temperature calculated from the heated surface temperature and the coolant bulk temperature. Since the flow of the applied coolant is parallel to the tool rake face and the back side of the chip, the forced convection effect can be considered as a fluid flow passing through parallel flat surfaces. The average heat transfer coefficient can be estimated by the Nusselt number from Equation (5.34).

In high-pressure coolant jet machining, the coolant is supplied at high pressure and flow rate. the relationships between coolant pressure, flow rate and the corresponding heat-transfer coefficient are now considered.

125

$$Re_j = \frac{\rho U_j D}{\mu} \quad \dots\dots\dots\dots\dots\dots\dots\dots\dots\dots\dots\dots\dots\dots\dots [5.35]$$

where, ρ and μ are the density and viscosity of the coolant respectively, D is the diameter of the jet nozzle and U_j is the velocity of the jet flow, which is given by.

$$U_j = \sqrt{\left(\frac{2P}{\rho} + \frac{Q^2}{A_p^2}\right)} \quad \dots\dots\dots\dots\dots\dots\dots\dots\dots\dots\dots\dots\dots [5.36]$$

Where, Q is the coolant flow rate, P is the coolant pressure and A_p is the cross-sectional area of the pipe. Considering the effect of coolant flow rate and coolant pressure, the effective heat transfer coefficient can be given as;

$$\overline{h}_{eff} = \Omega \overline{h} \quad \dots\dots\dots\dots\dots\dots\dots\dots\dots\dots\dots\dots\dots\dots\dots [5.37]$$

The coefficient, Ω, can be estimated experimentally. With both the secondary heat source and the heat loss due to convection. the temperature rise in the chip is $\Delta\theta_{c-s}$-$\Delta\theta_{t-hl}$. The temperature rise on the tool-chip interface is considered the same as that in the chip and in the tool. The heat partition function $B_1(x_i)$ is solved by the following relationship.

$$\theta_{c-p} + \theta_{c-s} = \theta_{t-f} + \theta_{t-hl} \quad \dots\dots\dots\dots\dots\dots\dots\dots\dots\dots\dots [5.38]$$

If a total of n points are of interest on the tool-chip interface, the same number of equations can be solved for the heat partition factors, $B_1^{(1)} \sim B_1^{(n)}$. Subsequently, the temperature distribution on the tool-chip interface can be obtained.

5.3   Experimental Model Validation

The validation of cutting temperatures in high-pressure coolant turning is verified by measuring the temperatures with a tool-work thermocouple located under the tool insert when turning C-60 steel with uncoated carbide tool inserts (SNMG-120408 and SNMM-120408, Sandvik) on a lathe under various cutting conditions, as shown in Table 5.2. The high-pressure coolant is applied through an external nozzle of 0.50 mm diameter along the auxiliary cutting edge. The high-pressure coolant system is used to supply the cutting oil of 6.0 l/min at a pressure of 80 bar. VG-68, cutting oil, is chosen as the cutting fluid. The cutting forces are recorded by a tool-post dynamometer (Kistler). The arrangement of the nozzle position and the thermocouple is shown in Fig.5.1.

Table 5.2   Test cutting conditions for sharp tools

Test No.	Cutting speed (m/min)	Feed rate (mm/rev)	Depth of cut (mm)
1	93	0.10	1.0
2	93	0.14	1.0
3	93	0.18	1.0
4	93	0.22	1.0
5	133	0.10	1.0
6	133	0.14	1.0
7	133	0.18	1.0
8	133	0.22	1.0
9	186	0.10	1.0
10	186	0.14	1.0
11	186	0.18	1.0
12	186	0.22	1.0
13	266	0.10	1.0
14	266	0.14	1.0
15	266	0.18	1.0
16	266	0 22	1.0

Assuming that the heat intensities are uniform on the shear plane and on the tool-chip interface, they can be calculated as:

$$q_p = \frac{F_c V}{w L} \qquad \dots\dots\dots\dots\dots\dots\dots\dots\dots\dots\dots\dots\dots\dots\dots\dots\dots\dots\dots\dots\dots\dots\dots[5.39]$$

$$q_s = \frac{F_t V}{w L_c} \qquad \dots\dots\dots\dots\dots\dots\dots\dots\dots\dots\dots\dots\dots\dots\dots\dots\dots\dots\dots\dots\dots\dots\dots[5.40]$$

where,

q_p	=	Heat intensity of primary heat source, J/cm-s
q_s	=	Heat intensity of secondary heat source, J/cm-s
F_c	=	Main cutting force, N
F_t	=	Feed force, N
V	=	Cutting speed. m/s
w	—	Width of cut, cm
L	=	Length of shear plane, cm
L_c	=	Natural chip-tool contact length, cm

The different heat generations in the cutting zones for dry and high-pressure coolant conditions are conveyed by the measured cutting forces which represent the lubricating effect in different circumstances. With the oil lubrication, the measured cutting forces in high-pressure coolant machining are expected smaller than those in dry cutting. The shear angle. φ and the contact length, L_c were obtained by [**Shaw 1996; Merchant 1945**]:

$$\frac{F_c}{F_t} = tan\,(\beta - \alpha) \qquad \dots\dots\dots\dots\dots\dots\dots\dots\dots\dots\dots\dots\dots\dots\dots\dots\dots\dots\dots[5.41]$$

$$\phi = \frac{\pi}{4} - \frac{1}{2}(\beta - \alpha) \qquad \dots\dots\dots\dots\dots\dots\dots\dots\dots\dots\dots\dots\dots\dots\dots\dots\dots[5.42]$$

$$L_c = \frac{t_o \, sin\beta}{sin\varphi \, cos(\varphi + \beta - \alpha)} \quad \text{...........[5.43]}$$

where,

t_o =   Uncut chip thickness. cm

β =   Friction angle in 2D force cutting model

α =   Rake angle

φ =   Shear plane angle

A carbide tool inserts (SNMG 120408 and SNMM 120408) with -6° rake angle and 6° clearance angle was used in this study. The material properties of the tool insert, the workpiece and the coolant are listed in Table 5.3. The estimated parameters according to the measured cutting forces for sharp tool are listed in Table 5.4 and Table 5.5.

Table 5.3   Properties of the insert, work material and cutting oil [**Shackelford et. al 1994; ASM handbook 1992**]

Insert	C 60 steel		Cutting oil			
Thermal conductivity (λ_t)	Thermal conductivity (λ)	Thermal diffusivity (a_c)	Density (ρ)	Prandtl number (Pr)	Absolute viscosity (υ)	Thermal conductivity (λ_o)
0.47 J/cm s °C	0.43 J/cm s °C	3.84 cm²/s	882 X 10⁻⁶ kg/cm³	754	68 X 10⁻⁶ m²/s	0.0015 J/cm s °C

Table 5.4   The estimated parameters for sharp SNMG insert

Test No.	Environment									
	Dry					High-pressure coolant				
	F_c	F_t	φ	β	L_c	F_c	F_t	φ	β	L_c
1	459	255	15.03	53.94	0.048	335	180	15.84	52.32	0.046
2	617	327	16.19	51.62	0.063	373	237	17.50	49.00	0.059
3	734	364	17.71	48.58	0.075	592	283	18.60	46.80	0.072
4	796	385	18.31	47.38	0.089	656	283	20.83	42.34	0.080
5	430	228	16.15	51.70	0.045	323	164	17.24	49.52	0.043
6	573	285	17.66	48.68	0.059	457	215	18.90	46.20	0.055
7	657	313	18.66	46.68	0.072	549	249	19.72	44.56	0.069
8	747	348	19.15	45.70	0.086	627	256	21.98	40.04	0.077
9	423	213	17.34	49.32	0.043	322	154	18.60	46.80	0.040
10	506	223	20.40	43.20	0.052	430	173	22.30	39.40	0.048
11	587	277	18.84	46.32	0.072	501	226	19.85	44.30	0.068
12	693	313	19.85	44.30	0.084	582	232	22.47	39.06	0.075
13	379	188	17.71	48.58	0.042	328	151	19.46	45.08	0.039
14	473	178	23.62	36.76	0.046	412	139	25.61	32.78	0.043
15	547	235	20.90	42.20	0.066	469	190	22.14	39.72	0.062
16	624	259	21.66	40.68	0.078	560	208	23.90	36.20	0.072

Table 5.5   The estimated parameters for sharp SNMM insert

Test No.	Environment									
	Dry					High-pressure coolant				
	F_c	F_t	φ	β	L_c	F_c	F_t	φ	β	L_c
1	483	248	16.89	50.22	0.044	350	168	18.49	47.02	0.040
2	620	311	17.45	49.10	0.059	447	183	21.90	40.20	0.049
3	686	337	17.92	48.16	0.074	529	187	24.78	34.44	0.057
4	706	341	18.31	47.38	0.089	573	178	27.09	29.82	0.065
5	467	219	19.02	45.96	0.039	352	145	21.74	40.52	0.035
6	567	253	20.12	43.76	0.053	431	157	24.18	35.64	0.045
7	671	294	20.54	42.92	0.066	532	164	27.21	29.58	0.053
8	704	299	21.20	41.60	0.079	604	172	28.46	27.08	0.062
9	435	182	21.42	41.16	0.036	356	126	24.78	34.44	0.032
10	542	214	22.64	38.72	0.048	463	148	26.62	30.76	0.042
11	622	241	23.07	37.86	0.060	539	143	29.55	24.90	0.049
12	662	247	23.80	36.40	0.072	596	158	29.55	24.90	0.060
13	376	145	23.07	37.86	0.033	323	93	28.20	27.60	0.028
14	482	177	24.09	35.82	0.045	406	110	29.27	25.46	0.039
15	533	190	24.68	34.64	0.073	477	115	30.86	22.28	0.047
16	621	210	25.61	32.78	0.068	578	138	31.01	21.98	0.058

5.4   Results and Discussion

The model-predicted temperatures and the measured temperatures under the tool insert for different cutting conditions are shown in Fig.5.8 and Fig.5.9. The deviations are within 9 % of error. Most of the predicted temperatures are a little bit higher or lower than the recorded temperature. The difference in cutting temperatures for dry and high-pressure coolant conditions is closely related to the difference in cutting forces. The greater the cutting forces the more heat is generated and consequently the higher cutting temperatures. Moreover, the average cutting temperature reduction, relative to dry machining, on the chip-tool interface in HPC machining is below 7%. This insignificant effect can be understood based on the mechanics of the cooling process. First, the tool rake face, where heat is removed, is far away from the cutting zone as compared to the dimensions of the heat sources. The temperatures difference between the tool rake face and the coolant are not as much as that between the coolants flow temperature and the maximum temperature at the tool-chip interface. Thus, the heat taken away from the tool rake face is relatively insignificant. Even if more cutting fluid is applied, the temperature reduction on the tool-chip interface is still limited by a low heat transfer coefficient. Secondly, the heat transfer rate is proportional to the heat coefficient of the medium. In this study, it was found that the heat intensity for the cooling process is almost two orders of magnitude less than the heat intensity generated in the primary shear zone or the tool-chip interface. Therefore, only a small portion of the heat can be removed from the cutting zone.
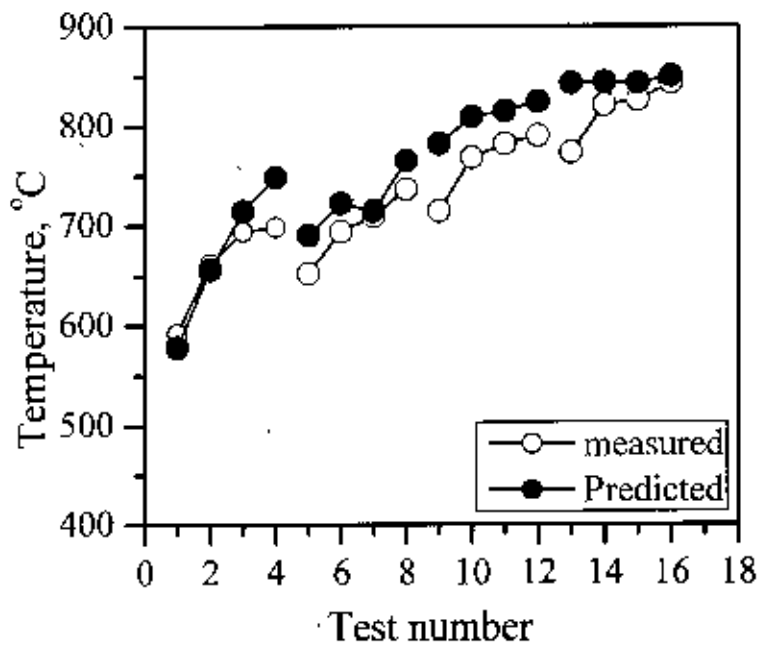
(a) Dry condition
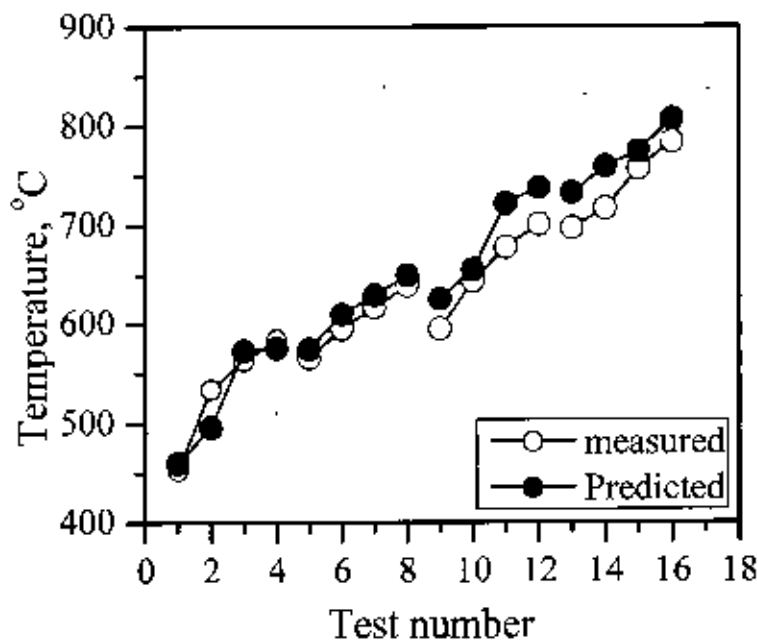
(b) HPC condition

Fig.5.8 Comparison of measured and predicted chip-tool interface temperature attained in (a) **Dry** and (b) **HPC** condition in machining **C-60 steel by SNMG** insert
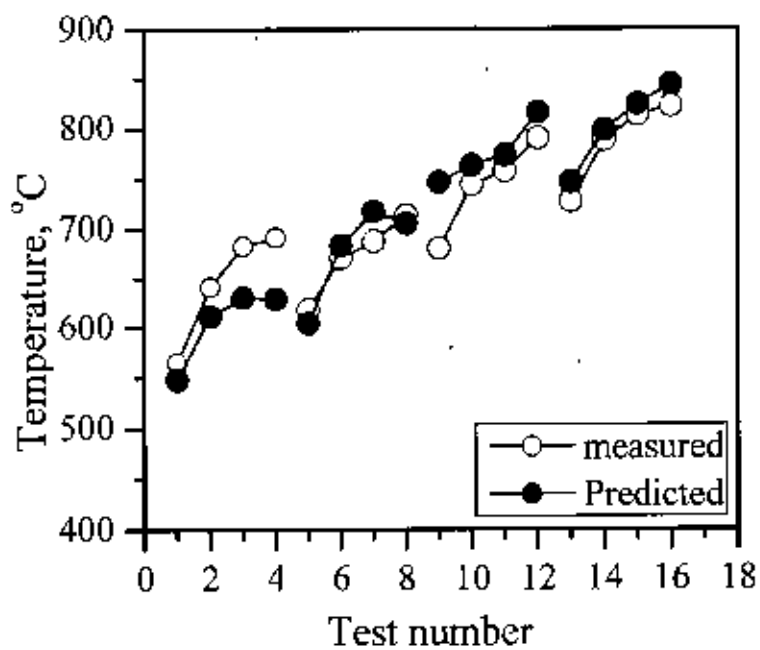
(a) Dry condition
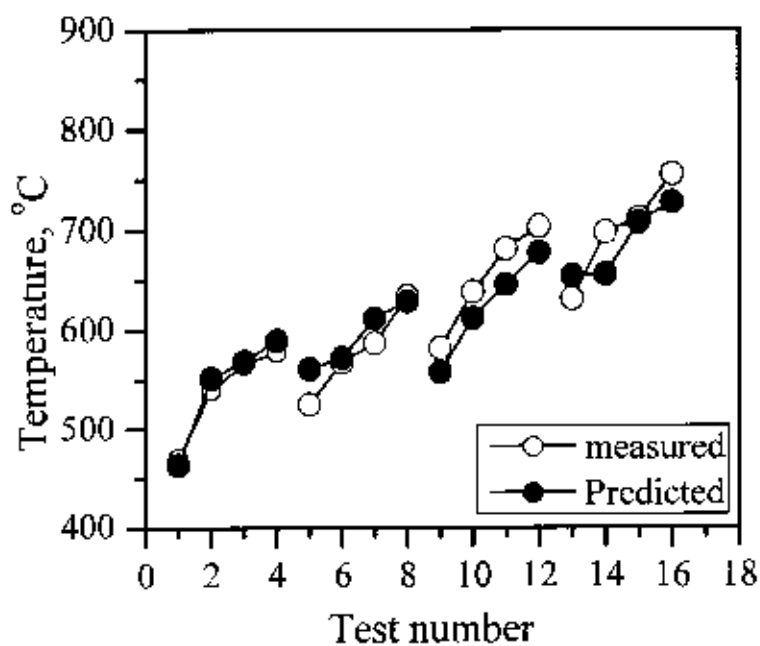
(b) HPC condition

Fig.5.9   Comparison of measured and predicted chip-tool interface temperature attained
in (a) Dry and (b) HPC condition in machining C-60 steel by SNMM insert

Chapter-6

Discussion on Experimental Results

6.1   Chip Formation

Chip thickness ratio, r_c (ratio of chip thickness before and after cut) is an important machinability index of chip formation and specific energy consumption for a given tool-work combination. For given cutting conditions, the value of chip thickness ratio depends upon the nature of chip-tool interaction, chip contact length and chip form all of which are expected to be influenced by high-pressure coolant (HPC) jet in addition to the levels of cutting speed and feed rate. Chip thickness ratio (r_c) is evaluated from the ratio,

$$r_c = \frac{t_a}{t_c} = \frac{\sin \varphi}{\cos(\varphi - \alpha)} \quad \text{..[6.1]}$$

where,

t_a = chip thickness before cut, cm

t_c = chip thickness after cut, cm

φ = shear angle, degree

α = rake angle, degree

In machining conventional ductile metals and alloys producing continuous chips, the value of r_c is generally less than 1.0 because chip thickness after cut (t_c) becomes

greater than chip thickness before cut (t_o) due to almost all sided compression and friction at the chip-tool interface. Smaller value of r_c means larger cutting forces and friction and is hence undesirable.

The effect of increase in V and f and the change in environment on the value of chip thickness ratio, r_c obtained during turning C-60 steel are shown in Fig.4.10 which depict some significant facts;

i.   values of r_c has all along been less than 1.0

ii.   reduction of cutting zone temperature by the application of high-pressure coolant jet increased the value of r_c further

iii.   the value of r_c increased with increase in V and f

In machining any conventional ductile metals like steels also r_c increases with increases in V due to plasticization and shrinkage of shear zone. With the increase in feed rate (i.e. uncut chip thickness) also the value of r_c increases due to increase in effective rake angle of the tool with edge beveling and its effect [Kronenberg 1943] on r_c is given by,

$$r_c = e^{-\mu\left(\frac{\pi}{2} - \alpha\right)} \quad \text{............................} \quad [6.2]$$

where,

μ =   apparent coefficient of friction at the chip-tool interface

α =   effective tool rake angle

The figures from Fig.4.10 to Fig.4.12 clearly show that throughout the present experimental domain the value of r_c gradually increased with the increase in V though in different degree for the different tool-work combinations, under both dry and HPC conditions. The value of r_c usually increases with the increase in V particularly at its lower range due to plasticization and shrinkage of the shear zone for reduction in friction and built-up edge formation at the chip-tool interface due to increase in temperature and sliding velocity. In machining steels by tools like carbide, usually the possibility of built-up edge formation and size and strength of the built-up edge, if formed gradually increase with the increase in temperature due to increase in V and also f and then decrease with the further increase in V due to too much softening of the chip material and its removal by high sliding speed.

Fig.4.10 shows that high-pressure coolant jet has increased the value of r_c particularly at lower values of V and f when the C-60 steel rod was machined by both the inserts. By high-pressure coolant jet applications, r_c is reasonably expected to increase for reduction in friction at the chip-tool interface and reduction in deterioration of effective rake angle by built-up edge formation and wear at the cutting edges mainly due to reduction in cutting temperature. In case of C-60 steel, more effective HPC cooling seemingly enabled more increase in r_c at lower V and f when machined by SNMM insert. In case of the other steel specimen, the degree of upsurge in r_c has been relatively much less as can be seen in Fig.4.11 and Fig.4.12 for both the inserts. This can be attributed mainly to less effective of high-pressure coolant at the chip-tool interface in case of those steels. Compared to the C-60 steel, 17CrNiMo6 steel and 42CrMo4 steel yielded lesser value of r_c (except when machining 42CrMo4 steel by SNMM insert) possibly for shorter chip-tool contact length and smoother chip formation respectively. The value of r_c has also been less affected by variation in V and f in case of 17CrNiMo6 steel as can be seen in the

concerned figures. This might be due to as such more stability of this steel against seizure and built-up edge formation even under dry machining.

The pattern of chips in machining ductile metals are found to depend upon the mechanical properties of the work material, tool geometry particularly rake angle, levels of V and f, nature of chip-tool interaction and cutting environment. In absence of chip breaker, length and uniformity of chips increase with the increase in ductility and softness of the work material, tool rake angle and cutting speed unless the chip-tool interaction is adverse causing intensive friction and built-up edge formation.

Table 4.3 shows that the C-60 steel, whose strength and hardness are much less compared to that of the other steels, when machined by the pattern type SNMG insert under dry condition produced loose arc chips. The geometry of the SNMG insert is such that the chips of this softer steel (C-60 steel) first came out continuously, got curled along normal plane and then hitting at the principal flank of this insert broke into pieces with regular size and shape. When machined under high-pressure coolant condition the form of these ductile chips did not change but their back surface appeared much brighter and smoother. This indicates that the amount of reduction of temperature due to high-pressure coolant enabled favourable chip-tool interaction and elimination of even trace of built-up edge formation. Fig.4.13 typically shows that the same tool-work combination provided loose arc chips when machined with high-pressure coolant jet. The colour of the chips have also become much lighter i.e. metallic from blue due to reduction in cutting temperature due to high-pressure coolant jet.

It is important to note in Table 4.3 as well as in Fig.4.14 that the role of high-pressure coolant jet has been more effective in respect of form and colour of the chips

when the same steel was machined by the groove type SNMM inserts. Such improvement can be attributed to effectively larger positive rake of the tool and better cooling by the jet coming along the groove parallel to the cutting edges.

The favourable effects of high-pressure coolant on chip formation were found to be relatively less in case of the other steels possibly because their stronger chips adhering intimately on the rake surface did not allow high-pressure coolant to reach and that effectively cool the chip-tool interface when those steels were machined by the SNMG inserts as can be seen in the tables from Table 4.4 and Table 4.5 as well the figures from Fig.4.15 to Fig.4.18. However, it is also evident from the aforesaid tables and figures that when those steels were machined by the SNMM inserts, high-pressure coolant jet could provide relatively more favourable effects on chips' form for the reasons already mentioned. However, the colour of the chips of the alloy steels significantly changed with the application of high-pressure coolant jet for both the cutting inserts. This seemingly happened due to post cooling by high-pressure coolant jet in addition to reduction in chip-tool and work-tool interface temperature.

Almost all the parameters involved in machining have direct and indirect influence on the thickness of the chips during deformation. The degree of chip thickening which is assessed by chip thickness ratio (r_c) plays sizeable role on cutting forces and hence on cutting energy requirements and cutting temperature. The role of high-pressure coolant jet on r_c have been discussed in the section dealing with cutting forces.

6.2 Cutting Temperature

High production machining and grinding are inherently associated with generation of large amount of heat and development of high cutting temperature at the

138

cutting zone. Such high cutting temperature not only reduces tool life but also impairs the dimensional accuracy and surface integrity of the component produced. Besides, this high temperature invites environmental problems when tried to be controlled by conventional cutting fluid application. The cutting temperature and its detrimental effects increase with

i.   increase in specific energy requirement for machining depending upon the tool material and the cutting tool geometry

ii.   increase in metal removal rate (MRR) i.e. cutting speed (V) and feed rate (f)

iii. absence or inadequate or ineffective cutting fluid application

Tool-work thermocouple technique is as such simple and reliable but limited to measurement of average cutting temperature. The understanding of temperature distribution in the cutting zone under high-pressure coolant condition is a prerequisite to the analysis of cutting tool wear behavior. Hence, the modelling of cutting temperature has been essential for evaluation of cutting temperature under high-pressure coolant condition and also for precisely determining the distribution of temperature in the cutting zone under any condition. But the modelling essentially need to be capable to predict temperature distribution reasonably accurately and reliably.

Fig.5.7 shows that the values of the average chip-tool interface temperature, θ predicted by the used model are adequately close agreement with their measured values. The deviations may be attributed mainly to the assumption that the entire cutting energy is converted into heat. Actually, a small fraction of the cutting energy remains frozen in the chips as residual strain and its percentage decreases with the increase in the level of the cutting temperature due to increase in cutting speed (V) and feed rate (f). However, the deviations between the predicted and the measured temperatures within the domain of the present study, excepting at few points, have been within around 10%, which is reasonably

acceptable from engineering point of view [Ding and Hong 1998]. The pattern of temperature distribution at the cutting zone attained by the present model for dry machining are also matching with the corresponding results reported earlier [Ding and Hong 1998, Muraka et al. 1979, Stevenson et al. 1983, Strenskovski and Kyung-jin 1990 and Tay et al. 1974]. Therefore, the presently used model could be considered reasonably accurate and valid for evaluation of cutting temperature.

A temperature model based on heat source and heat sink mechanisms for high-pressure coolant machining is presented. With cutting forces and the material properties as inputs, the average tool-chip interface temperature are obtained. The cooling effect in high-pressure coolant situations is modeled as heat losses on the tool rake face and the chip surface. In addition, the lubricating effect on cutting temperatures in high-pressure coolant machining is considered by the change of cutting forces which lead to different heat intensities in the cutting zone. For the temperature rise in the chip on the tool-chip interface, the effects of the shearing heat source on the shear plane and the frictional heat source on the tool-chip interface are modeled as moving heat sources. For the temperature rise in the tool on the tool-chip interface, the effects of the secondary heat source due to friction and the heat loss due to cooling on the tool rake face are modeled as stationary heat sources. The results also show that the cutting speed plays an important role for the temperature rise in turning processes. Moreover, the reduction in the cutting temperatures is small by considering the lubricating effect as the reduction in cutting forces, and consequently the cooling effect on the tool rake wear face is insignificant when the differences in cutting forces between dry and high-pressure turning are small.

The cutting temperature generally increases with the increase in V and f, though in different degree, due to increased energy input and it could be expected that high-pressure

coolant would be more effective at higher values of V and f. The average chip-tool interface temperature (θ) have been determined by using tool-work thermocouple technique and plotted against cutting speed for different work-tool combinations, feed rates and environments undertaken. The figures from Fig.4.19 to Fig. 4.21 are showing how and to what extent θ has decreased due to high-pressure coolant application under the different experimental conditions. With the increase in V and f, θ increased as usual, even under high-pressure coolant condition, due to increase in energy input. The difference in θ noted for the different work-tool combinations under dry machining and same V-f conditions has been mainly due to difference in specific energy requirement or value of F_c and F_t which largely depend upon the dynamic yield shear strength, τ_s of the work material and geometry of the cutting tool. The magnitude of F_c and F_t are again likely to be affected by high-pressure coolant jet which may change the nature of chip-tool interaction and also the value of τ_s to some extent.

Apparently more drastic reductions in θ are expected by employing high-pressure coolant jet But practically it has not been so because the high-pressure coolant has been employed in the form of thin jet along the cutting edge and towards only the chip-tool interface instead of bulk cooling. Also the jet, like any cutting fluid, could not reach deeply in the chip-tool interface for plastic or bulk contact. particularly when V and f are large.

The percentage saving in θ attained by high-pressure coolant for different tool-work combinations, cutting speed and feed rate have been extracted from the previous figures and shown in Table 6.1 for different work-tool combinations. Saving in the cutting forces, F_c and F_t are also shown in Table 6.2. The tables indicate that the role of variation of the process parameters; V and f and tool configuration on percentage reduction of θ as well as cutting forces, F_c and F_t due to high-pressure coolant jet have not been uniform for

141

the different work materials. Table 6.1 shows that in case of C-60 steel, high-pressure coolant enabled sizeable reduction in θ as well as F_c and F_t and the degree of their reduction decreased quite uniformly with the increase in f and V. Also the SNMM type insert provided more effective in high-pressure coolant machining seemingly through more sizeable reduction in the cutting forces. But such trends are absent in case of the other two steels. Besides that, in case of those steels though high-pressure coolant provided lesser savings in θ and cutting forces but there is no clear trend in the relation between the patterns of savings in θ and the cutting forces. This may be attributed to variation in the chip forms particularly chip-tool contact length, L_c which for a given tool widely vary with the mechanical properties and behaviour of the work material under the cutting conditions. The value of L_c affects not only the cutting forces but also the cutting temperature.

Table 6.1   Reduction in average chip-tool interface temperature due to high-pressure coolant jet in turning different steels by SNMG and SNMM inserts.

f mm/rev	V m/min	C-60 steel		17CrNiMo6 steel		42CrMo4 steel	
		SNMG	SNMM	SNMG	SNMM	SNMG	SNMM
0.10	93	14.36	16.81	10.10	12.87	11.54	13.97
	133	10.43	14.89	11.44	11.60	10.03	12.41
	186	14.15	14.41	11.87	12.45	10.36	13.04
	266	10.09	13.20	12.31	11.42	11.23	12.30
0.14	93	13.54	15.76	10.46	10.57	11.34	11.89
	133	11.67	15.22	11.91	11.20	10.77	11.39
	186	13.80	14.25	12.50	11.58	11.66	10.46
	266	10 48	11.55	11.44	11.35	10.40	11.54
0.18	93	14.27	17.01	10.63	12.41	12.14	10.56
	133	10.44	15.78	11.86	10.79	11.28	11.84
	186	11.00	10.04	10.51	11.33	10.43	11.07
	266	10.24	12.55	11.62	10.26	11.76	10.29
0.22	93	13.75	16.35	10.96	12.09	12.69	10.48
	133	10.60	11.08	10.68	10.94	10.81	11.61
	186	11.25	11.01	10.06	10.41	10.94	11.96
	266	10.70	11.38	10.36	10.51	10.55	10.60

6.3 Cutting Forces

Machinability, i.e. ease of machining any material is judged by

i.   magnitude of cutting forces

ii.   level of cutting temperature

iii. tool wear and tool life

iv.   surface integrity of the product

Productivity, product quality and overall economy of machining of any material is governed mainly by its machinability characteristics which can be improved without scarifying material removal rate (MRR) by reducing cutting forces and temperature and enhancing tool life and surface quality.

Large cutting forces means high specific energy requirement for machining and high cutting temperature that adversely affect the tool life as well as dimensional accuracy and surface finish of the products. The magnitude of the cutting force increases almost proportionately with the increase in chip load (f X d) and shear strength of the work material. But, the actual values of cutting forces are also governed by several other factors such as tool life and machining environment. However, attempts should always be made to minimize the magnitude of cutting forces without sacrificing the MRR and product quality.

The role of major factors on the magnitude of the cutting force components (as shown in Fig.6.1) in machining like turning of ductile materials are generally expressed by the following expressions,
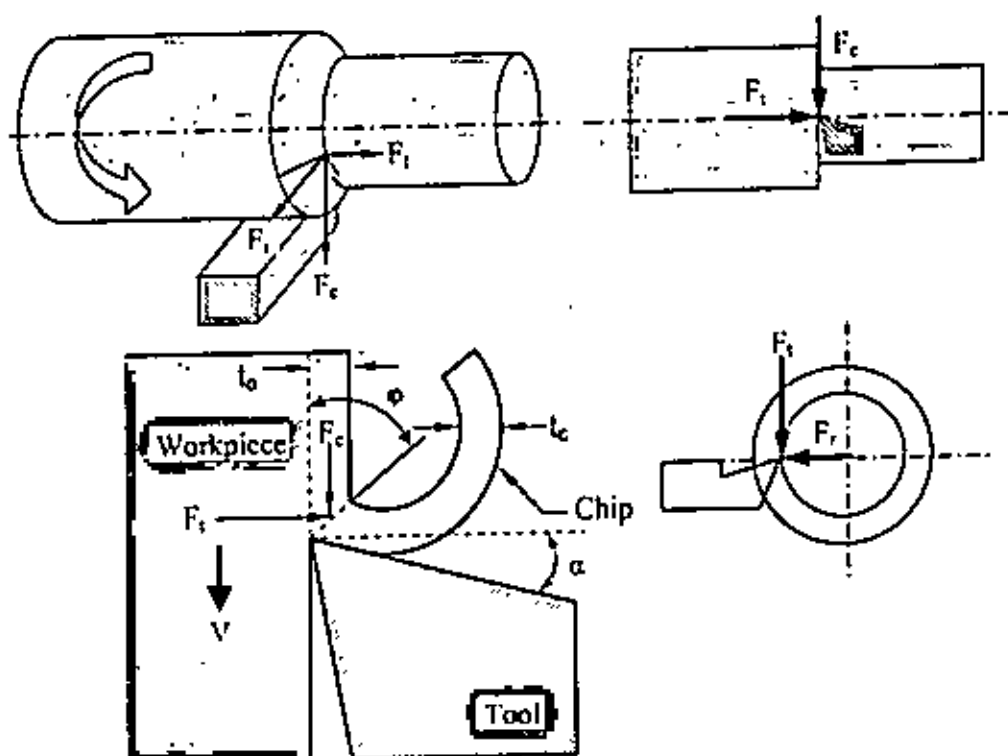
Fig.6.1 Component of cutting forces acting on the tool

$$F_c = d f \tau_s \left(\cot \varphi + I \right) \quad \text{...[6.3]}$$

$$F_t = d f \tau_s \left(\cot \varphi - I \right) \quad \text{...[6.4]}$$

where,

F_c = tangential component of the cutting force, N

F_t = axial component of the cutting force (thrust force), N

d = depth of cut, cm

f = feed rate, mm/rev.

τ_s = shear strength of the work material,

φ = shear angle (Fig.6.1) of chip formation

F_c is the major component, which also decides power consumption, and F_t is an indirect indicator of the nature of chip-tool indicator like friction. For machining conventional materials producing continuous chips the shear angle φ can be replaced by r_c

as.

144

$$\cot \varphi = \frac{1}{r_c} - \tan \alpha \qquad \text{[6.5]}$$

then the equations 6.3 and 6.4 become

$$F_c = d \, f \, \tau_s \left(\frac{1}{r_c} - \tan \alpha + 1 \right) \qquad \text{[6.6]}$$

$$F_t = d \, f \, \tau_s \left(\frac{1}{r_c} - \tan \alpha - 1 \right) \qquad \text{[6.7]}$$

In machining ductile metals, particularly steels, the actual value of τ_s is affected [Abuladze 1962] by the values of tool rake angle and r_c as,

$$\tau_s = 0.74 \, \sigma_u \, \varepsilon^{0.6\Delta} \qquad \text{[6.8]}$$

where,

σ_u =   ultimate tensile strength of the work material at normal condition

Δ =   percentage elongation of the work material

ε =   average cutting strain [Bhattacharyya 1984]

$$\varepsilon = \cot \varphi + \tan(\varphi - \alpha) \qquad \text{[6.9]}$$

where,

φ =   shear angle

α =   rake angle

The figures from Fig.4.10 to Fig.4.12 clearly show that throughout the present experimental domain the value of r_c gradually increased with the increase in V though in different degree for the different tool-work combinations, under both dry and high-pressure coolant conditions. It is also noted in those figures that r_c increased all along also

with the increase in f expectedly due to increase in average rake angle with increase in uncut chip thickness.

It clearly appears in all the figures from Fig.4.22 to Fig.4.27 that both the cutting force components, F_c and F_t have gradually decreased with the increase in V almost in the opposite way the value of r_c increased. Equations 6.6 and 6.7 also indicate that for the same chip load the magnitude of the cutting forces are governed mainly by the value of r_c. According to equations 6.5, 6.8 and 6.9, the value of τ_s also decreases, though in lesser degree, with the increase in r_c. But τ_s may also increases to some extent with the increase in V due to softening of the work material by cutting temperature, particularly if it is very high for the work material. Therefore, it can be concluded that the main reasons behind decrease in cutting forces with the increase in V are that which cause increase in r_c with increase in V. It is also interesting and important to note that though apparently and according to equations 6.6 and 6.7, the magnitude of F_c and F_t should increase proportionally with the increase in feed rate, f but actually the rate of increase of F_c and F_t with that of f has been much less, though in different degree for different tool-work combinations and environments undertaken, as can be seen in the given figures. This can be attributed mainly to upsurge in r_c with the increase in f for increase in average effective rake angle of the tool with the increase in uncut chip thickness.

The experimental results are showing that though the 17CrNiMo6 and 42CrMo4 steels provided much lesser value of r_c compared to that provided by the C-60 steel, the difference in the cutting forces have been quite less. This is obvious for higher strength of the 17CrNiMo6 and 42CrMo4 steels. But inspite of providing almost same value of r_c, the stronger 17CrNiMo6 steel required lesser cutting forces compared to softer C-60 steel during dry machining particularly at lower V. This can be explained by the fact that under

cutting condition, the dynamic yield shear strength, τ_s of 17CrNiMo6 steel did not increase that much like that of C-60 steel due to lesser percentage elongation of the former steel.

Fig.4.22 shows that the main cutting force, F_c decreased sizeably when C-60 steel was machined by high-pressure coolant jet expectedly mainly for upsurge in r_c due to favourable change in the chip-tool interaction and reduction of adverse change in the tool rake angle by controlling cutting temperature. Such reduction in F_c has been more predominant reasonably at lower ranges of V and f when high-pressure coolant jet was more effective.

It is also evident from Fig.4.22 that high-pressure coolant provided more significant reduction in F_c expectedly when C-60 steel was machined by the SNMM insert which enabled more favourable chip form and larger upsurge in r_c by more effective high-pressure coolant. But reduction in F_c by the application of high-pressure coolant jet have been considerably less in case of the other two steels, as can be seen in Fig.4.23 and Fig.4.24 and also in the Table 6.2. Inability of the high-pressure coolant jet to reach and cool the chip-tool interface effectively and increase r_c seems to be the main reason behind such lesser reduction in F_c by high-pressure coolant application. However, effect of high-pressure coolant jet in respect of F_c has been somewhat better when these steels were machined by the SNMM inserts which seemingly allowed coolant to reach closer to the chip-tool interfaces.

Fig.4.22, Fig.4.25 and Table 6.2 reveal that the high-pressure coolant jet had more favourable effect on F_t than on F_c expectedly because chip-tool friction and configuration of the tool rake surface and any change in them have physically more influence on F_t the direction of which is almost parallel to the rake surface. Equations 6.6 and 6.7 also indicate

that any change in value of r_c' would have more impact (in terms of percentage variation) on F_t than on F_c. It is further evident from those figures and table that high-pressure coolant jet reduced F_t also more successfully when C-60 steel was machined by the SNMM type inserts.

Table 6.2   Percentage reduction in cutting forces due to high-pressure coolant in turning different steels by SNMG and SNMM inserts

f mm/rev	V m/min	C-60 steel				17CrNiMo6 steel				42CrMo4 steel			
		SNMG		SNMM		SNMG		SNMM		SNMG		SNMM	
		F_c	F_t	F_c	F_t	F_c	F_t	F_c	F_t	F_c	F_t	F_c	F_t
0.10	93	13.29	16.08	15.11	20.75	8.75	12.20	12.88	19.94	9.05	13.05	10.55	18.69
	133	11.16	15.28	15.91	25.75	6.52	9.73	11.33	17.25	9.41	13.33	11.87	19.89
	186	9.14	13.94	13.73	25.88	9.09	15.22	9.61	17.40	7.01	13.44	8.68	17.72
	266	8.97	15.78	11.17	22.93	9.09	14.19	11.92	20.33	4.83	12.00	7.62	18.68
0.14	93	14.10	18.76	16.96	25.72	11.26	16.71	10.87	18.29	8.78	14.01	11.08	19.10
	133	11.52	16.21	14.91	24.00	9.18	15.03	9.81	16.56	6.08	12.12	9.42	22.11
	186	11.07	14.03	13.01	26.02	6.93	15.83	5.80	14.95	5.44	14.07	7.30	17.08
	266	11.21	17.89	11.62	26.47	8.14	14.08	9.41	19.49	4.40	12.38	5.46	15.03
0.18	93	12.53	15.94	14.41	24.80	10.32	16.41	9.91	17.82	8.86	12.07	9.10	18.73
	133	11.72	16.27	11.68	22.22	10.39	15.87	9.06	16.11	7.14	13.17	8.93	21.18
	186	11.41	21.36	12.79	26.10	8.12	13.49	7.20	15.80	5.45	10.16	5.28	14.08
	266	10.05	19.70	9.94	24.88	6.27	10.98	6.05	15.91	3.59	8.13	4.77	16.61
0.22	93	11.31	17.63	12.18	23.55	9.80	16.51	11.82	19.78	8.75	13.82	10.71	21.40
	133	10.31	17.30	12.06	22.66	8.50	15.60	8.33	16.23	6.11	12.97	8.13	17.17
	186	5.59	14.01	10.88	23.39	4.65	11.85	9.40	17.22	4.04	9.48	5.55	16.87
	266	5.13	15.76	9.82	24.72	2.32	12.42	9.65	18.60	2.67	9.62	3.19	10.46

The figures from Fig 4.22 to Fig.4.27 as well as Table 6.2 clearly visualise that reduction in the cutting forces by high-pressure coolant jet happened to be much less in case of the alloy steels compared to the C-60 steel. However, in case of those alloy steels

also, the benefit of the high-pressure coolant has been relatively higher in respect of F_t than F_c and when those steels were machined by the SNMM type inserts.

6.4   Tool Wear and Tool Life

Machining operations are accomplished using cutting tool. The high forces and temperatures during machining create a very harsh environment for the tool. If cutting force becomes too large, the tool fractures. If cutting temperature becomes too high, the tool material softens and fails. And if neither of those conditions causes tool failure, continual wearing action on the cutting tool ultimately leads to failure.

It is already mentioned that wear of cutting tools are generally quantitatively assessed by the magnitudes of VB, VS, KT etc. shown in Fig.4.28, out of which VB is considered to be the most significant parameter at least in R&D work.

It was reported [Paul et al. 2000 and Seah et al. 1995] earlier that application of conventional cutting fluid does not help in reducing tool wear in machining steels by carbides rather may aggravate wear.

It is also evident from Fig.4.29 that usual flood cooling by soluble oil could not reduce flank wear (VB) in any of the carbide inserts while machining C-60 steel. Such wet cutting causes faster oxidation and corrosion of the tool surfaces and rapid micro fracturing of the cutting edges by thermo-mechanical shocks due to fluctuation in temperature and stresses, which compensates or often surpasses the reduction of adhesion and diffusion wear of the carbide inserts expected due to cooling and lubrication by the cutting fluid in continuous machining like turning of steels. But application of high-pressure coolant jet has substantially reduced growth of VB as can be seen in Fig.4.29. Such improvement by

149

high-pressure coolant jet can be attributed mainly to retention of hardness and sharpness of the cutting edge for their steady and intensive cooling, protection from oxidation and corrosion and absence of built-up edge formation, which accelerates both crater and flank wear by flaking and chipping. Fig.4.29 also shows that VB increased much faster in case of SNMG inserts than in SNMM inserts irrespective of the environments of machining. The possible reasons have already been mentioned. It appears from the SEM view graphs in Fig.4.35, Fig.4.36, Fig.4.37 and Fig.4.38 that principal flank wear remained more or less uniform after machining the C-60 steel specimen under different environments particularly under high-pressure coolant condition.

The SEM views of the worn out SNMG insert after machining C-60 steel at a particular V-f-d combination under different environments are shown in Fig.4.35 and fig.4.36 which clearly indicates that use of conventional cutting fluid did not significantly improve the nature and extent of wear, whereas application of high-pressure coolant jet has provided remarkable improvement and even after 48 minutes of machining, both flank and crater wear have been much uniform and much smaller in magnitude and without any notch wear. Only a small notch appeared on the auxiliary flank. In the process of systematic growth of cutting tool wear, the cutting tools usually first undergo rapid wear called break-in wear at the beginning of machining due to attrition and micro-chipping and then uniformly and relatively slow mechanical wear followed by faster wear at the end. But the SNMG tool attained so less wear when used in machining the C-60 steel under high-pressure coolant condition.

Fig.4.37 and Fig.4.38 show that compared to the SNMG insert the SNMM type insert wore out much less under both dry, wet and high-pressure coolant conditions, which indicates that tool geometry plays substantial role on wearing of tool and also on the

150

effectiveness of high-pressure coolant on control of tool wear. This difference might be due to straight and sharp cutting edges of the SNMM inserts.

The auxiliary flank wear, which occurs due to rubbing of the tool tip against the finished surface, causes dimensional inaccuracy and worsens the surface finish. Gradual increase in depth of the auxiliary flank wear, which is proportional to the width of that wear, increases the diameter of the job in straight turning with the progress of machining. And the irregularity developed in the auxiliary cutting edge due to wear impairs the surface finish of the product.

Fig.4.35 and Fig.4.36 show that after machining the C-60 steel rod for 48 minutes under dry condition the SNMG insert attained sizeable wear with wide notch at the auxiliary flank. Wet machining under the same condition has not provided any significant improvement rather the notch has become much deeper expectedly for added chemical wear. Whereas, high-pressure coolant application has resulted much lesser wear and uniform wear. Fig.4.32 also shows that the value of average auxiliary flank wear, VS not only grew quite rapidly when machining by the SNMG inserts under dry as well as wet condition. Application of high-pressure coolant jet, which is aligned towards the auxiliary kept the magnitude and rate of growth of VS all along much low even upto 48 minutes of machining. The adverse and favorable effects of respectively wet and high-pressure coolant machining on auxiliary flank wear of SNMM type insert are also evident in Fig.4.32 and Fig.4.38 respectively.

The results of the experimental study presently carried out on tool wear in machining C-60 steel under different environments clearly depict that in machining steels, at least like C-60 steel, by carbide inserts, application of conventional method and type of

cutting fluid like soluble oil does not help in reducing wear or improving tool life. But proper application of high-pressure coolant in the form of jet provides substantial improvement. Such benefit of high-pressure coolant jet may be attributed mainly to reduction of abrasive and chemical wear at the tool flanks and also possible control of chip-tool interaction and thereby built-up edge formation which not only adds flaking wear but also accelerates chipping of the cutting edges by inducing vibration.

In machining research, a cutting tool is generally said to have failed when its VB reaches a specific value, mostly 300 μm. It is very important to note in Fig.4.29 that tool life has improved from 22 minutes to 45 minutes in case of SNMG inserts and from about 19 minutes to 48 minutes in case of SNMM inserts, i.e. almost by two to three times increase in tool life have been possible by high-pressure coolant. Or in other words, for same span of tool life the material can be machined at much higher cutting speed, which will drastically enhance productivity and economy if such cooling technique be employed.

Cutting tool wear and tool life tests usually consume lot of time and work material. Inspite of that in case of C-60 steel machining was continued over long period i e. 20 to 50 minutes to explore thoroughly the nature and extent of growth of the different features of tool wear till reaching the stage of tool failure i.e. VB is close to/reaches/exceeds 300 μm. But for the other two steels, the tool wear test runs were discontinued when the trend of growth of wear and effect of high-pressure coolant on that become adequately clear.

The mechanism and rate of growth of cutting tool wear depend much on the mechanical and chemical properties of tool and the work materials and their behavior under the cutting condition. Fig.4.30 shows that VB grew quite fast in both the inserts in

machining 17CrNiMo6 steel expectedly for its higher strength and hardness. But high-pressure coolant jet enabled sharp reduction in VB with the progress of machining. In uninterrupted machining of ductile metals by tools like carbides at reasonably high V and f, crater wear is governed mainly by adhesion and diffusion for rubbing at higher stresses and temperature and flank wear mainly by abrasion for lesser pressure and temperature. But adhesion and diffusion type temperature sensitive wear may also occur, in addition to abrasion wear, at the tool flanks if the flank temperature becomes high. Turning of ductile but strong metal like 17CrNiMo6 steel at reasonably high V (193 m/min) and f (0.18 mm/rev) under dry condition is expected to cause sufficiently high temperature at the tool flanks. Therefore, adhesion and diffusion are also likely to have contributed in the flank wear in the present case, and high-pressure coolant jet seemingly prevented such temperature sensitive adhesion and diffusion as well as reduced abrasion wears.

It appears from Fig.4.29 and Fig.4.30 that compared to the C-60 steel, the 17CrNiMo6 steel specimen provided relatively lesser flank wear for both the tools and both the environments. But while machining 17CrNiMo6 steel the main cutting edge of the inserts were found to suffer from chipping and flaking seemingly due to formation of minute built-up edge. However, in machining this steel also VB have sufficiently decreased for both the inserts by high-pressure coolant jet application as can be seen in Fig.4.30. Like VB, VS has also been quite low in machining this steel as can be seen in Fig.4.33, Fig.4.40 and Fig.4.42. High-pressure coolant has reduced auxiliary flank wear as usual and more effectively due to easier entry of high-pressure coolant jet.

The SEM views of the worn out inserts after machining of 17CrNiMo6 steel for different times spans, shown in Fig.4.39, Fig.4.40, Fig.4.41 and Fig.4.42, qualitatively indicate that high-pressure coolant has provided sizeable reduction in overall wear of the

inserts. It clearly appears from Fig.4.39 and Fig.4.41 that the principal flank of the SNMG and SNMM inserts attained wide flaking while dry machining of 17CrNiMo6 steel expectedly for high strength and hardness of this steel. But such detrimental flaking remarkably decreased, as can be seen in Fig.4.30, Fig.4.39 and Fig.4.41, when high-pressure coolant was employed, which reduced both abrasive and chemical wear at the tool flanks. Fig.4.39 and Fig.4.41also show that flank wear occurred more or less uniformly along the main cutting edge of both the tools and under both the environments in machining the 17CrNiMo6 steel. Substantial reduction in average auxiliary flank wear, VS in SNMG and SNMM inserts enabled by present high-pressure coolant in machining 17CrNiMo6 steel has been revealed in Fig.4.33, Fig.4.40 and Fig.4.42.

Beneficial role of high-pressure coolant on tool wear has been found to be more predominant in case of machining the high alloy steel, 42CrMo4 steel. The SNMG insert failed by large fracturing, as shown in Fig.4.43 and Fig.4.44, within 14 minutes of machining this steel under dry condition at the V-f-d levels undertaken. But high-pressure coolant allowed machining smoothly (Fig.4.31) even upto 20 minutes after which a part of the main cutting edge was found to chip-off (Fig.4.43) and flank wear also got aggravated. But interestingly, the SNMM insert survived in dry machining at least up to 15 minutes though attained wider flank wear (Fig.4.31 which, again, remarkably decreased by high-pressure cooling allowing machining at least upto 15 minutes after which macro chipping started occurring at the main cutting edge. While machining this steel, no notching was found to develop in any of the inserts even under dry machining condition possibly for less hardenability and more chemical stability of this steel. Fig.4.34 and Fig.4.44 and Fig.4.46 are showing the beneficial role of high-pressure coolant jet on VS in machining 42CrMo4 steel by SNMG and SNMM type carbide inserts.

154

The life of the cutting tool like turning insert is generally evaluated on the basis of the limiting value of average flank wear, VB. But depending upon the situation, depth of crater wear, KT alone or together is also used. For machining ductile material, which causes crater wear, even eroding the cutting edge, the amount of cutting edge depression may be taken as tool life criteria.

However, considering VB=300 μm as tool life criteria, the approximate tool life values obtained for both the inserts (SNMG and SNMM) under different conditions have been presented in Table 4.6.The graphical representation of tool life shown in Fig.4.47 and fig.4.48 depict that in machining C-60 steel by uncoated carbide tool, the tool life decreases with the increase of V and f as usual under all the environments undertaken. Tool life improved to some extent particularly when this material was machined at relatively lower V and f but high-pressure coolant jet enhanced tool life more pronouncedly though the benefit gradually decreased with the increase in cutting speed and feed rate. The present high-pressure coolant system increased tool life by 30% to 75% when turning C-60 steel by SNMG insert and 80% to 140% when machining by SNMM insert.

6.5   Surface Roughness

Surface finish is also an important index of machinability or grindability because performance and service life of the machined/ground component are often affected by its surface finish, nature and extent of residual stresses and presence of surface or subsurface microcracks, if any, particularly when that component is to be used under dynamic loading or in conjugation with some other mating part(s) Generally, good surface finish, if essential, is achieved by finishing processes like grinding but sometimes it is left to machining. Even if it is to be finally finished by grinding, machining prior to that needs to

be done with surface roughness as low as possible to facilitate and economize the grinding operation and reduce initial surface defects as far as possible. The major causes behind development of surface roughness in continuous machining processes like turning, particularly of ductile metals are:

i.   feed marks or scallop marks inherently left by the tool tip

ii. built-up edge formation, if any

iii. vibration in the tool work system

iv. irregular deformation of the tool nose due to chipping, wear and fracturing

The surface roughness geometrically caused by feed marks only depends upon the value of feed rate, f and the tool nose radius, r as

$$h_m = \frac{f^2}{8r}$$ ....[6.10]

where, h_m is the peak value of the feed marks as schematically shown by offset BD in the Fig.6.2 (b). In actual machining, often the peak value h_m may decrease, like from BD to EF as schematically shown in Fig.6.2 (b) due to rubbing over the feed mark ridges by the inner sharp edge of the flowing chips. Further deterioration may occur as indicated in Fig.6.2(c) due to micro or macro deformation of the cutting edge by micro chipping, fracturing, wear etc. at the tool tip. Besides BUE formation if any and vibrations for any reason also aggravates surface roughness.

The level of feed rate, f directly and almost proportionately governs the surface roughness in machining by single point cutting tools but the value of cutting speed V also

156

affects the pattern and extent of surface finish, though indirectly through deformation of the tool nose profile, BUE formation and vibration.
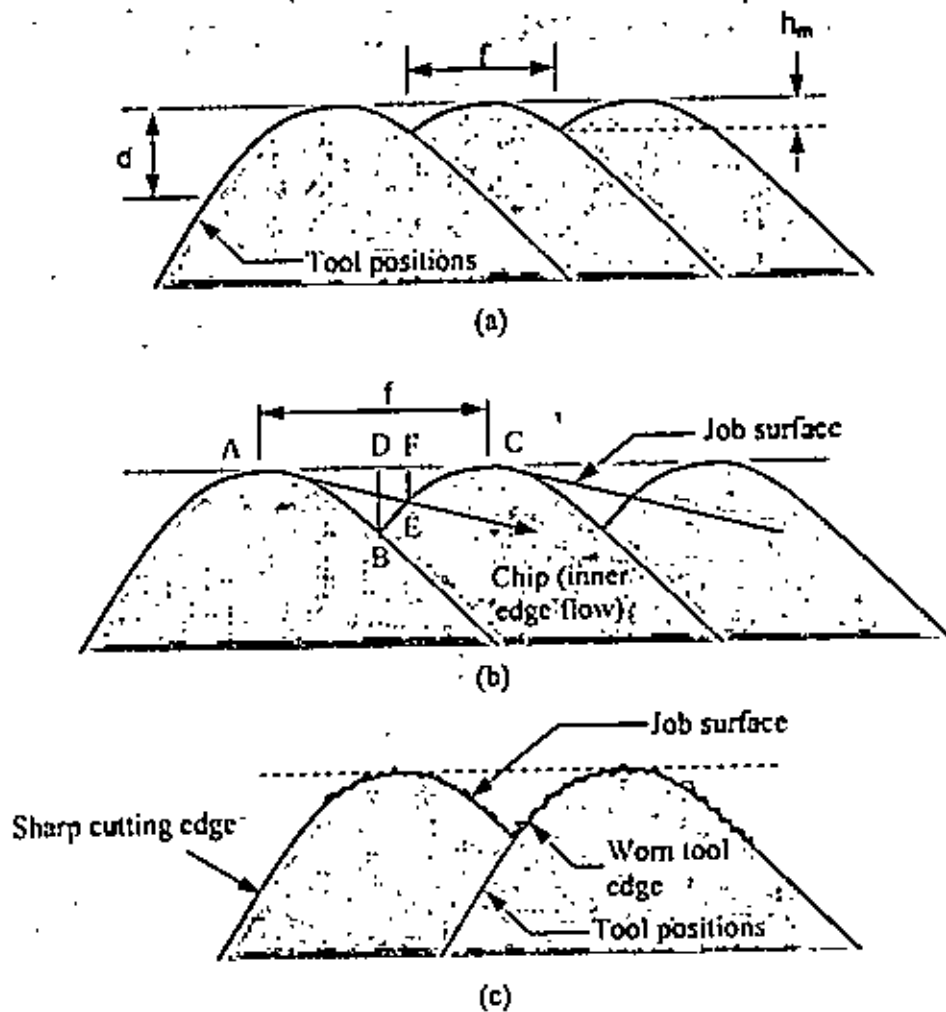
Fig.6.2 Pattern of surface roughness in turning

Fig.4.49 shows the variation of Ra values of surface roughness after 45 seconds of turning the C-60 steel rod at different V-f combinations under dry and high-pressure coolant condition by the (a) SNMG and (b) SNMM inserts. Assuming sinusoidal distribution of surface roughness caused only by feed marks, the Ra values for the present inserts having 0.8 mm nose radius have been evaluated and found to be around 0.55 μm, 1.08 μm, 1.80 μm and 2.67 μm for f equal to 0.10, 0.14, 0.18 and 0.22 mm/rev respectively. But the actual values of Ra have been much larger than the aforesaid values

excepting when V and f are very large. This indicates that in the present machining conditions, the effects of chipping, wear and notching of the auxiliary flank near the tool tips on surface roughness are prevalent. Built-up edge formation is also quite likely to have some role on surface roughness in machining the present steels by carbide inserts. In some of the present conditions, particularly with the increase in V and f, the actual Ra value has been even lower than the corresponding Ra value expected only due to feed marks as can be seen, for instance, in Fig.4.49. This might be due to either truncation of the feed marks as has been indicated in Fig.6.2(c) or flattening of the radiused tip of the cutting insert by more rapid break-in wear due to intensive temperature and pressure. Simultaneous action of both the factors is also possible.

Fig.4.49 clearly shows that surface roughness as such increased with the increase in feed rate, f and decreased with the increase in V. Increase in f raised Ra mainly according to the equation 6.10. Reduction in Ra with the increase in V may be attributed to smoother chip-tool interface with lesser chance of built-up edge formation in addition to possible truncation of the feed marks and slight flattening of the tool-tip. Increase in V may also cause slight smoothing of the abraded auxiliary cutting edge by adhesion and diffusion type wear and thus reduced surface roughness. It is evident in Fig.4.49 that high-pressure coolant could provide marginal improvement in surface finish at the beginning of machining with the fresh cutting edges. This has been more or less true for all the work-tool combinations undertaken as can be seen in Fig.4.49 to Fig.4.51. The slight improvement in surface finish by high-pressure coolant might be due to reduction in break-in wear and also possibly reduction or prevention of built-up edge formation depending upon the work material and cutting condition. Compared to C-60 steel, the alloy steels (17CrNiMo6 steel and 42CrMo4 steel) showed lesser effect of V and high-pressure coolant on surface roughness. This may reasonably be attributed to more stability of those steels

158

against attrition and built-up edge formation. It is also to be noted that there was no significant difference in *Ra* values provided by the present two types of inserts within such a short period of machining any steel. Therefore, any difference observed in *Ra* values provided by the different alloy steels may be attributed mainly to difference in break-in wear and nature of work-tool interactions.

Surface roughness for each treatment was also measured at regular intervals while carrying out machining for tool wear study. It was found that surface roughness grew substantially, though in different degree under different tool-work-environment combinations, with the progress of machining. Comparison of the figures from Fig.4.52 to Fig.4.54 with those from Fig.4.32 to Fig.4.34 reveals that the pattern of growth of surface roughness bears close similarity with that of growth of auxiliary flank wear, *VS* in particular. This has been more or less true for all the tool-work-environment combinations undertaken. Such observations indicate distinct correlation between auxiliary flank wear and surface roughness also like dimensional deviation. Wear at the tool flanks is caused mainly by micro-chipping and abrasion unlike crater wear where adhesive and diffusion wear are predominant particularly in machining steels by uncoated carbides. The minute grooves produced by abrasion and chipping roughen the auxiliary cutting edge at the tool-tip, as has been indicated in Fig.4.28, which is directly reflected on the finished surface. Built-up edge formation also is likely to affect surface finish directly being particularly sticked to the cutting edge as well as finished surface and indirectly by causing chipping and flaking at the tool tip.

Fig.4.52 clearly shows that machining C-60 steel by both SNMG and SNMM type carbide inserts results sizeable surface roughness with the progress of dry machining. Wet cutting, which aggravated auxiliary flank wear (Fig.4.32), has further deteriorated the

surface whereas, like *VS* and dimensional deviation, surface roughness also decreased substantially by application of high-pressure coolant jet (Fig.4.52). In case of alloy steels (Fig.4.53 and Fig.4.54), which as such produced higher surface roughness under dry machining expectedly due to more intensive temperature and stresses at the tool-tips, high-pressure coolant jet appeared to be more effective in reducing surface roughness as it did for auxiliary flank wear. However, it is evident that high-pressure coolant jet substantially improves surface finish depending upon the work-tool materials and mainly through controlling the deterioration of the auxiliary cutting edge by abrasive, chipping and built-up edge formation.

6.6 Dimensional Deviation

High-pressure coolant provided remarkable benefit in respect of controlling the increase in diameter of the finished job with machining time as can be seen in Fig.4.55. In plain turning the finished job diameter generally deviates from its desired value with the progress of machining i.e. along the job-length mainly for change in the effective depth of cut due to several reasons which include wear of the tool nose, over all compliance of the Machine-Fixture-Tool-Work (*M-F-T-W*) system and thermal expansion of the job during machining followed by cooling. Therefore, if the *M-F-T-W* system is rigid, variation in diameter would be governed mainly by the heat and cutting temperature. With the increase in temperature the rate of growth of auxiliary flank wear and thermal expansion of the job will increase. High-pressure coolant takes away the major portion of heat and reduces the temperature resulting decrease in dimensional deviation desirably.

Fig.4.55 and Fig.4.32 show that the nature of increase of dimensional deviation with the progress of machining C-60 steel rod is quite similar to that of growth of *VS* for

160

both the inserts. Dimensional inaccuracy has been respectively enhanced and reduced by application of soluble oil and high-pressure coolant, expectedly, in the way VS has been respectively raised and reduced. Therefore, increase in diameter is almost directly related to that of average auxiliary flank wear. However, it is clear that use of the conventional cutting fluid significantly aggravated dimensional inaccuracy which on the other hand substantially decreased by high-pressure coolant jet.

The machining tests conducted for studying the role of high-pressure coolant on dimensional inaccuracy were separately carried by fresh inserts after completion of tool wear tests. Dimensional deviation, for each tool-work-environment combination, was measured along the jog axis after one complete pass. It can be noted in Fig.4.56 and Fig.4.57 that both 17CrNiMo6 and 42CrMo4 steels resulted much lesser dimensional deviation, even under dry machining, compared to that resulted by the C-60 steel (Fig.4.55). This difference seems to be due to much lesser break-in wear or initial wear and absence of notching at the auxiliary flank of the inserts as can be seen in Fig.4.40, Fig.4.42, Fig.4.44 and Fig.4.46.

Fig.4.56 shows how dimensional deviation decreased spectacularly in case of machining 17CrNiMo6 steel by any of the inserts due to high-pressure, which enabled such reduction in VS (Fig.4.33) also. While machining 42CrMo4 steel at 193 m/min, the SNMG insert failed and both the tools attained sizeable edge-chipping. That speed might be too high for machining this alloy steel by uncoated carbide inserts. But under such condition also high-pressure coolant was found to reduce dimensional deviation quite substantially, particularly in case of SNMG inserts, as can be seen in Fig.4.57. Here also, the effect of high-pressure coolant on VS (Fig.4.34) shows similar trend.

161

Chapter-7

Conclusions and Recommendations

7.1   Conclusions

This study led to the evaluation of the effectiveness of the high-pressure coolant system. The feasibility of improving the machinability of different materials was also explored in this study. The results clearly indicate the advantages of using high-pressure coolant over dry and flood cooling while machining these materials. Based on the observations made and the experimental results obtained, the following conclusions are made:

i.   The present high-pressure coolant system enabled reduction in average chip-tool interface temperature upto 17% depending upon the work materials, tool geometry and cutting conditions and even such apparently small reduction, unlike common belief, enabled significant improvement in the major machinability indices.

The application of coolant (water soluble oil) did not improve machinability rather accelerated auxiliary tool flank wear, dimensional inaccuracy and surface roughness in machining C-60 steel by enhancing chipping and chemical wear at the cutting edges particularly at the auxiliary cutting edge where stresses and temperature are relatively higher.

The predicted values of the chip-tool interface temperature have been in close agreement with the corresponding experimental results. The deviation might be due to the several factors which have some influence on the cutting temperature but could not be incorporated in the model.

ii. Due to high-pressure coolant jet, the form and colour of the steel chips became favourable for more effective cooling and improvement in nature of interaction at the chip-tool interface. In the case of application of high-pressure coolant jet through an external nozzle, friction is reduced at the chip-tool interface due to the fragmentation of the chip by the impinging jet which prevents intimate contact at the chip-tool interface, consequently leading to bending and self breakage of chips.

iii. High-pressure coolant enabled favourable chip formation modes leading to reduction of the cutting forces by about 5% to 27%. F_t decreased more predominantly than F_c. Such reduction has been more effective for those tool-work combinations and cutting conditions, which provided lower value of, chip thickness ratio, r_c for adverse chip-tool interaction causing large friction and built-up edge formation at the chip-tool interface. Favourable change in the chip-tool interaction and retention of cutting edge sharpness due to reduction of cutting zone temperature seemed to be the main reason behind reduction of cutting forces by the high-pressure coolant jet.

iv. High-pressure coolant jet reduced the cutting tool wear, flank wear in particular in machining the steels by the carbide inserts undertaken. which would enable either remarkable improvement in tool life or enhancement of

163

productivity allowing higher cutting speed and feed rate. Such reduction in tool wear might have been possible for retardation of abrasion and notching, decrease or prevention of adhesion and diffusion type thermal sensitivity wear at the flanks and reduction of built-up edge formation which accelerates wear at the cutting edges by chipping and flaking. Notching and grooving, which are very detrimental and may cause premature and catastrophic failure of the cutting tools, are remarkably reduced by high-pressure coolant jet.

The present high-pressure coolant system increased tool life by 30% to 75% when turning C-60 steel by SNMG insert and 80% to 140% when machining by SNMM insert.

v. The surface finish obtained is much better than that obtained in the case of dry machining. Under certain condition, the surface finish obtained with the use of high-pressure coolant is comparable to that obtained in case of grinding operation. The welding of hot chip to the cutting edge which is a common problem while machining ductile steel is completely eliminated with the application of high-pressure coolant jet, leading to an improvement in surface quality and tool life.

Dimensional accuracy also substantially improved mainly due to significant reduction in cutting temperature due to application of high-pressure coolant jet.

vi. The geometry of cutting tools played significant role on the degree of improvement in machinability of the steels by high-pressure coolant jet

which becomes more effective when the tool geometry allows more intensive cooling of the chip-tool interface and the tool flanks.

vii. Further, the enhanced effectiveness of the coolant/lubrication by applying the cutting oil at high-pressures in the form of a narrow jet, leads to a reduction in the quantity of the cutting oil being used, reducing the amount of disposal, which is a primary concern of environmental protection authorities.

7.2   Recommendations

i.   In this research work only one high-pressure coolant (HPC) jet is applied along the rake surface. Other application methods, for example, along the main cutting edge and flank surface, can be further investigated in the future. The best solution of application methods to control cutting temperature, forces, tool wear and product quality can be offered through studying those configurations.

ii.   All testing presented in this work used uncoated carbide insert with SNMM and SNMG tool geometry, although it is not expected that this geometry is optimal for any or all cases. Previous work has shown that tool types and geometry affects nearly everything about the process. chip formation mode, cutting temperature, cutting forces, tool wear and failure, surface finish, residual stresses. and white layer generation. The types and geometry of the cutting tool should also be considered in dry and HPC cutting because the type and geometry of the cutting tool is an important factor for machinability of steel.

iii. In this research work an analytical model for cutting temperature is developed. For better understanding other analytical models can be developed to predict cutting forces, tool wear, tool life and surface roughness under high-pressure coolant (HPC) condition.

iv. In this work, the pattern of flow is not considered. So for future investigations the pattern of flow of jet can be measured, i.e., whether it is laminar or turbulent. Though turbulent flow is able to transport more heat in comparison to laminar jet, but for more thinning of jet lamina flow jet is preferable. With increase in oil pressure, flow rate and nozzle tip diameter, the effective laminar flow pattern for more effective and efficient cooling can be easily maintained.

v. This research work only focused on the effect of high-pressure coolant (HPC) jet on machinability of steels like chip formation mode, cutting temperature, forces, tool wear and product quality. To achieve a better understanding of the machining process planning with environmental concerns as a factor of consideration, the cutting fluid atomization behavior in high-pressure coolant (HPC) turning process in order to estimate the resulting air quality can be further investigated in the future.

References

Abrao, A. M., Aspinwall, D. K. and Ng, E.G., "Temperature Evaluation when Machining Hardened Hot Work Die Steel using PCBN Tooling", Ind. Diamond Rev., Vol. 56. pp. 40-44, 1996.

Abuladze, N. G., "Character and the Length of Tool-Chip Contact (In Russian), In: Proc. Machinability of Heat-Resistant and Titanium Alloys", Kuibyshev, pp. 68–78, 1962.

Alaxender, A., Varadarajan, A. S. and Philip, P. K., "Hard Turning with Minimum Cutting Fluid: A Viable Green Alternative on the Shop Floor", Proceedings 18th All India Conference MTDR, pp. 152-155. 1998.

Aronson, R. B., "Using High-Pressure Fluids, Cooling and Chip Removal are Critical", Manufacturing Engineering, June 2004, Vol. 132(6), 2004.

Aronson, R.B., "Why Dry Machining?", Manufacturing Engineering, Vol. 114, pp. 33-36, 1995.

Arunachalam, R. and Mannan, M. A., "Machinability of Nickel-based High Temperature Alloys", Journal of Machining Science and Technology, Vol. 4(1), pp. 127–168, 2000.

Attanasio, A., Gelfi, M., La Vecchia, M., Pedrazzani, R. and Remino, C., "Minimum Quantity Lubrication in Turning: Tool Life Test", Lubrication Engineering, pp. 1497–1503, 2004.

A S M Handbook, *ASM International*, Materials Park, Ohio, 1992.

Beaubien, S. J. and Cattaneo, A. G., "A Study of the Role of Cutting Fluid in Machining Operations", Lubrication Engineering, Vol. 10, pp. 74-79, 1964.

Bennett, E. O and Bennett, D. L., "Occupational Airway Diseases in the Metal-working Industry", Tribology International, Vol. 18(3), pp. 169-176, 1987.

Bennett, E. O., "Water Based Cutting Fluids and Human Health", Tribology International, Vol. 18, pp. 133–136, 1983.

Bhattacharyya, A., "Metal Cutting-Theory and Practice", *Central Book Publishers*, India, pp. 324-329, 1984.

Bhattacharyya, A., Roy, T. K and Chattopadhyay, A. B., "Application of Cryogenic in Metal Machining", Journal of Institution of Engineers, India, 1972.

Bouzid, W., Zghal, A.and Ben Ayed, K., "Carbide and Ceramic Tool Life in High Speed Turning", International Journal of Vehicle Design, Vol. 39(1-2), pp. 140-153, 2004.

Byrne, G., Dornfeld, D. and Denkena, B., "Advancing Cutting Technology", Annals of CIRP, Vol. 52(2), pp. 483–507, 2003.

Carlsaw, H. S. and Jaeger, J. C., "Conduction of Heat in Solids", Oxford UK, *Oxford University Press*, 1959.

Cassin, C. and Boothroyed, G., "Lubrication Action of Cutting Fluids", Journal of Mechanical Engineering and Science, Vol. 7(1), pp. 67-81, 1965.

Chandrasekaran, H., Thuvander, A. and Johansson, J. O., "The Influence of Cutting Fluid on Tool Temperature Distribution in Single Point Turning of Steel", 18th AIMTDR Conference, IIT Kharagpur, India, pp. 219-224, 1998.

Chattopadhyay, A. B. and Bhattacharya, A., "Cutting Characteristics of Constant Pressure", Journal of Engineering for Industry, ME-2, pp. 255-275, 1968.

Chattopadhyay, A. K. and Chattopadhyay. A. B., "Wear and Performance of Coated Carbides and Ceramic Tools", Wear, Vol. 80, pp. 239-253, 1982.

Childs, T.H.C., Mackawa, K., and Maulik, P., "Effects of Coolant on Temperature Distribution in Metal Machining", Materials Science and Technology, Vol. 4(11), pp. 1006-1019, 1988.

Choudhury, S. K. and Appa Rao, I. V. K., "Optimization of Cutting Parameters for Maximizing Tool Life", International Journal of Machine Tools and Manufacture, Vol. 39, pp. 343–353, 1999.

Cozzens, D. A., Olson, W. W., Sutherland, J. W. and Panetta, J. M., "An Experimental Investigation into the Effect of Cutting Fluid Conditions on the Boring of Aluminum Alloys," Concurrent Product and Process Engineering, ASME Bound Volume - MED Vol. 1/DE Vol. 85, pp. 251-257, November 1995.

169

Crafoord, R., Kaminski, J., Lagerberg, S., Ljungkrona, O. and Wretland, A., "Chip Control in Tube Turning using a High-Pressure Water Jet", Proceedings of the Institution of Mechanical Engineers, Part B, Vol. 213, pp. 761–767, 1999.

Davies, M. A., Chou, Y. and Evans, C. J., "On Chip Morphology, Tool Wear and Cutting Mechanics in Finish Hard Turning", Annals of CIRP, Vol. 45(1), pp. 77-82, 1996.

Dhar N. R. and Kamruzzaman, M., "Effect of High-Pressure Coolant on Tool Wear, Tool Life and Surface Roughness in Turning Medium Carbon Steel by SNMG Insert", 9th Cairo University International Conference on Mechanical Design and Production (MDP-9), Cairo, pp. 555-565. January. 2008.

Dhar N. R., Paul S. and Chattopadhyay A. B., "Beneficial Effects of Cryogenic Cooling over Dry and Wet Machining on Tool Wear and Surface Finish in Turning AISI 1060 Steel", Journal of Materials Processing Technology, Vol. 116, pp. 44-48, 2001.

Dhar, N. R. and Kamruzzaman, M., "An Experimental Study of Cryogenic Cooling in Grinding Steels: Chip Formation, Temperature and Surface Roughness", Journal of Mechanical Engineering, IEB, Vol. ME 34, pp.35-45, June and December, 2005.

Dhar. N. R. and Kamruzzaman, M., "Cutting Temperature, Tool Wear, Surface Roughness and Dimensional Deviation in Turning AISI-4037 Steel under Cryogenic Condition", International Journal of Machine Tool and Manufacture, Vol. 47, pp. 754-759, 2007.

Dhar, N. R. and Kamruzzaman, M., "Effect of Cryogenic Cooling by Liquid Nitrogen Jet on Tool Wear and Product Quality in Turning AISI-9310 Steel", ARPN Journal of Engineering and Applied Sciences, Vol. 1(1), pp. 1-7, June 2006.

Dhar, N. R. and Kamruzzaman, M., "Wear of Coated Carbide Tool, Surface Finish and Dimensional Deviation in Turning Steel under Cryogenic Cooling", AEESEAP Journal of Engineering Education, Vol. 31(1), pp. 62-71, 2005.

Dhar, N. R., Islam, M. W., Islam, S. and Mithu, M. A. H., "The Influence of Minimum Quantity Lubrication (MQL) on Cutting Temperature, Chip and Dimensional Accuracy in Turning AISI 1040 Steel", Journal of Materials Processing Technology, Vol. 171, pp. 93-99, 2006.

Dhar, N. R., Islam, S. and Kamruzzaman, M., "Effect of Minimum Quantity Lubrication (MQL) Tool Wear and Surface Roughness and Dimensional Deviation in Turning AISI-4340 Steel", G.U. Journal of Science, Vol. 20(2), pp. 23-32, January-June, 2007.

Dhar, N. R., Islam, S. and Kamruzzaman, M., "Experimental Investigation on Effect of Minimum Quantity Lubrication (MQL) in Machining Steel", International Journal of Manufacturing Technology and Research, Vol. 2(1 & 2), pp. 45-52, January-June, 2006.

Dhar, N. R , Islam, S. and Kamruzzaman, M., "Experimental Investigation on Effect of Minimum Quantity Lubrication (MQL) in Machining Steel", Journal of Engineering and Technology, Vol. 4(1), pp. 13-24, 2005.

Dhar, N. R., Islam, S., Kamruzzaman, M., and Paul, S., "Wear Behavior of Uncoated Carbide Inserts under Dry, Wet and Cryogenic Conditions in Turning C-60 Steel", Journal of Brazilian Society of Mechanical Science and Engineering, Vol. 28(2), pp. 146-152, 2006.

Dhar, N. R., Kamruzzaman, M. and Ahmed Mahiuddin, "Effect of Minimum Quantity Lubrication (MQL) on Tool Wear and Surface Roughness in Turning AISI 4340 Steel", Journal of Materials Processing Technology, Vol. 172, pp. 299-304, 2006.

Dhar, N. R., Kamruzzaman, M., Khan, M.M.A and Chattopadhyay, A. B., "Effect of Cryogenic Cooling by Liquid Nitrogen Jets on Tool Wear, Surface Finish and Dimensional Deviation in Turning Different Steels", International Journal of Machining and Machinability of Materials, Vol. 1(1) pp. 115-131, 2006.

Dhar, N. R., Nandakishore, S. V., Paul, S. and Chattopadhyay, A. B., "The Effects of Cryogenic Cooling on Chips and Cutting Forces in Turning of AISI 1040 and AISI 4320 Steels", Journal of Engineering Manufacture (IMechE-2002), Part B, Vol. 216, pp. 713-724, 2002

Dhar, N. R., Paul, S. and Chattopadhyay, A. B., "Role of Cryogenic Cooling on Cutting Temperature in Turning Steel", Transaction of the ASME, Vol. 123, pp. 146-154, 2002.

Dhar, N. R., Paul, S. and Chattopadhyay, A. B., "Machining of AISI 4140 Steel under Cryogenic Cooling-Tool Wear, Surface Roughness and Dimensional Deviation", Journal of Materials Processing Technology, Vol. 123, pp. 483-489, 2002.

Dhar, N. R., Paul, S. and Chattopadhyay, A. B., "The Influence of Cryogenic Cooling on Tool Wear, Dimensional Accuracy and Surface Finish in Turning AISI 1040 and E4340C Steels", Wear, Vol. 249, pp. 932-942, 2002.

Ding, Y. and Hong, S. Y., "Improvement of Chip Breaking in Machining Low Carbon Steel by Cryogenically Precooling the Workpiece", Transaction of the ASME, J. of Manuf. Science and Engg., Vol. 120, pp. 76-83, 1998.

Ding, Y. and Hong, S. Y., "Improvement of Chip Breaking in Machining Low Carbon Steel by Cryogenically Pre-cooling the Workpiece", Transaction of the ASME, Vol. 120, pp. 76-83, 1998.

Duan, C. and Wang, M., "Some Metallurgical Aspects of Chips Formed in High Speed Machining of High Strength Low Alloy Steel", Scripta Materialia, Vol. 52(10), pp.1001–1004, 2005.

Ekinovic, S., Dolinsek, S. and Begovic, E., "Machinability of 90MnCrV8 Steel during High-Speed Machining", Journal of Materials Processing Technology, Vol. 162–163, pp. 603–608, 2005.

Ekinovic, S., Dolinsek, S. and Ekinovic, E., "Frequency of Segmentation and Shape and Dimensions of Chip Segments at 52 HRC Steel High-speed Machining", Journal of Mechanical Engineering, Mašinstvo, Vol. 6(3), pp. 143–148, 2002.

Ezugwu, E. O., "High speed machining of aero-engine alloys", Journal of the Brazilian Society of Mechanical Sciences and Engineering, Vol. 26(1), Technical Paper, 2004.

Ezugwu, E. O. and Bonney, J., "Effect of High-Pressure Coolant Supply when Machining Nickel-Base, Inconel 718, Alloy with Coated Carbide Tools", <u>Journal of Materials Processing Technology</u>. Vol. 153–154, pp. 1045–1050, 2004.

Ezugwu, E. O. and Bonney, J.. "Effect of High-Pressure Coolant Supply when Machining Nickel-Base, Inconel 718, Alloy with Coated Carbide Tools", <u>International Conference on Advances in Materials and Processing Technologies (AMPT)</u>, Dublin City University, Dublin, Republic of Ireland, pp. 787–790, 8–11 July, 2003.

Ezugwu, E. O. and Tang, S. H., "Surface Abuse when Machining Cast Iron (G-17) and Nickel-Base Superalloy (Inconel 718) with Ceramic Tools", <u>Journal of Materials Processing Technology</u>, Vol. 55, pp. 63–69, 1995.

Ezugwu, E. O. and Wang, Z. M., "Performance of PVD and CVD Coated Tools when Machining Nickel-Based, Inconel 718 Alloy", <u>Progress of Cutting and Grinding</u>, Vol. 111, pp. 102–107, 1996.

Ezugwu, E. O., Bonney. J. and Yamane, Y., "An Overview of the Machinability of Aeroengine Alloys", <u>Journal of Materials Processing Technology</u>, Vol. 134, pp. 233–253, 2003.

Ezugwu, E. O.. Machado, A. R., Pashby, I. R. and Wallbank, J., "The Effect of High-Pressure Coolant Supply when Machining a Heat-Resistant Nickel-Based Superalloy", <u>Journal of Tribology and Lubrication Engineering</u>, Vol. 47(9), pp. 751–757, 1990.

Ezugwua, E. O., Bonney, J., Fadare, D. A. and Sales, W. F., "Machining of Nickel-base, Inconel 718, Alloy with Ceramic Tools under Finishing Conditions with Various Coolant Supply Pressures", Journal of Materials Processing Technology, Vol. 162-163. pp. 609–614, 2005.

Ezugwua, E. O., Da Silvaa, R. B., Bonney, J. and Machado, A. R., "Evaluation of the Performance of CBN Tools when Turning Ti–6Al–4V Alloy with High Pressure Coolant Supplies", International Journal of Machine Tools & Manufacture, Vol. 45, pp. 1009–1014, 2005.

Fang, N., "Machining with Tool-Chip Contact on the Tool Secondary Rake Face. Part II Analysis and Discussion", International Journal of Mechanical Sciences, Vol. 44, pp. 2355–2368, 2002.

Farook, A., Varadarajan, A. S. and Philip, P. K., "Machinability Studies on Steel using Hard Metal Inserts with Soft Material Deposit", Proceedings of 18th All India Conference MTDR, pp. 152-155, 1998.

Fillippi, A. D. and Ippolito, R., "Face Milling at 1800C", Annals of CIRP, Vol. 19(1), 1970.

Goldstein, R. J and Frankchett, M. E, "Heat Transfer from a Flat Surface to an Oblique Impinging Jet", Journal of Heat and Mass Transfer, Transaction of the ASME, Vol. 110, pp 84-90, 1988.

Hahn, R. S., "On the Temperature Developed at the Shear Plane in the Metal Cutting Processes", Proc. U. S. Nat. Congress of Applied Mechanics, Transaction of the ASME, pp. 661, 1951.

Heisel, U., Lutz, D., Wassmer, R., Walter, U., "The Minimum Quantity Lubricant Technique and its Application in the Cutting Process", Machines and Metals Magazine, Brazil, Vol. 386, February, pp. 22-38, 1998.

Heisel, U, Lutz, M., Spath, D., and Wassmer, R., "Application of Minimum Quantity Cooling Lubrication Technology in Cutting Process", Production Engineering, Vol. 2(1), pp. 49-54, 1994.

Hong, S. Y., Ding, Y. and Ekkins, R. G., "Improving Low Carbon Chip Breakability by Cryogenic Cooling", International Journal of Machine Tool and Manufacture, Vol. 39, pp. 1065-1085, 1999.

Hong, S. Y., Markus, I. and Jeong, W., "New Cooling Approach and Tool Life Improvement in Cryogenic Machining of Ti–6Al–4V", International Journal of Machine Tools and Manufacture, Vol. 41, pp. 2245–2260, 2001.

Huang, Y. and Liang, S. Y., "Modeling of the Cutting Temperature Distribution under the Tool Flank Wear Effect", Proceedings of the Institution of Mechanical Engineers, Part C: Journal of Mechanical Engineering Science, Vol. 217(11), pp. 1195-1208, 2003.

Iowa Waste Reduction Centre, "Cutting Fluid Management in Small Machine Shop Operations", *University of Northern, Iowa75 Biology Research Complex*, Cedar Falls, Iowa 50614-0185319/273-2079, 1996.

Jaeger, J. C., "Moving Sources of Heat and the Temperature at Sliding Contacts", Proceedings of the Royal society of NSW, Vol. 76, pp. 203-211, 1942.

Jaspers, S. P. F. C. and Dautzenberg, J. H., "Material Behaviour in Metal Cutting: Strains, Strain Rates and Temperature in Chip Formation", Journal of Materials Processing Technology, Vol. 43, pp. 1–13, 2002.

Jawahir, I. S. and van Luttervelt, C. A., "Recent Development in Chip Control Research and Application", Annals of CIRP, Vol. 42(2), pp. 659-693, 1993.

Jawahir, I. S., "The Tool Restricted Contact Effect as a Major Influencing Factor in Chip Breaking: An Experimental Analysis", Annals of CIRP, Vol. 37(1), pp. 121-126, 1988.

Kaminski, J. and Alvelid, B., "Temperature in the Cutting Zone in Water-Jet Assisted Turning", Journal of Materials Processing Technology, Vol. 106, pp. 68–73, 2000.

Kennedy, S. M., "Acute Pulmonary Responses among Automobile Workings Exposed to Aerosols of Machining Fluids", American J. of Industrial Medicine, Vol.15, pp. 627-641, 1989.

Khamsehzadeh, H., "Behaviour of Ceramic Cutting Tools When Machining Superalloys", *Ph. D Thesis*, University of Warwick, England, 1991.

177

Kitagawa, T., Kubo, A. and Maekawa. K., "Temperature and Wear of Cutting Tools in High Speed Machining of Inconel 718 and Ti-6V-2Sn", Wear, Vol. 202, pp. 142-148, 1997.

Klocke, F., Eisenblatter, G., "Dry Cutting", Annals of the CIRP, Vol. 46 (2), pp. 519-526. 1997

Komanduri, R. and Hou, Z. B., "Thermal Modeling of the Metal Cutting Process - Part II: Temperature Rise Distribution due to Frictional Heat Source at the Tool-Chip Interface", International Journal of Mechanical Sciences, Vol. 43(1), pp. 57-88, 2001.

Komanduri, R. and Hou, Z. B., "Thermal Modeling of the Metal Cutting Process Part 1 - Temperature Rise Distribution due to Shear Plane Heat Source", International Journal of Mechanical Sciences, Vol. 42(9), pp. 1715-1752, 2000.

Komanduri, R. and Schroeder, T. A. "On Shear Instability in Machining a Nickel-Iron base Superalloy", Journal of Engineering for Industry, Vol. 108, pp. 93-106, 1993.

Konenberge, M., "Cutting Angle Relationship on Metal Cutting Tools", Mechanical Engineering, December, pp. 901, 1943.

Kosa, T. and Ney, R. P., "Metals Handbook", Vol. 16, ASM, pp. 681-707, 1989.

Kovacevic, R., "Apparatus and Method of High Pressure Water Jet Assisted Cooling/Lubrication in Machining", Patent No. 5, 288,186, 22nd February, 1994.

Kovacevic, R., Cherukuthota, C. and Mazurkiewicz, M., "High-pressure Water Jet Cooling/Lubrication to Improve Machining Efficiency in Milling", International Journal of Machine Tools and Manufacture, Vol. 35(10), pp. 1459–1473, 1995.

Kurimoto, T. and Barroe, G., "The Influence of Aqueous Fluids on the Wear Characteristics and Life of Carbide Cutting Tools", Annals of CIRP, Vol. 31(1), pp. 19-23, 1982.

Li, X., "Effect of Coolant Flow Rate on Cooling in Machining", Proceedings of the NAMRC XXIII Conference, SME, Houghton, MI, USA, pp. 109-114, 1996.

Liao, Y. S. and Shiue, R. H., "Carbide Tool Wear Mechanism in Turning of Inconel 718 Superalloy", Wear, Vol. 193, pp. 16–24, 1996.

List, G., Nouari, M., G'ehin, D., Gomez, S., Manaud, J. P., Le Petitcorps, Y. and Girot, F., "Wear Behavior of Cemented Carbide Tools in Dry Machining of Aluminum Alloy", Wear, Vol. 259, pp. 1177–1189, 2005.

Liu, X. L., Wen, D. H., Li, Z. J., Xiao, L. and Yan, F. G., "Experimental Study on Hard Turning Hardened GCr15 Steel with PCBN Tool", Journal of Materials Processing Technology, Vol. 129, pp. 217-221, 2002.

Loewen, E. G. and Shaw M. C., "On the Analysis of Cutting Tool Temperature", Transaction of the ASME, Vol. 76, pp. 217-231. 1954.

Luo, S. Y., Liao, Y. S. and Tsai, Y. Y., "Wear Characteristics in Turning High Hardness Alloy Steel by Ceramic and CBN Tools", Journal of Materials Processing Technology, Vol. 88. pp. 114–121, 1999.

Machado, A. R. and Wallbank J., "The Effect of Extremely Low Lubricant Volumes in Machining", Wear, Vol. 219, pp. 76–82, 1997.

Machado, A. R. and Wallbank, J., "The Effect of High-Pressure Jet on Machining", Proceedings of the Institution of Mechanical Engineers (Part B), Vol. 208, pp. 29–38, 1994.

Masatoshi Hirao, Toru Fuse, Keiichi Shirase, Takeshi Yasui, Tetsuo Shiraga and Nobuyuki Ishikawa, "Improved Machinability of Nitriding Steel (SACM 645)", Journal of Materials Processing Technology, Vol. 62, pp. 370-373, 1996.

Mazurkiewicz, M., Kubala, Z. and Chow, J., "Metal Machining with High Pressure Water-Jet Cooling Assistance-A New Possibility", Journal of Engineering for Industry, Vol. 111, pp. 7–121, 1989.

Merchant, M. E., "Mechanics of the Metal Cutting Process. II. Plasticity Conditions in Orthogonal Cutting", Journal of Applied Physics, Vol. 16, pp. 318-324, 1945.

Molinari, A. and Nouari, M., "Modeling of Tool Wear by Diffusion in Metal Cutting", Wear, Vol. 252, pp.135–149, 2000.

Molinari, A. and Nouari, M., "Tool Wear in High Speed Machining", Journal de Physique, Vol. 10, pp. 541–547, 2000.

Muller, C. and Blumke, R., "Influence of Heat Treatment and Cutting Speed on Chip Segmentation of Age Hardenable Aluminum Alloy", Material Science and Technology, Vol. 17, pp. 651-654, 2001.

Muraka, P. D., Barrow, G. and Hinduja, S., "Influence of the Process Variables on the Temperature Distribution in Orthogonal Machining using the Finite Element Method", International Journal of Machine Tool Design and Research, Vol. 21, p.445, 1979.

Nabhani, F., "Machining of Aerospace Titanium Alloys", Robotics and Computer Integrated Manufacturing. Vol. 17, pp. 99–106, 2001.

Nagpal, B. K. and Sharma, C. S., "Cutting Fluids Performance-Part 1-Optimization of Pressure for 'Hi-Jet' Method of Cutting Fluid Application", Journal of Engineering for Industry, Transactions of the ASME, pp. 881–889, 1973.

Narutaki, N., Yamane, Y. and Okushima, K., "Tool Wear and Cutting Temperature of CBN Tools in Machining of Hardened Steels", Annals of CIRP, Vol. 28(1), pp. 23-28, 1979.

Nedess, C. and Hintze, W., "Characteristics Parameters of Chip Control in Turning Operations with Indexable Three Dimensionally Shaped Chip Formers", Annals of CIRP, Vol. 38(1), pp. 75-79, 1989.

Ng E., El-Wardany T. I., Dumitrescu M., Elbestawi M. A., "Physics based Simulation of High Speed Machining", International Journal of Machining Science and Technology, Vol. 6(3), pp. 301-329, 2002.

Novaski, O. and Dörr, J., "Machining without Coolant", Machines and Metals Magazine, Vol. 399, pp. 18–27, 1999.

Oxley, P. L. B., "The Mechanics of Machining: An Analytical Approach to Assessing Machinability", *E. Horwood New York*, 1989.

Pashby, I. R., Wallbank J. and Boud, F. "Ceramic Tool Wear when Machining Austempered Ductile Iron", Wear, Vol. 162, pp. 22-33, 1993.

Paul, S. and Chattopadhyay, A. B., "Effects of Cryogenic Cooling by liquid Nitrogen Jet on Forces, Temperature and Surface Residual Stresses in Grinding", Cryogenics, Vol. 35, pp. 515-523, 1995.

Paul, S., Dhar, N. R. and Chattopadhyay, A. B., "Beneficial Effects of Cryogenic Cooling over Dry and Wet Machining on Tool Wear and Surface Finish in Turning AISI 1060 steel", Journal of Materials Processing Technology, Vol. 116(1), pp. 44-48, 2001.

Paul, S., Dhar, N. R. and Chattopadhyay, A. B., "Beneficial Effects of Cryogenic Cooling over Dry and Wet Machining on Tool Wear and Surface Finish in Turning AISI 1060 steel", Proceedings of ICAMT-2000, Malaysia, pp. 209-214, 2000.

Peter, C. R., Steven, C. and David, L., "Evaporation of Polydisperse Multi Component Oil Droplets", American Industrial Hygiene Association, 1996.

Rahman, M., Seah, W. K. H. and Teo, T. T., "The Machinability of Inconel 718", Journal of Materials Processing Technology, Vol. 63(1-3), pp.199–204, 1997.

Reed, R. P. and Clark, A. F., "Materials at Low Temperatures", American Society for Metals, Carnes Publication, Metal Park, OH. 1983.

Rosenthal, D., "The Theory of Moving Sources of Heat and its Application to Metal Treatment", Transactions of the ASME, Vol. 68, pp. 849-866, 1946.

Sadik, M. I. and Lindstrō̈m, B., "The Role of Tool-Chip Length in Metal Cutting", Journal of Materials Processing Technology, Vol. 37, pp. 613–627, 1993.

Satoshi, I., Teiji, Y., Shinichi, M. and Kazuo, M., "Machinability of Ni_3Al based Intermetallic Compounds", Journal of Materials Processing Technology, Vol. 63(1-3), pp. 181-186, 1997.

Seah, K. H. W., Li, X. and Lee, K. S., "The Effect of Applying Coolant on Tool Wear in Metal Machining", Journal of Materials Processing Technology, Vol. 48, pp. 495-501, 1995.

Shackelford, J. F., Alexander, W. and Park, J. S., "CRC Materials Science and Engineering Handbook", 2nd ed, CRC Press, Boca Raton, 1994.

Shaw, M. C., Pigott, J. D. and Richardson, L. P., "The Effect of Cutting Fluid upon Chip-Tool Interface Temperature", Transactions of the ASME, Vol 71, pp. 45-56, 1951.

Shaw, M. C, "Metal Cutting Principles", Oxford University Press, New York, 1996.

Shigeki, O., Yoshinobu, N. and Suehisa, K., "Cooling Action of Grinding Fluid in Shallow Grinding", International Journal of Machine Tools and Manufacture, Vol. 33(1), pp. 13–23, 1993.

Singh, S B., Chakraborty, A. K. and Chattopadhyay, A. B., "A Study of the Effects of Inclusion Contact on the Machinability and Wear Characteristics of 0.24% Carbon Steel", Journal of Materials Processing Technology, Vol. 66, pp. 90-96, 1997.

Sokovic, M., Mijanovic, K., "Ecological Aspects of the Cutting Fluids and its Influence on Quantifiable Parameters of the Cutting Processes", Journal of Materials Processing Technology, Vol. 109(1-2), pp. 181-189, 2001.

Stephenson, D. A., "Tool-work Thermocouple Temperature Measurement: Theory and Implementation Issue", Transaction of the ASME, Vol. 115, pp. 432-437, 1993.

Stevenson, M. G., Wright, P. K., and Chow, J. G., "Further Developments in Applying the Finite Element Method to the Calculation of Temperature Distributions in Machining and Comparisons with Experiment", ASME J. Eng. Ind., Vol. 105, pp. 149-154, 1983.

Strafford, K. N. and Audy, J., "Indirect Monitoring of Machinability in Carbon Steels by Measurement of Cutting Forces", Journal of Materials Processing Technology, Vol. 67, pp. 150-156, 1997.

Strenskovski, J. S., and Kyung-jin, Moon, "Finite Element Prediction of Chip Geometry and Tool and Workpiece Temperature Distributions in Orthogonal Cutting", Transaction of the ASME, J. of Manuf. Science and Engg., Vol. 112, pp. 313-318, 1990.

Sutter, G., "Chip Geometries during High-Speed Machining for Orthogonal Cutting Conditions", International Journal of Machine Tools & Manufacture, Vol. 45, pp. 719–726, 2005.

Tay, A. O., Stevenson, M. G., and Davis, G. V., "Using the Finite Element Method to Determine Temperature Distribution in Orthogonal Machining", Proc. Inst. Mech. Eng., Vol. 188, pp. 627–638, 1974.

Thiele, J. D. and Melkote, S. N., "Effect of Cutting Edge Geometry and Work-piece Hardness on Surface Generation in the Finish Hard Turning of AISI 52100 Steel", Journal of Materials Processing Technology, Vol. 94, pp. 216–226, 1999.

Thony, C., Thony, J. Lafontaine, M. and Limasset, J. C., "Occurrence of Polycyclic Aromatic Hydrocarbons in Some Cutting Oils. Study of the Corresponding Risk", Arch. Mal. Prof Med. Trav. Sec. Soc., Paris 36, pp. 37-52, 1975.

Thoors, H and Chandrasekaran, H., "Influence of the Cutting Medium on Tool Wear during Turning", Swedish Institute for Metal Research, Report No IM-3118, 1994.

Thornburg, J. and Leith, D., "Mist Generation during Metal Machining", Journal of Tribology, Transactions of the ASME, Vol.122 (3), pp.544-549, 2000.

Toropov, A. and Ko, S. L., "Prediction of Tool-Chip Contact Length using a New Slip-Line Solution for Orthogonal Cutting", International Journal of Machine Tools & Manufacture, Vol. 43, pp. 1209–1215, 2003.

Trent, E. M., "Metal Cutting", Butterworths, London & Boston, 1984.

Trent, E. M., "The Tribology of Metal Cutting, Industrial Tribology, the Practical Aspect of Friction", Lubrication and Wear, Elsevier, Amsterdam, pp. 446-470, 1983.

Trent, E. M., "Metal Cutting", *Third edition, Butterworth*, London, 1991.

Uhera, K. and Kumagai, S., "Chip Formation, Surface Roughness, Cutting Forces and Tool Wear in Cryogenic Machining", Annals of CIRP, Vol. 17(1), 1968.

Uhera, K. and Kumagai, S., "Mechanisms of Tool Wear", Journal of Japanese Society of Precision Engineering, Vol. 35(9), pp. 43-49, 1969.

U.S. Department of Health and Human Services, "Occupational Exposure to Metalworking Fluids", *NIOSH Publication* No. 98-102, January 1998.

Venkatesh, V. C., "Experimental Techniques in Metal Cutting", *Prentice Hall, India*, 1987.

Vernon, A. and Ozel, T., "Factors Affecting Surface Roughness in Finish Hard Turning", Proceedings of the Manufacturing Automation and Research Laboratory (MARL-03), New Jersey, January 2003.

Vleugels, J., "Machining of Steel with Sialon Ceramics: Influence of Ceramic and Workpiece Composition on Tool Wear", Wear, Vol. 189, pp. 32-44, 1995.

Wang, Z. Y., Rajurkar, K. P. and Murugappan, M., "Cryogenic PCBN Turning of Ceramic (Si_3N_4)", Wear, Vol. 195, pp. 1-6, 1996.

Weiner, J. H., "Shear-Plane Temperature Distribution in Orthogonal Cutting", Transaction of the ASME, Vol. 77(8), pp. 1331-1344, 1955.

Welter, E.S., "Manufacturing Exposure to Coolant-Lubricants", Journal of Occupied. Med., Vol. 20, pp. 535-538, 1978.

Wrethim, R., Rotberg, J. and Ber, A., "Influence of High Pressure Flushing through the Rake Face of Cutting Tool", Annals of CIRP, Vol. 41(1), pp. 101-106, 1992.

Wright, P. K. and Trent, E. M., "Metallographic Methods of Determining Temperature Gradients in Cutting Tools", Journal of Iron and Steel Institute, pp. 364-368, 1973.

Wu, D. W. and Matsumoto, Y. "The Effect of Hardness on Residual Stresses in Orthogonal Machining of AISI 4340 Steel", Journal of Engineering for Industry, Vol. 112. pp. 245-252, 1990.

List of Publications

01. Kamruzzaman, M. and Dhar, N. R., "Effect of High-Pressure Coolant on Temperature, Chip, Force, Tool Wear, Tool Life and Surface Roughness in Turning AISI 1060 Steel", GU Journal of Science, Vol. 22 (4), pp. 359-370, 2009.

02. Kamruzzaman, M. and Dhar, N. R., "The Effect of Applying High-Pressure Coolant (HPC) Jet in Machining of 42CrMo4 Steel by Uncoated Carbide Inserts", Journal of Mechanical Engineering. Vol. ME39 (2), pp.71-77, 2009.

03. Kamruzzaman, M. and Dhar. N. R., "The Influence of High Pressure Coolant on Temperature, Tool Wear and Surface Finish in Turning 17CrNiMo6 and 42CrMo4 Steels", Journal of Engineering and Applied Sciences, Vol.4 (6), pp. 1-11, 2009.

04. Kamruzzaman, M. and Dhar, N. R., "Effects of High-Pressure Coolant (HPC) Jet on Temperature, Chips and Forces in Turning AISI1060 Steel and AISI4320 Steel", Proceedings of the International Conference on Mechanical Engineering (ICME-2009), Bangladesh, ICME09-RT-32, pp. 1-7.

05. Kamruzzaman, M. and Dhar, N. R., "Performance Evaluation of Carbide Inserts in Turning C-60 Steel and 42CrMo4 Steel under High-pressure Coolant (HPC) Condition", Proceedings of the International Conference on Mechanical Engineering (ICME-2009), Bangladesh, ICME09-RT-31, pp. 1-7.

06. **Kamruzzaman M.**, Chowdhury M.M.H. and Dhar N.R., "Effect of High-Pressure Coolant (HPC) Jet in Machining AISI 1060 Steel by Uncoated Carbide Insert", Proceedings of the 2nd Intl. and 23rd AIMTDR conf., Chennai, India, pp.679-684, December, 2008.

07. **Kamruzzaman. M.** and Dhar, N. R., "The Effect of Applying High Pressure Coolant on Temperature, Force, Chips and Product Quality in Machining C-60 Steel with SNMM Insert", Proceedings of 12th Annual Paper Meet, The Institution of Engineers, Mechanical Engineering Division, Bangladesh, Paper ID: 189-EN10, pp.1-8, February, 2008.

08. **Kamruzzaman, M.** and Dhar, N. R., "Experimental Investigation into Tool Wear, Tool Life and Product Quality in Turning C-60 Steel under High-Pressure Coolant Condition", Proceedings of 12th Annual Paper Meet, The Institution of Engineers, Mechanical Engineering Division, Bangladesh, Paper ID: 190-EX10, pp.1-7, February, 2008.

09. Dhar N.R. and **Kamruzzaman, M.**, "Effect of High-Pressure Coolant on Tool Wear, Tool Life and Surface Roughness in Turning Medium Carbon Steel by SNMG Insert", 9th Cairo University International Conference on Mechanical Design and Production (MDP-9), Cairo, pp. 555-565, January, 2008.

10. **Kamruzzaman, M.** and Dhar, N. R., "An Experimental Study of Effect of High-Pressure Coolant on Tool Wear, Tool Life and Roughness in Turning 16MnCr5 steel by SNMG Insert", Proceedings of the International Conference on Mechanical Engineering (ICME-2007), Bangladesh, Paper ID: AM-33, pp.1-7, December, 2007.

189

11. **Kamruzzaman, M.** and Dhar, N. R., "Wear Behavior of Carbide Insert under High-Pressure Coolant Jet Assisted Machining of 42CrMo4 Steel", Proceedings of the All India Conference on Recent Developments in Manufacturing & Quality Management (RDMQM-2007), India, pp.178-187, October, 2007.

12. **Kamruzzaman, M.** and Dhar, N. R., "Effects of High Pressure Coolant Jet on Temperature, Chip and Force in Turning 42CrMo4 Steel", Proceedings of the National Conference on Advances in Materials and Manufacturing Technology (AMMT-2007), India, pp.14-20, September, 2007.

13. Dhar, N. R. and **Kamruzzaman, M.,** "A Study of Effects of High-Pressure Coolant on Chips, Temperature and Cutting Force in Turning AISI-8740 Steel", Proceedings of the International Conference on Manufacturing Automation (ICMA-2007), Singapore, pp.159-168, May, 2007.

14. Dhar, N. R., **Kamruzzaman, M.** and Rashid, M. H., "On Effect of High-Pressure Coolant on Tool Wear and Surface Finish in Turning AISI-8740 Steel", Proceedings of the International Conference on Manufacturing Automation (ICMA-2007), Singapore, pp.695-703, May, 2007.

15. **Kamruzzaman, M.,** Dhar, N. R. and Rashid, M. H., "Effect of High-Pressure Coolant on Chip, Temperature and Cutting Force in Turning AISI-1060 Steel", Proceedings of the National Conference on Design, Dynamics and Manufacturing (NCDDM-2007), Punjab, India, pp.199-204, March, 2007.

16. **Kamruzzaman, M.** and Dhar, N. R., "An Experimental Investigation into Tool Wear, Tool Life and Product Quality in Turning Steel under High-Pressure Coolant

Condition", <u>Proceedings of the Global Conference on Production and Industrial Engineering</u> (CPIE-2007), Jalandhar, India, pp.1-6. March, 2007.

17.   Kamruzzaman, M. and Dhar, N. R., "Machining of 17CrNiMo6 Steel under High-Pressure Coolant Condition - Chip, Temperature, Forces, Tool Wear and Surface Roughness", <u>JZUS-Journal of Zhejiang University of Science</u>, 2008 (Submitted)

18.   Kamruzzaman, M. and Dhar, N. R., "Effects of Pressure and Coolant Flow Rates in Machining of AISI 4230 Steel by Uncoated Carbide Inserts", <u>Journal of Materials Processing Technology</u>, 2008 (Submitted)

19.   Kamruzzaman, M. and Dhar, N. R., "Role of High-pressure Coolant on Cutting Temperature in Turning Steels", <u>Journal of Manufacturing Science and Engineering</u>, 2008 (Submitted)

20.   Kamruzzaman, M. and Dhar, N R., "Prediction of Chip and Tool Temperature in Turning C-60 Steel under High-Pressure Coolant Conditions", <u>International Journal of Manufacturing Research (IJMR)</u>, 2009 (Submitted)